

Characterization of red blood cell functions in health and coronary artery disease

Inaugural-Dissertation

zur Erlangung des Doktorgrades
der Mathematisch-Naturwissenschaftlichen Fakultät
der Heinrich-Heine-Universität Düsseldorf

vorgelegt von

Christina Monika Panknin
aus Radevormwald

Düsseldorf, März, 2017

Aus dem kardiologischen Labor, Klinik für Kardiologie, Pneumologie und Angiologie
der Heinrich-Heine-Universität Düsseldorf

Gedruckt mit der Genehmigung der
Mathematisch-Naturwissenschaftlichen Fakultät der
Heinrich-Heine-Universität Düsseldorf

Referent: Prof. Dr. rer. nat. Dr. M. M. Cortese-Krott

Korreferent: Prof. Dr. rer. nat. P. Proksch

Tag der mündlichen Prüfung: 08.06.2017

Eidesstattliche Erklärung

Hiermit erkläre ich an Eides Statt, dass ich die vorliegende Arbeit selbstständig und nur unter Zuhilfenahme der ausgewiesenen Hilfsmittel angefertigt habe. Sämtliche Stellen der Arbeit, die im Wortlaut oder dem Sinn nach anderen gedruckten oder im Internet verfügbaren Werken entnommen sind, habe ich durch genaue Quellenangaben kenntlich gemacht.

Düsseldorf, den

Christina Panknin

Zusammenfassung

Vieles deutet darauf hin, dass Erythrozyten, neben ihrer Rolle als Gas- und Nährstofftransporter, weitere nicht-klassische Funktionen besitzen. Es wird vermutet, dass Erythrozyten am Stickstoffmonoxid (NO) Metabolismus und an der Freisetzung von ATP zur Regulierung des vaskulären Tonus beteiligt sein könnten. Zusätzlich sind sie in der Lage, über die Präsentation von Phosphatidylserin (PS) auf der extrazellulären Seite ihrer Plasmamembran, ihre Lebensdauer selbst zu regulieren. Das präsentierte PS wird anschließend in der Milz von Makrophagen als „find me“ Signal für alte oder geschädigte Erythrozyten erkannt. Die unterliegenden Regulationsmechanismen dieser nicht-klassischen Funktionen sind bisher noch nicht gänzlich aufgeklärt worden. Die vorliegende Arbeit basiert auf der Hypothese, dass die nicht-klassische Funktionen der Erythrozyten in kardiovaskulären Krankheiten verändert sein und/ oder Einfluss auf den klinischen Outcome haben könnten. Daher war das Hauptziel der Studie, die nicht-klassischen Funktionen der Erythrozyten in gesunden Erythrozyten und in Erythrozyten von Patienten mit koronarer Herzkrankheit und Niereninsuffizienz zu charakterisieren. Die Teilziele bestanden darin, die Signalwege zu analysieren, die an der Regulation der ATP Freisetzung (1.) und der PS-Präsentation (2.) beteiligt sind. Zusätzlich sollten die nicht-klassischen Funktionen von Erythrozyten von Patienten mit koronarer Herzkrankheit und Niereninsuffizienz im Vergleich zu gleichaltrigen Kontrollen charakterisiert werden (3.). Die Hauptergebnisse dieser Studie bestanden darin, dass die erythrozytäre ATP Freisetzung unabhängig vom Guanylatzyklase/cGMP- und cAMP-Signalweg reguliert wird. Diese Studie zeigte weiterhin, dass die ATP Freisetzung durch hypotonischen Stress und Phosphodiesterase (PDE)-Inhibierung induziert wird, dass diese jedoch unabhängig vom Pannexin-1 Kanal reguliert wird. Jedoch konnte gezeigt werden, dass die PDE -vermittelte ATP Freisetzung „downstream“ über den Cystic Fibrosis Transmembrane Conductance Regulator kontrolliert wird. Das Hauptergebnis bei der Analyse der PS-Präsentation bestand darin, dass NO die Ca^{2+} /Calciumionophor/N-Ethylmaleimide induzierte Präsentation von PS auf der Erythrozytenoberfläche inhibiert, dass dieser Mechanismus jedoch unabhängig vom Guanylatzyklase/cGMP-Signalweg wirkt. Der letzte Teil der Studie beschäftigte sich mit der Analyse des Zustandes der nicht-klassischen Funktionen der Erythrozyten in kardiovaskulären-und Nierenerkrankungen. Die Ergebnisse der Studie haben ergeben,

dass der zelluläre Redox-Status, NO Metaboliten, Membransymmetrie, Verformbarkeit sowie Aggregationsfähigkeit der Erythrozyten in koronarer Herzkrankheit aufrechterhalten sind, woraus sich schließen lässt, dass die nicht-klassischen Funktionen Erythrozyten unter diesen pathologischen Bedingungen nicht beeinflusst werden.

Summary

Beside the role of red blood cells (RBCs) as transporter of oxygen and nutrients to the tissues, there is accumulating evidence that RBCs exert non-canonical functions, which might contribute to regulation of vascular tone or cardioprotection. RBCs were proposed to participate to nitric oxide (NO) metabolism and to release ATP to regulate vascular tone. In addition, RBCs were shown to control their own half-life by exposing phosphatidylserine (PS) on their surface, which is recognized by macrophages as a “find me signal” for old/damaged erythrocytes in the spleen. The mechanisms underpinning these non-canonical functions of RBCs are not fully understood so far. This work is based on the hypothesis that non-canonical functions may be affected by cardiovascular disease (CVD), and/or might contribute to its clinical outcome. Therefore, the main aim of the study was to characterize non-canonical RBC functions in healthy RBCs and in RBCs from patients with coronary artery disease (CAD) and chronic kidney disease (CKD). The main goals of the study were to analyze pathways regulating (1.) ATP release and (2.) PS exposure of RBCs, as well as (3.) to characterize non-canonical RBC functions in RBCs taken from patients with CAD or CKD as compared to age-matched controls. The main findings in the analysis of ATP signaling were that soluble guanylyl cyclase (sGC)/cGMP as well as cAMP signaling do not regulate ATP release from RBCs. Moreover, the study showed that ATP release is induced by hypotonic stress and phosphodiesterase (PDE) inhibition and that this release is not controlled via pannexin-1, but PDE mediated effects are downstream regulated via cystic fibrosis transmembrane conductance regulator. The main finding in the analysis of PS exposure was that treatment of RBCs with NO inhibits Ca^{2+} /calcium ionophore/ N-ethylmaleimide induced exposure of PS in RBCs, but sGC/cGMP signaling is not involved in this regulation. The last part of the study aimed to analyze the status of non-canonical functions in cardiovascular- and renal disease. The results indicated that cellular redox-state, NO metabolites, RBC deformability and membrane symmetry are preserved in CVD indicating that RBC functions are not affected in these pathological conditions.

Table of content

Zusammenfassung	IV
Summary	VI
1 Introduction	1
1.1 Canonical and non-canonical functions of red blood cells	1
1.1.1 RBCs in the regulation of NO metabolism	2
1.1.1.1 Role of endogenous NO in the modulation of vascular tone	2
1.1.1.2 Role of RBCs in NO metabolism	4
1.1.2 Redox-regulation of RBCs	5
1.1.3 ATP release from RBCs	6
1.1.3.1 Role of second messengers cAMP and cGMP	6
1.1.3.2 Role of PDEs	7
1.1.3.3 Role of ion channels: Cystic fibrosis transmembrane conductance regulator and pannexin-1 ...	8
1.1.4 Regulation of PS exposure in RBCs	9
1.1.5 Rheological properties of RBCs	10
1.2 RBC dysfunction and anemia	11
2 Aim of the work	13
3 Material and methods	15
3.1 Material	15
3.2 Methods	20
3.2.1 RBC purification	20
3.2.1.1 Human samples	20
3.2.1.2 Murine samples	20
3.2.2 Analysis of ATP signaling from RBCs	20
3.2.2.1 ATP determination	20

3.2.2.2	Hb detection	22
3.2.3	Flow cytometric analysis of RBCs	22
3.2.3.1	Detection of PS exposure	22
3.2.3.2	Detection of NO-, ROS- and reduced thiols-levels	23
3.2.4	Cell culture experiments	24
3.2.4.1	Cultivation of HUVECs.....	24
3.2.4.2	Cell lysis	25
3.2.4.3	Protein determination.....	25
3.2.5	Analysis of red cell eNOS expression	26
3.2.5.1	Cell lysis	26
3.2.5.2	Protein determination.....	26
3.2.5.3	Bead coupling and immunoprecipitation of red cell eNOS.....	26
3.2.5.4	Detection of red cell eNOS expression by western blot.....	27
3.2.6	RBC NO ₂ ⁻ detection via chemiluminescence	27
3.2.7	Analysis of rheological properties of RBCs.....	29
3.2.7.1	Aggregability measurement.....	29
3.2.7.2	Deformability measurement.....	31
3.3	Study design: CVD	32
3.4	Study design: CKD	35
3.5	Statistics	35
4	Results	36
4.1	Part 1: Measurement of ATP release from RBCs.....	36
4.1.1	Assay Optimization.....	36
4.1.1.1	Time-dependent decrease of ATP levels from RBCs	36
4.1.1.2	Hemolysis is a confounding parameter in ATP measurement	37

4.1.1.3	ATP measurement requires normalization.....	39
4.1.1.4	Hypotonic stress induces ATP release in mouse RBCs independent of hemolysis.....	42
4.1.2	Intracellular signaling of ATP release from murine RBCs.....	44
4.1.2.1	PDE-inhibition induces ATP release in RBCs.....	44
4.1.2.2	No effect of extracellular cGMP on ATP release	46
4.1.2.3	No effect of extracellular cAMP on ATP release.....	47
4.1.3	No effect of sGC stimulation on ATP release	49
4.1.4	Role of ion channels in ATP release	50
4.1.4.1	Hypotonic stress induces ATP release but is independent of Pnx-1.....	50
4.1.4.2	PDE 5 regulated ATP release is Pnx-1 independent.....	51
4.1.4.3	Hypotonic stress induces hemolysis in RBCs from CFTR KO mice	52
4.1.4.4	PDE 5 regulated ATP release is CFTR dependent.....	53
4.1.5	No Correlation of Hb levels and ATP.....	54
4.2	Part 2: Regulation of PS exposure in human RBCs	55
4.2.1	Induction of PS exposure in RBCs by NEM, CaCl ₂ and Ca-I.....	55
4.2.2	NO-donor DEA/NO inhibits NEM/ CaCl ₂ / Ca-I mediated PS exposure.....	58
4.2.3	PS exposure is sGC/cGMP independent	59
4.3	Part 3: Patient study I	61
4.3.1	Red cell eNOS expression is decreased in CKD.....	61
4.3.2	Patient study II: Role of RBC functions in CAD and ACS.....	63
4.3.2.1	Red cell eNOS expression is decreased in CAD	66
4.3.2.2	Levels of NO and NO ₂ ⁻ are unchanged in CAD	66
4.3.2.3	Redox-state is preserved in CAD and ACS	68
4.3.2.4	PS exposure is unchanged in patients with CAD and ACS	70
4.3.2.5	Rheological parameters.....	70

4.3.2.5.1	Aggregability is increased in ACS.....	71
4.3.2.5.2	Deformability is unchanged in CAD and ACS.....	72
5	Discussion.....	73
5.1	Part 1: ATP release from RBCs.....	74
5.1.1	Technical hurdes of measurement of ATP release: Hemolysis	74
5.1.2	Hypotonic stress induces ATP release independent of hemolysis	75
5.1.3	PDE inhibition induces ATP release.....	76
5.1.4	ATP release is independent of sGC/cGMP signaling	77
5.1.5	Role of ion channels: Pnx-1 and CFTR	78
5.1.5.1	Hypotonic stress induced ATP release is Pnx-1 independent	78
5.1.5.2	PDE mediated ATP release is CFTR dependent, but Pnx-1 independent.....	79
5.1.6	Limitations and perspectives	80
5.2	Part 2: Regulation of PS exposure	80
5.3	Part 3: Analysis of RBC functions in CAD and CKD.....	82
5.3.1	Red cell eNOS expression is decreased in CKD.....	82
5.3.2	Non-canonical RBC functions are preserved in CAD and ACS	83
6	Summary and Conclusion	86
7	References.....	88
	Acknowledgment	112
	Curriculum vitae.....	114

Table index

Table 1: Instruments and consumables.....	15
Table 2: Software	16
Table 3: Chemicals,buffers, kits and antibodies part 1	16
Table 4: Chemicals,buffers, kits and antibodies part 2	17
Table 5: Chemicals,buffers, kits and antibodies part 3	18
Table 6: Formulation of HBSS	21
Table 7: Formulation of KH buffer.....	21
Table 8: Stimulators and inhibitors used in ATP determination assay	21
Table 9: Formulation of PS buffer	23
Table 10: Chemicals for PS analysis	23
Table 11: Fluorochromes used in flow cytometric analysis.....	24
Table 12: Formulation of RIPA buffer	25
Table 13: Formulation of preservation solution.....	28
Table 14: Formuation of reduction solution	28
Table 15: Aggregation settings	30
Table 16: Elongation settings	32
Table 17: Demographic and clinical characteristics of the study population (CKD) [204].....	61
Table 18: Demographic and clinical characteristics of the study population (CAD, ACS).....	65

Figure index

Figure 1: Overview of canonical and non-canonical functions in RBCs.....	2
Figure 2: Depiction of the NO/ soluble guanylyl cyclase signaling pathway in the smooth muscle cell [35]	3
Figure 3: Classification of Anemia [3]	12
Figure 4: Aims and goals of the study	14
Figure 5: Measurement principle of ATP assay	22
Figure 6: Treatments for flow cytometry of DAF, DCF and TT@.....	24
Figure 7: Syllectogram of RBC aggregability [208].....	30
Figure 8: RBC deformability curve [208].....	31
Figure 9: Study design of CAD and ACS study	33
Figure 10: Study protocol of of CAD and ACS study	34
Figure 11: Basal ATP levels are decreasing with time in RBC suspensions	36
Figure 12: Hemolysis is a confounding parameter in ATP measurement.....	38
Figure 13: ATP measurement requires normalization	41
Figure 14: Hypotonic stress induces ATP release from RBCs independent of hemolysis	43
Figure 15: PDE 5 inhibition induces ATP release in murine RBCs.....	45
Figure 16: No effect of CPT-cGMP on ATP release from murine RBCs.....	46
Figure 17: No effect of CPT-cAMP on ATP release in murine RBCs.....	48
Figure 18: sGC stimulation has no impact on ATP release	49
Figure 19: Hypotonic effect on ATP release is Pnx-1 independent.....	51
Figure 20: Pnx-1 is not involved in ATP release via phosphodiesterase 5 inhibition	52
Figure 21: Hypotonic stress induces strong hemolysis in RBCs from CFTR KO mice	53
Figure 22: CFTR is participating in PDE 5 mediated ATP release.....	54
Figure 23: Hemolysis control of performed experiments	55
Figure 24: NEM/Ca-I/CaCl ₂ increases phosphatidyserine exposure of human RBCs.....	56

Figure 25: NEM/Ca-I/CaCl ₂ treatment changes human RBC morphology	57
Figure 26: DEA/NO decreases NEM/Ca-I/CaCl ₂ induced PS exposure	58
Figure 27: Effects of DEA/NO on PS exposure in RBCs are independent of sGC/cGMP signaling	60
Figure 28: Red cell eNOS expression is decreased in CKD	63
Figure 29: Study design of CAD and ACS study	64
Figure 30: Overview of CAD and ACS study	64
Figure 31: Red cell eNOS expression is decreased in CAD and ACS.....	66
Figure 32: Levels of NO and NO ₂ ⁻ are unchanged in CAD and ACS.....	67
Figure 33: No differences of ROS ⁻ and thiol levels in CAD and ACS	68
Figure 34: No changes of glutathione levels in CAD and ACS	69
Figure 35: No changes in PS exposure in patients with CAD and ACS.....	70
Figure 36: RBC Aggregability is increased in ACS	71
Figure 37: RBC deformability is unchanged in CAD and ACS.....	72
Figure 38: Aims and goals of the present study.....	73
Figure 39: Main findings of the present study.....	86

Abbreviations

(-)	without CaCl ₂ + MgCl ₂
(+)	with CaCl ₂ + MgCl ₂
•O ₂ ⁻	superoxide anion
8-CPT-	8-(4-chlorophenylthio)
AC	adenylate cyclase
ACS	acute coronary syndrome
ADP	adenosine diphosphate
AI	aggregation index
AMP	adenosine monophosphate
AMP	erythrocyte aggregation amplitude
ATP	adenosine triphosphate
BAY-41	BAY-41-2272
BSA	bovine serum albumin
calcium	intracellular calcium concentration
CAD	coronary artery disease
Ca-I	calcium ionophore
Ca ²⁺ _i	Intracellular calcium concentration
cAMP	cyclic adenosine monophosphate
CF	cystic fibrosis
CFTR	cystic fibrosis transmembrane conductance regulator
cGMP	cyclic guanosine monophosphate
CKD	chronic kidney disease
CLD	chemiluminescence detector

CRP	C-reactive protein
CTRL	control
CVD	cardiovascular disease
DAF-FM-DA	4-amino-5-methylamino-2',7'-difluorofluorescein diacetate
db-cGMP	dibutyl-cyclic GMP
DCF	2',7'-dichlorodihydrofluorescein-diacetate
DEA/NO	diethylamine nonoate diethylammonium salt
DMSO	dimethylsulfoxide
DPTA	DTPA
ECG	electrocardiography
EI	elongation index
eNOS	endothelial nitric oxide synthase
FCS	fetal calf serum
FI	fluorescence intensity
FMD	flow-mediated dilation
FSC	forward scatter
GCP	good clinical practice
geo. MFI	geometric mean fluorescence intensity
GSH	free glutathione (reduced)
GSSG	glutathione disulfide
GTP	guanosine triphosphate
H ₂ CO ₃	carbonic acid
H ₂ O ₂	hydrogen peroxide
Hb	hemoglobin

HBSS	Hank's balanced salt solution
Hct	hematocrit
Hepes	4-(2-hydroxyethyl)-1-piperazineethanesulfonic acid
HUVEC	Human Umbilical Vein Endothelial Cells
IBMX	3-isobutyl-1-methylxanthine
KH buffer	Krebs-Henseleit-buffer
KO	knock out
LDL	low density lipoprotein
LDS	lithium dodecyl sulfate
L-NAME	<i>n</i> ω -nitro-L-arginine methyl ester hydrochloride
Lorca	Laser-assisted Optical Rotational Cell Analyzer
MRP4	Multidrug resistance-associated protein 4
NEM	N-ethylmaleimide
NO	nitric oxide
NO ₂ ⁻	nitrite
NO ₃ ⁻	nitrate
NSTEMI	non ST-segment elevation myocardial infarction
o.n.	over night
O ₂	oxygen
ODQ	1h-[1,2,4]oxadiazolo[4,3,-a] quinoxalin-1-one
ONOO ⁻	peroxynitrite
PBS	phosphate buffer saline
PDE	phosphodiesterase
PKC	protein kinase C

PKG	protein kinase G
PL	phospholipid
Pnx-1	pannexin-1
PS	phosphatidylserine
RBC	red blood cell
RIPA buffer	radioimmunoprecipitation assay buffer
ROS	reactive oxygen species
RT	room temperature
SDS	sodium dodecyl sulfate
SEM	standard error of the mean
sGC	soluble guanylyl cyclase
Sil	sildenafil citrate salt
SNP	sodium nitroprusside
SRA	sample reducing agent
STEMI	ST-segment elevation myocardial infarction
TA	tris-acetat
TBS-T	tris-buffered saline with Tween-20
tGSH	total glutathione
TT®	ThiolTracker®
w/o	without
WT	wild type

1 Introduction

1.1 Canonical and non-canonical functions of red blood cells

Red blood cells (RBCs) play an important role in the body due to their ability to transport oxygen (O_2) and carbon dioxide (CO_2) through the body and to maintain the acid/base equilibrium in the blood. Moreover, they have unique characteristics and are highly abundant. They have been firstly characterized in 1674 by Lee Van Hock and until now, the process of analysis has not come to the end [1]. RBCs represent a volume of about 99% and a cell number of 4.5×10^{12} per liter in human whole blood. They are shaped as biconcave discs of $7.5 \mu m$ diameter with a thickness of $2 \mu m$, which provides them the ability of a high gas exchange due to their high surface and short diffusion ways [2].

The main protein in RBCs is hemoglobin (Hb). Together with the enzyme carbonic anhydrase, it contributes to the major canonical functions of RBCs, which is the transport of O_2 and CO_2 through the body and the preservation of the systemic acid/base balance of the blood [2, 3]. The regulatory mechanisms of these functions are intertwined [3].

Hb is a tetrameric protein whose subunits consist of a globulin chain and a heme-group. The heme mediates its O_2 binding capacity by containing a central Fe^{2+} -atom, which is able to bind O_2 dependent of O_2 -partial pressure, acid/base balance and temperature. The binding of O_2 to Hb results in a conformation change of the protein from a tense T-state to a relaxed R-state [2]. Hb also functions as a buffer system by binding of free H^+ ions to its histidine residues. Furthermore, the histidine residues are also able to bind CO_2 resulting in generation of carbamino-Hb. Thereby, Hb contributes to the transport of CO_2 from the tissues. However, the major mechanism of RBCs to transport CO_2 to the lungs is the hydration of CO_2 to carbonic acid (H_2CO_3) via carbonic anhydrase. Thereby, the enzyme contributes to the regulation of the blood pH-value. The generated H_2CO_3 dissociates to HCO_3^- and H^+ and free H^+ -ions are buffered by Hb [2].

However, beside their commonly known function as O₂ transporters, RBCs might have additional non-canonical functions (Figure 1).

These include the release of vasoactive metabolites like (1.) adenosine triphosphate (ATP) [4-7] and (2.) nitric oxide (NO) [8-11], which are proposed to contribute to the regulation of vascular tone [5, 12]. Furthermore, (3.) regulation of membrane functions like deformability and aggregation [13-15], but also phosphatidylserine (PS) exposure [16, 17] as well as (4.) redox regulation [18, 19] are believed to play an important role in human physiology.

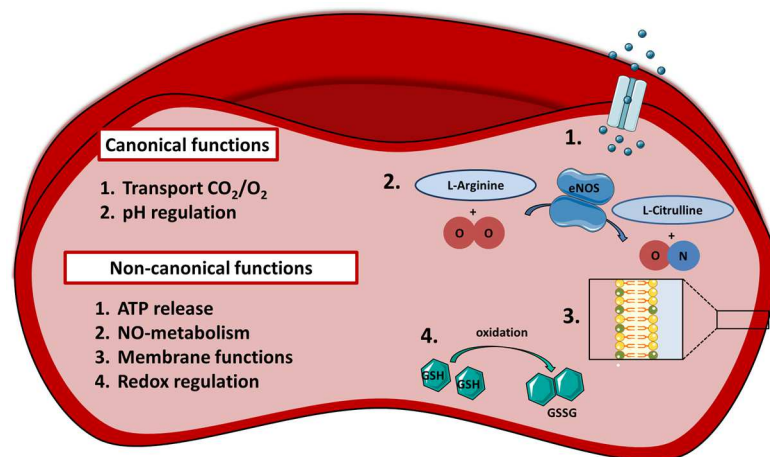


Figure 1: Overview of canonical and non-canonical functions in RBCs

Until today, complexity of RBC non-canonical functions is not completely understood. Moreover, it remains to be investigated whether non-canonical functions of RBCs are changed in cardiovascular disease (CVD).

1.1.1 RBCs in the regulation of NO metabolism

NO is a short living, but highly important signaling molecule in the human body. It represents an important vasoactive molecule in the endothelium-dependent regulation of vascular tone and blood flow [2] and this regulation is highly connected to cardiovascular physiology [20].

1.1.1.1 Role of endogenous NO in the modulation of vascular tone

In the endothelium, NO is generated by the constitutively expressed endothelial NO synthase (eNOS) [21, 22]. The eNOS enzyme in the endothelium generates NO via conversion of L-arginine and O₂ to L-citrulline. It is tightly regulated by

variety of calcium-dependent and -independent pathways, of which most are connected to each other [23-27]. eNOS is activated by increase of intracellular calcium concentrations (Ca^{2+}_i) with subsequent binding of Ca^{2+} /calmodulin [28, 29] to its eNOS binding region [30]. Furthermore, enzyme activation is dependent on multiple cofactors like tetrahydrobiopterin, flavin mononucleotide, flavin adenine dinucleotide and nicotinamide adenine dinucleotide phosphate [31]. Beside the calcium-dependent activation, eNOS is also activated by shear stress [20, 28, 32-34]. Although NO is highly reactive, it is able to diffuse from endothelial cells into the smooth muscle cells where it mediates vasodilatory effects in a complex intracellular signaling pathway [35] (Figure 2).

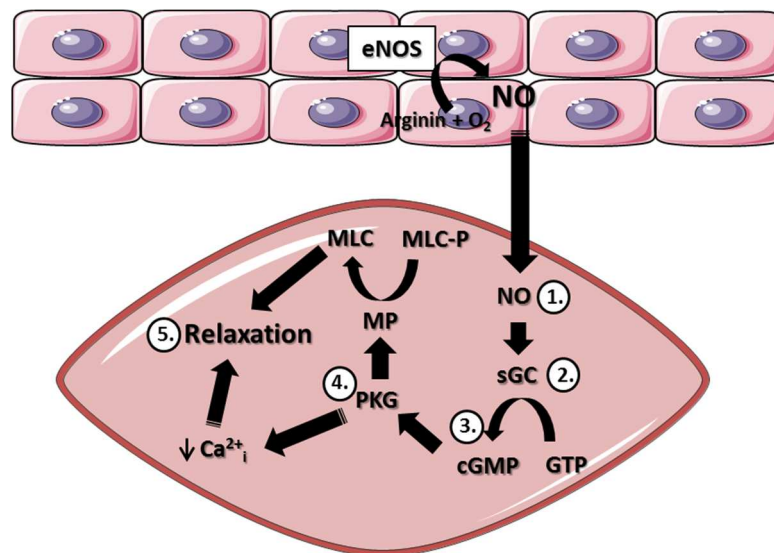


Figure 2: Depiction of the NO/ soluble guanylyl cyclase signaling pathway in the smooth muscle cell [35]

First (1.), NO diffuses through the membrane of the smooth muscle cell and binds to soluble guanylyl cyclase (sGC) [2]. The enzyme contains a heme domain [36, 37], which is activated by NO via binding to the Fe^{2+} atom of the heme group [38, 39] and thus converts cyclic guanosine monophosphate (cGMP) from guanosine triphosphate (GTP) [40]. The enzyme is typically found as a heterodimer, consisting of a larger α -subunit (α_1/α_2 isoforms) and a smaller heme binding β -subunit (β_1/β_2 isoforms) [41], but also homodimers of these subunits are existing rarely (sGC α/α or β/β) [42]. The heme subunit consists of a central Fe^{2+} - atom, which is associated with four nitrogens and an axial ligand histidine-105 [43]. Binding of NO leads to a generation of a nitrosyl-heme-complex and a

conformation change of sGC [43, 44] resulting in an increase in enzyme activity up to the 200 fold [45]. The heme complex functions as the NO binding site since its removal leads to abolishment of NO activation of the enzyme [46, 47]. For activation of sGC, just small amounts of NO in nM range are necessary [43]. Moreover, the chemical compound BAY-412272 (BAY-41) synthesized by BAYER AG is able to potentiate the effect of NO in a heme-dependent manner [43]. Removal of heme-group as well as oxidation of sGC by 1h-[1,2,4]oxadiazolo[4,3,-a]quinoxalin-1-one (ODQ) abolishes the effect of NO [48, 49]. Changes in redox-state may happen via reactive oxygen species (ROS) and nitrogen species such as superoxide anion (O_2^-) and peroxynitrite (ONOO^-) and are increased under oxidative stress conditions [50].

The generated cGMP from sGC affects diverse protein kinases, ion channels and phosphodiesterases (PDEs) [44]. As shown in Figure 2, cGMP (3.) binds to protein kinase G (PKG) (4.) in the smooth muscle cell. Thereby, it activates the kinase. PKG further phosphorylates multiple factors, which lead to a decrease of Ca^{2+} and to dephosphorylation of the myosin light chain. In result, relaxation of the smooth muscle cells (5.) is induced [35, 51]. There is strong evidence that downregulation of eNOS activity might be correlated to pathological conditions like atherosclerosis [52-54] and diabetic vascular disease [55].

1.1.1.2 Role of RBCs in NO metabolism

For a long time, RBCs have been considered as scavengers of free NO [56], because they are able to convert NO to nitrate (NO_3^-) via generation of metHb. Small quantities of NO are converted to nitrite (NO_2^-) via reaction with free O_2 [57-61]. Since NO-scavenging is increased in aged RBCs, RBCs have been proposed to play a key role in the impairment of NO bioavailability during blood transfusion or pathological conditions [62, 63].

However, RBCs not only function as NO sinks, but also are able to store, synthesize and transport NO [8, 10]. NO_2^- has been proposed to function as a main marker for NO bioavailability [64]. Moreover, the majority of NO_2^- in whole blood is present in RBCs [65]. Under hypoxic conditions, RBCs release NO to the blood stream [66]. Thereby, stored NO_2^- serves as a source of NO via reaction

with deoxyHb and generation of methHb [67] and thus might participate to the regulation of vasodilation [64, 68].

In the past years, we and others have shown that besides the endothelium, a functional eNOS also exists in RBCs (red cell eNOS) [9, 69]. We demonstrated this by purification and concentration of the red cell eNOS-enzyme by magnetic beads and mass spectrometry analysis and showed further that RBCs are able to synthesize NO [69]. This was supported by the finding that the isolated enzyme is not present in RBCs from eNOS^{-/-} mice [70].

Therefore, RBCs might play an important role in the regulation of NO bioavailability in the human body.

1.1.2 Redox-regulation of RBCs

Oxidative stress is generally described as an imbalance between production of ROS and their degradation via anti-oxidative molecules [71]. The main intracellular source of oxidative stress of RBCs is based in autoxidation reactions of Hb [72].

Therefore, RBCs are equipped with a number of anti-oxidative systems consisting of enzymatic and non-enzymatic components [3]. These include antioxidants like glutathione, thioredoxin, ascorbic acid and vitamin E, but also enzymatic anti-oxidative factors such as superoxide dismutase, catalase, glutathione peroxidase, glutathione reductase and methHb reductase [73-76]. Because of their high abundance of anti-oxidative enzymes, RBCs may function as potent ROS neutralizing cells for the whole human body [18, 19].

Reduced glutathione (GSH) is described as the main antioxidant in RBCs [77, 78] and about 10% of total GSH (tGSH) in the body are present in RBCs [79-81]. Beside its role as an antioxidant, it also serves as modulator of detoxification, cell proliferation or apoptosis [82, 83]. In RBCs, GSH is generated from glutamate, cysteine and glycine. The intracellular concentration is defined as equilibrium of GSH synthesis, consumption and efflux. GSH is a cofactor of glutathione peroxidase, which catalyzes the reduction of hydrogen peroxide (H₂O₂) to H₂O and thereby oxidizes GSH to glutathione disulfide (GSSG). The generated GSSG

is reduced to GSH by glutathione reductase via NADPH oxidation, but some parts of GSSG efflux out of the cell, which contribute to loss of intracellular GSH [84].

It has been proposed that oxidative stress might play a major role in several disease states like atherosclerosis [85], diabetes [86] and CVD [87]. However, it remains to be investigated whether changes in redox state of RBCs occur in CVD.

1.1.3 ATP release from RBCs

Beside its role as an energy transporter, ATP serves as a potent signaling molecule in RBCs. RBCs contain intracellular concentrations of about 5 mM ATP, which is mainly generated by glycolysis [5]. There is evidence that RBCs might be involved in the control of O₂ supply and vascular tone via release of ATP [88]. Several studies showed that vessels exposed to fully saturated RBCs dilate in response to a decrease of O₂ tension [89, 90]. This showed a relationship between vasodilation, RBCs and O₂, but did not clarify the underlying mechanisms. Until today, a lot of new aspects of ATP signaling have been investigated.

ATP released in the lumen interacts via purinergic receptors on the endothelium [91-93], which results in a release of vasoactive molecules such as NO and eNOS dependent vasodilation [94-96].

ATP release from RBCs is induced by extracellular stimuli like hypoxia and deformation [97, 98], but also by activation of prostacyclin- and β -adrenergic receptors [99].

1.1.3.1 Role of second messengers cAMP and cGMP

Cyclic adenosine monophosphate (cAMP) and cGMP both are second messengers involved in the regulation of cellular processes of various organs like heart, brain or kidney [2], but also have been proposed to play a regulatory role in ATP release from RBCs [100, 101]. cAMP is generally converted from ATP by membrane bound adenylate cyclase (AC) [40] and its main targets are protein kinase A [102] and cAMP-regulated ion channels [103]. AC is ubiquitarily expressed in mammalian tissues [104] and exists of a family of at least 9 isoforms

[105]. The enzyme is regulated via extracellular agonists like adrenaline, noradrenaline, glucagon or histamine, which act extracellular via heptahelical receptors [40]. These receptors further activate or inhibit AC via intracellular guanine nucleotide proteins (G-proteins) and thus function as molecular switches [40]. In an inactive state, the heterotrimeric G-proteins consists of a complex build from a $G_{\alpha_{s/i}}$, G_{β} - and G_{γ} -subunit [2]. The $G_{\alpha_{s/i}}$ domain is bound to GDP. Activation of heptahelical receptors results in exchange of GDP and GTP and breakdown of the trimeric complex. The released G_{α} binds to AC and thus activates (G_{α_s}) or inactivates (G_{α_i}) the enzyme depending of the type of G-protein [40].

AC type II is mainly expressed in the brain and lungs [106, 107], but also in rabbit RBCs [108]. Although G_i is generally known as an AC inhibiting protein [40], it acts as an activating molecule at AC type II in RBCs [104, 108-110]. It has been shown that activation of G_s as well as G_i results in generation of cAMP from ATP in RBCs [108, 111, 112]. Furthermore, deformation and hypoxia both lead to activation of G_i in RBCs [111, 113-115]. However, regulatory effects of G_i on AC type II in other tissues have not been clarified yet [116, 117].

The other important second messenger proposed to play a role in ATP release from RBCs is cGMP. It is converted from GTP by all isoforms of guanylyl cyclases [43, 118] and its main targets are PKG and cGMP-activated channels [2].

1.1.3.2 Role of PDEs

There is strong evidence that regulation of cAMP and cGMP in RBCs might be additionally regulated by compartmentalization of the specific PDEs [119-121]. The general role of PDEs is the control of intracellular cAMP and cGMP levels by specific hydrolyzation of the second messengers. The individual isoforms are classified by their specificity for either one or both nucleotides [119, 122]. Moreover, cGMP controls cAMP levels via cGMP-mediated regulation of PDEs [122-124]. cGMP- and cAMP- specific PDEs are present in RBCs, which include PDE2, -3, -4 and -5 [125-127]. Furthermore, it was indicated that PDE3 is involved in prostacyclin-mediated ATP release via potentiation of intracellular cAMP-increase, but not in β -adrenergic signaling [119, 126]. This indicates the

existence of at least more than one regulatory mechanism of ATP signaling within RBCs.

1.1.3.3 Role of ion channels: Cystic fibrosis transmembrane conductance regulator and pannexin-1

Deformation and hypoxia mediated ATP release of RBCs involves the cystic fibrosis transmembrane conductance regulator (CFTR) [7] as well as the pannexin-1 channel (Pnx-1) [4, 7]. The CFTR is a cAMP-regulated chloride channel, which is mainly present at the apical membrane of epithelial cells of pancreas, airways and other fluid-transporting tissues [128, 129]. Furthermore, the channel is a member of the ATP-binding cassette transporter [130]. It is activated via cAMP/protein kinase K mediated phosphorylation [131] and ATP hydrolysis [132, 133]. Moreover, mutation of the CFTR gene (DF508) is associated to the development of cystic fibrosis (CF), which results in organ pathology [134, 135]. Recent studies indicate that CFTR is also present at the RBC plasma membrane and that CFTR expression is reduced in CF patients [136]. Furthermore, deformation-induced ATP release from RBCs is CFTR-dependent [137]. However, prostacyclin-mediated ATP release is regulated via CFTR, but not via Pnx-1 [7], indicating presence of at least two independent signal cascades within the RBCs.

The Pnx-1 channel builds a pore by oligomerization of 6 equally structured subunits [138]. It has been shown that the channel is expressed ubiquitously in human tissues like brain, heart, endothelium or RBCs [139]. Pnx-1 is activated via shear stress [140], caspase cleavage [141] or membrane depolarization [140]. Moreover, it has been proposed that Pnx-1 inhibition is controlled via negative feedback of ATP release [142] or pharmacological inhibition by probenecid and carbenoxolone [143-145]. Furthermore, ATP release from RBCs induced by hypoxia [7], shear stress and hypotonic stress [145] is Pnx-1-dependent.

Until today, the exact molecular mechanisms of ATP release from RBCs have not been fully understood and intracellular signaling mechanisms of ATP release remain to be investigated. In detail, it is unknown whether PDE and cGMP

signaling is involved in the regulation of ATP release. Furthermore, the involved transport channels have not been identified in detail so far.

1.1.4 Regulation of PS exposure in RBCs

RBCs have a unique membrane composition consisting of cholesterol and phospholipids (PLs) and an anchored elastic cytoskeleton [146, 147]. The cholesterol is evenly distributed in the inner and outer side of the plasma membrane. In contrast, the main phospholipids like PS, phosphatidylcholine, phosphatidylethanolamine and sphingomyelin are asymmetrically distributed. In healthy RBCs, PS and PE are mainly present inside of the cell membrane [148, 149]. In case of senescence, cell activation or damage, the PS is exposed to the outer face of the membrane representing a signal for phagocytosis to the surrounding macrophages [150-155]. In this way, RBCs are removed from the blood stream. Regulation of membrane asymmetry is controlled via PL-translocators, which vary in their specificity and regulation mechanisms [156]. PL-translocation is proposed to be controlled via ATP-dependent flippases, which continuously move phospholipids from the outer to the inner side of the membrane [147] and ATP-independent scramblases, which reallocate the PLs randomly from one side to the other. Until today, the exact regulatory mechanisms of the enzyme groups are unknown [157]. However, it was demonstrated that scramblase activity is increased via calcium influx or modifications via protein-SH groups or oxidation [157-160]. Furthermore, it was shown that also flippase activity is controlled via sulfhydryl modifications resulting in a decrease of enzyme activity [159, 161]. However, there is a disagreement about the existence of scramblases and flippases in RBCs [147] and scramblase is the only enzyme that has been characterized so far [162].

Possible intracellular signaling mechanisms concerning the control of RBC death have been focused in the past decades. Since RBCs lack mitochondria and nucleus, differently cell death mechanisms have been proposed compared to other cell types. PS exposure is induced by oxidative stress [163], glucose depletion and calcium ionophore (Ca-I) treatment [164] via uptake of Ca^{2+}_i [164] and activation of several calcium/cation channels [165, 166]. Furthermore, Ca^{2+}_i -

uptake results in scramblase activation [167-169] and/or flippase inhibition [170] and might lead to enhancement of PS exposure at the RBC surface and RBC removal from the blood stream. Ca^{2+}_i increase is also followed by activation of calcium activated potassium channels and accompanied by cell shrinkage [171]. Loss of membrane symmetry is found in RBCs from patients with several clinical disorders like diabetes [163], heart failure [172] or hemolytic anemia [173]. Furthermore, it was demonstrated that application of NO donors and stable cGMP derivate blunt the increase of PS exposure evoked by Ca-I [164]. In detail, it was shown that application of NO donor sodium nitroprusside (SNP) from 1 nM to 1000 nM significantly decreases PS exposure in presence of Ca-I treatment and that application of 1 mM dibutyryl-cGMP (db-cGMP) has the same effect [164]. However, it remains to be investigated whether sGC signaling plays a role in the regulation of membrane symmetry in RBCs.

1.1.5 Rheological properties of RBCs

Blood is physically defined as a "non-Newtonian, shear-thinning fluid" [174], in which viscosity decreases by accelerating shear rates in a non-linear manner. The characteristics of blood viscosity are influenced by RBC deformability and aggregation [13-15]. Therefore, deformability is the factor dominantly influencing viscosity at high shear rates and aggregation at low shear rates [175].

Deformability of RBCs is defined as their ability to change their shape, when they are exposed to high shear forces, from their biconcave form to a ellipsoidal structure [14]. These alterations of RBC shape results in a decrease of blood viscosity [175] and thus make it a key regulator of blood rheology. Deformability of RBCs is mainly allowed by the structure of their unique cytoskeleton, which enables RBCs to be highly flexible [176]. Besides their ability to deform in response of high shear situations, RBCs are able to aggregate in situations of low shear forces or stasis. In these conditions, RBCs discs tend to form linear aggregates, commonly known as "rouleaux formation" [177, 178]. The aggregates contribute to an increase of blood viscosity due to increased particle size and flow resistance [175]. It was demonstrated that regulation of aggregation is highly dependent on type and concentration of plasma proteins [179]. It was

demonstrated that deformability is affected by disease states like circulatory disorders, diabetes, infections or pulmonary disorders [180, 181]. It was further shown that changes of aggregability are related to myocardial infarction, chronic inflammation, infections or trauma, probably due to increased levels of fibrinogen [182-184]. It has also been proposed that increased RBCs aggregability may be considered as an indicator of bad clinical outcome in angina pectoris [185]. Oxidative stress was shown to influence both deformability and aggregability depending on the source of ROS [186]. In the large vessels, RBCs control blood viscosity [13]. In smaller vessels their deformability has a regulatory impact on flow resistance [187, 188]. In capillaries, the deformability is of high importance due to the fact that RBCs have to pass vessels, which are even smaller than their diameter. Thus, they strongly contribute to blood flow regulation in capillaries [189, 190].

1.2 RBC dysfunction and anemia

The World Health Organization (WHO) describes anemia as a pathological condition, which is defined by decreased concentrations of Hb in the whole blood, being Hb <12 g/dL in females and <13 g/dL in males [191]. As shown in Figure 3 [3], anemia classification can be done accordingly to (A) changes in morphology/size of circulating RBCs, (B) decrease of Hb, or (C) etiopathology, which itself is caused by (1.) defects in erythropoiesis, (2.) increased hemolysis or RBC uptake, (3.) bleeding or (4.) disorders of cell distribution [3, 192]. Taken together, anemia is characterized by loss of RBC integrity resulting in impairment of RBC mediated canonical functions in the body [193]. Interestingly, there is clinical evidence that anemia is a common comorbidity in CVD [194] and associated to cardiovascular complications [194-196]. Specifically, clinical cohort studies with patients with CVD have shown that anemia is related to increased mortality in this disease state [194] even under mild anemic conditions [197, 198]. Moreover, it was shown that anemia is associated to multiple severe complications in CVD, which include thromboembolic events or bleeding complications [199].

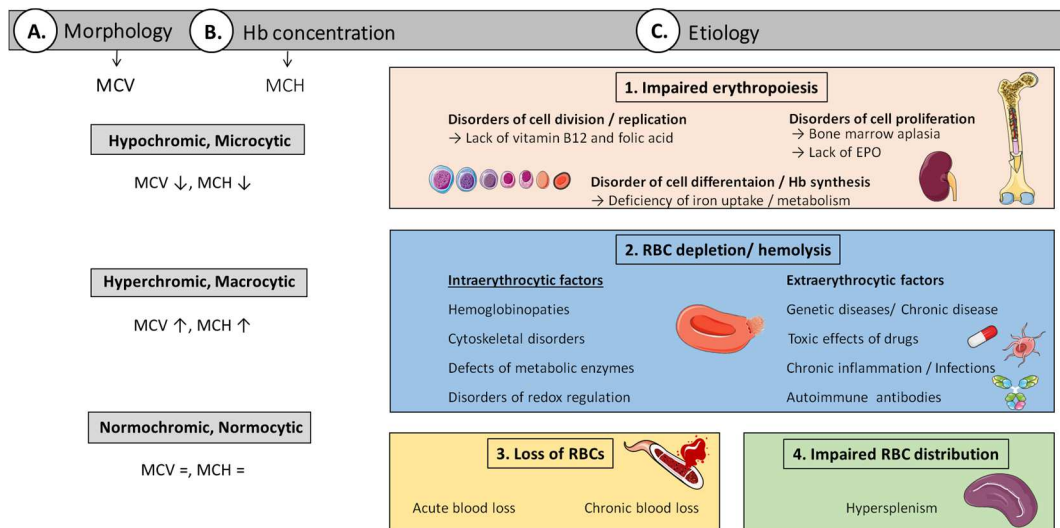


Figure 3: Classification of Anemia [3]

Anemic conditions can be classified according to (A) changes in morphology/size of the circulating RBCs, (B) decrease of Hb, or (C) etiopathology, which itself may be caused by (1.) changes in erythropoiesis, (2.) increased hemolysis, or RBC depletion, (3.) bleeding, or (4.) disorders of cell distribution.

However, the underlying mechanisms of these complications are unclear. As described in §1.1, there is accumulating evidence that RBCs exert additional non-canonical functions and therefore have been proposed to play a role in cardiovascular protection [3]. However, it is unknown whether non-canonical RBC functions are affected in CVD. Since CVD is the most frequent cause of death in the western countries [202], it is of high interest to identify underlying molecular mechanisms and to find new perspectives for therapeutic approaches. The WHO defines CVD as a group of disorders of the heart and blood vessels, which include coronary artery disease (CAD), cerebrovascular disease, peripheral arterial disease and others. [203]. CAD is classified as the manifestation of atherosclerosis in the coronary arteries. Due to flow-limited coronary stenosis, it results in coronary insufficiency and to an impairment of O₂ supply of the heart. The most abundant manifestation of myocardial ischemia are angina pectoris (40%), acute coronary syndrome (ACS; 50%) and sudden heart death (10%). In the clinical practice, ACS is defined as the event of unstable pectoris, acute myocardial infarction or sudden heart death. These are categorized due to electrocardiogram -changes in non ST-segment elevation myocardial infarction (NSTEMI) and ST-segment elevation myocardial infarction (STEMI) [202].

2 Aim of the work

Beside the role of RBCs as transporter of O₂ and nutrients to the tissues, there is accumulating evidence that RBCs may exert non-canonical functions. RBCs were proposed to participate to NO metabolism and to release of ATP and thereby may contribute to regulate vascular tone or cardioprotection. In addition, RBCs were shown to control their own half-life by exposing PS on their surface, which is recognized by macrophages as a “find me signal” for old/damaged erythrocytes in the spleen. The mechanisms underpinning these non-canonical functions of RBCs are not fully understood so far.

This work is based on the hypothesis that non-canonical functions of RBCs may be affected by CVD, and/or might contribute to its outcome.

Therefore, the main aim of the study was to characterize non-canonical RBC functions in healthy RBCs and in RBCs from patients with CAD and chronic kidney disease (CKD). The main goals of the study were to analyze pathways regulating (1.) ATP release and (2.) PS exposure of RBCs, as well as (3.) to characterize non-canonical RBC functions in RBCs taken from patients with CAD or CKD as compared to age-matched controls (Figure 4).

Specifically:

- (1.) Previous data indicate that sGC/cGMP signaling might be involved in the regulation of ATP release from RBCs. Furthermore, the Pnx-1 and CFTR channels have been proposed to be involved in ATP export from RBCs. Here, the role of cGMP signaling and PDE inhibition in control of ATP release, and the involvement of Pnx-1 and CFTR in ATP release induced by hypotonic stress will be investigated.

(2.) There is evidence that the NO and cGMP pathway are involved in the regulation of membrane symmetry and PS exposure. Therefore, the present study will investigate whether sGC activation by NO is involved in the control of PS exposure from RBCs.

(3.) Anemia has been described to be associated to increased mortality in patients with CAD and CKD. However, it is unknown whether non-canonical RBC functions affected by CVD. Therefore, the present study will analyze whether selected RBC functional properties including NO metabolism, changes in redox state and maintenance of membrane symmetry (PS exposure), RBC deformability and aggregability are changed in RBC from patients with CAD, ACS and CKD as compared to age-matched controls.

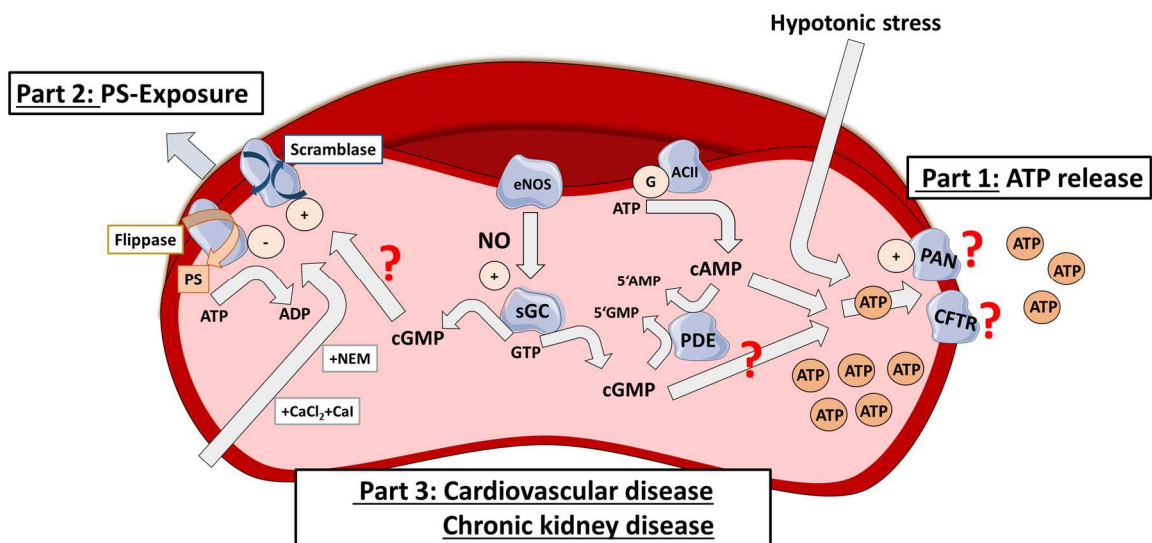


Figure 4: Aims and goals of the study

3 Material and methods

3.1 Material

Table 1: Instruments and consumables

Applicance/Consumable	Purchased by
TH 15 Incubator	Edmund Bühler
Autoclave DX-65	Systemec
Rotina 38 R	Hettich
Ritina 380 R	Hettich
Mikro 200R	Hettich
Micro Star 17R	VWR
FluoStar Omega	BMG Labtech
ImageQuant LAS4000	GE healthcare
Eppendorf tubes	Starstedt
Pipettes with tips	Eppendorf
Corning® 96 well plates, UV-transparent	#CLS3635, Sigma
96 well plate, F-bottom, white	#655083, Greiner Bio one
96 well plate, ELISA, U-bottom, transparent	#650001, Greiner Bio one
Omega Software, 2007-2012	BMG, Labtech
Omega data Analysis Software V2.41	BMG Labtech
FACS Verse	BD
Magnetic particle concentrator	#12001d, Invitrogen
Eppendorf tube rotator	Neolab
Shaker KL-2	Edmund Bühler
Hamilton syringe	VWR
Pipetboy	lbs Integra
XCell II™ Blot Module	Invitrogen
XCell SureLock™ Mini-Cell Electrophoresis System	Invitrogen
Milli-Q Millipore	Reference
Cell culture flasks (250ml) with filter	Greiner Bio one
Waterbath VWB 12	VWR
Cleanbench CA/REV 4	Biohazard
CO ₂ incubator Hera Cell240	Heraeus
DFC450 microscope	Leica
Neubauer counting chamber	Roth

Table 2: Software

Software	Purchased by
FluoStar Omega	BMG Labtech
ImageQuant LAS4000 Software Version1.2	GE healthcare
Omega Software, 2007-2012	BMG, Labtech
Omega data Analysis Software V2.41	BMG Labtech
FlowJo V10	FlowJo
GraphPadPrism 6.0.1	GraphPad, Inc.
FACS Suite V1.0.53841, 2013	BD
SPSS Statistica V23.0.0.0	IBM
Leica Application Suite V4.3.0	Leica Microsystems
NIS Elements V4.30.02	Laboratory Imaging

Table 3: Chemicals, buffers, kits and antibodies part 1

Article	Purchased by	Article no.
3-8% Tris-Acetate (TA) Gel	Invitrogen	EA0375Box
8-(4-chlorophenylthio) –cAMP (8-CPT-cAMP)	Sigma	C3912
8-CPT-cGMP	Sigma	C5438
Albumin Fraction V	Roth	8076.3
Annexin V-PE	BD	556422
Antioxidant	Invitrogen	NP0005
ATP Determination kit	Invitrogen	A22066
BAY-41	Bayer AG	-
CaCl ₂	Sigma	C7902
CaCl ₂ x2H ₂ O	Sigma	C3881
Ca-I	Sigma	C7522
Carbogen	Linde	-
4-amino-5-methylamino-2',7'-difluorofluorescein diacetate (DAF-FM-DA)	Invitrogen	D23844
DC protein assay (Lowry assay)	Biorad	5000116
Diethylamine NONOate diethylammonium salt (DEA/NO)	Sigma	D5431

Table 4: Chemicals, buffers, kits and antibodies part 2

Article	Purchased by	Article no.
DMEM medium	Invitrogen	A14430-01
Dimethylsulfoxid (DMSO)	Roth	5179.1
Dynabeads® Antibody Coupling Kit	Invitrogen	14311D
Endothelial cell medium + supplement	Promocell	c-22010
Ethanol 70%	VWR	20905296
FACS clean	BD	340345
FACS flow	BD	342003
Fetal calf serum (FCS)	Sigma	12133C
Glucose	Sigma	G5767
Glutathione Fluorescent Detection Kit, 5 Plate	Arbor	K006-F5
2',7'-dichlordihydrofluorescein-diacetat (DCF)	Invitrogen	D-399
H ₂ O ₂ 30% wt	Sigma	216763
Acetic acid	Roth	3738.4
Diethylenetriaminepentaacetic acid (DTPA)	Sigma	D1133
Hanks balanced salt solution (HBSS) + CaCl ₂ +MgCl ₂ , no phenolrot (HBSS (+))	Invitrogen	14025-100
HBSS without (w/o) CaCl ₂ +MgCl ₂ , no phenolrot (HBSS (-))	Invitrogen	14175095
HCl	VWR	1.09911.0001
Heparin 25000 I.E	Ratiopharm	PZN3029843
4-(2-hydroxyethyl)-1-piperazineethanesulfonic acid (Hepes)	Sigma	H3375
Hepes solution for cell culture	Invitrogen	15630-080
HPLC-water	VWR	83.650.320
human umbilical vein endothelial cell (HUVEC) vials c-pooled (lot.399Z014)	Promocell	c-12203
IGEPAL	Sigma	I3201-50m
J ₂	Sigma	I3380
K ₃ Fe(CN) ₆	Roth	P745.1
KCl	Sigma	P9333
KH ₂ PO ₄	Sigma	1551139
KJ	Merck	1.050.430.25
Magic Marker	Invitrogen	LC5602
Methanol	VWR	83.638.320

Table 5: Chemicals, buffers, kits and antibodies part 3

Article	Purchased by	Article no.
MgSO ₄ ·7H ₂ O	Sigma	230391
NaCl	Sigma	s7653
NaHCO ₃	VWR	144-55-8
NaOH	Sigma	s8045
NaOH	Sigma	s8045-1kg
<i>N</i> -ethylmaleimide (NEM)	Sigma	E3876
NP40	Sigma	74385
NuPage LDS Sample Buffer (4x)	Invitrogen	NP0007
ODQ	VWR	ACRO328800100
Phosphate buffer saline (PBS (+))	Sigma	D8537
PBS (-)	Sigma	D8662
Penicillin/Strepomycin	Invitrogen	15140122
Ponceau S solution	Sigma	1441194
Reagent A	Biorad	500-0113
Reagent S	Biorad	500-0115
Reagent B	Biorad	500-0114
Sodium dodecyl sulfate (SDS, 10%-solution)	Aglichem	A06760599
Sildenafil citrate salt (Sil)	Sigma	PZ-0003
Sodium deoxycholate	Sigma	30970
Sample reducing agent (SRA) (10X)	Invitrogen	NP0004
SuperSignal™ West Femto Maximum Sensitivity Substrate	Invitrogen	34095
Tris buffered saline with Tween-20 (TBS-T), (10X)	Biorad	170-6435
Thiol Tracker® (TT®)	Invitrogen	T10095
Toluol	Roth	7346.2
Transfer buffer (20X)	Invitrogen	NP006-1
TA-Buffer (20X)	Invitrogen	LA0041
Trypsin/EDTA	Invitrogen	R-001-100
Tween-20	Sigma	P9416

Animals

Male 12-20 weeks old C57Bl/6J mice were used as wild type (WT) control mice (Janvier Labs, Saint-Berthevin, France). For CFTR-KO experiments, mouse blood was freshly delivered from Bayer AG, Wuppertal. The used CFTR^{tm1UNC} knock out mice (CFTR KO) had C57Bl/6J background and were purchased from Jackson Laboratory, Maine, U.S.A. Animal care was in accordance with the institutional guidelines. All experiments were performed according to the criteria outlined in the NHLBI Animal Care and Use Committee and the LANUV Nordrhein-Westfalen (no. 84-02.04.2013.A228).

Human blood donors

For analysis of healthy human RBCs, blood was obtained from the antecubital vein of healthy individuals (25-33 years). The study was approved by the local ethics committee (no. 3857) and performed in accordance to the Declaration of Helsinki and the guidelines of good clinical practice (GCP). The study has been performed according to the legal data protection requirements. Written informed consent was obtained from all subjects taking part in the study.

CVD study

The study was led by Prof. Dr. med. M. Kelm, head of the cardiology department and coordinated by Prof. Dr. rer. nat. Dr. M. M. Cortese-Krott. The study was approved by the local ethics committee (no. 4460) and performed in accordance to the Declaration of Helsinki and the guidelines of GCP. The study has been performed according to the legal data protection requirements. Written informed consent was obtained from all subjects taking part in the study. The study was performed together with Dr. med. G. Wolff and the medical students Thirumakal Manokaran, Claudio Parco and Jonathan Schmidt.

CKD study

The study was approved by the Ethics Committee of the University of Chieti and was performed in accordance to the Declaration of Helsinki. Written informed consent was obtained from all subjects taking part in the study [204].

3.2 Methods

3.2.1 RBC purification

3.2.1.1 Human samples

Human blood was collected in heparin tubes. Whole blood was centrifuged at 800 x g for 10 minutes at room temperature (RT) and buffy coat and plasma were removed. RBC pellets were washed three times with the corresponding buffer of the specific experiment (as described in §3.2.2.1 for ATP determination, §3.2.3.1 for PS exposure and §3.2.5.1 for western blot) at 300 x g at RT for 10 minutes. In the patient study, heparinized whole blood was used for flow cytometric- and (Laser-assisted Optical Rotational Cell Analyzer (Lorca) measurements.

3.2.1.2 Murine samples

Murine blood was collected in heparinized tubes. Mice were anesthetized by injection of ketamine (100 mg/kg bodyweight) and xylazin (10 mg/kg bodyweight) and blood was taken from the heart. Murine blood was centrifuged at 3000 x g for 3 minutes at RT, and plasma and buffy coat was removed. RBC pellets were washed three times with the corresponding buffer described in §3.2.2.1 at 300 x g at RT for 10 minutes.

3.2.2 Analysis of ATP signaling from RBCs

3.2.2.1 ATP determination

After RBC separation as described in §3.5.1 and §3.5.2, cells were diluted either in Krebs-Henseleit (KH buffer) or HBSS (+) + 0.5% bovine serum albumin (BSA, Table 6 and 7) in a total volume of 150 µl to the corresponding hematocrit (Hct) as described in §4.1. Afterwards, suspensions were incubated with the used stimulators and inhibitors from Table 8. Hypotonic stress was induced by incubation of RBC suspension with 1:2 diluted buffer (in millipore water) for 30 seconds.

Table 6: Formulation of HBSS

Components	Concentration (mM)
CaCl ₂ , anhydrous	1.26
MgCl ₂	0.49
MgSO ₄	0.41
KCl	5.33
KH ₂ PO ₄	0.44
Na ₂ CO ₃	4.17
NaCl	137.93
NaHCO ₃	0.34
Glucose	5.56

KH buffer was prepared as followed and flushed with carbogen for 30 minutes:

Table 7: Formulation of KH buffer

Compound	Concentration (mM)
KH ₂ PO ₄	1.2
KCl	4.7
MgSO ₄ x7H ₂ O	1.2
CaCl ₂ x2H ₂ O	1.25
NaCl	118
NaHCO ₃	25
Glucose	11

Table 8: Stimulators and inhibitors used in ATP determination assay

Substance	Concentration/diluent
DEA/NO	0,5-1000 μM/ 10 mM NaOH
BAY-41	10 μM/ DMSO (<0.1%)
8-CPT-cGMP	1-1000 μM/ millipore water
Sil	100μM/ millipore water
Carbenoxolone	100 μM/ millipore water
Probenecid	4 mM/ KH buffer

The ATP assay is based on the reaction of ATP serving as a substrate for luciferase to convert D-luciferin into oxyluciferin and light. The emitted light of wavelength of 560 nm was measured via luminescence (Figure 5).

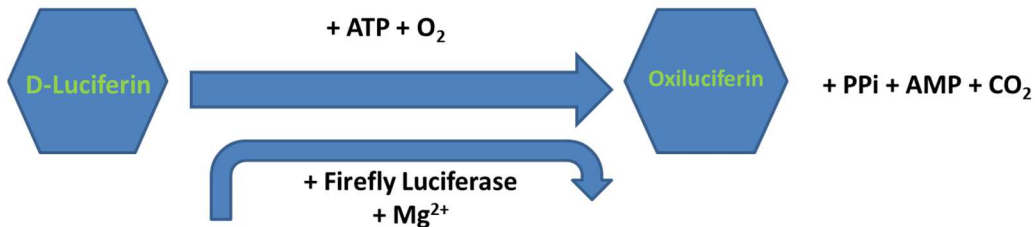


Figure 5: Measurement principle of ATP assay

The assay is based on the enzymatic reaction of firefly luciferase, which converts D-luciferin to oxyluciferin and light in presence of ATP and other cofactors. The emitted light was detected via luminescence.

After incubation with the stimulators and inhibitors, RBC suspensions were centrifuged at 300 x g at RT for 5 minutes and the supernatant was transferred to a new tube. Luciferin-Luciferase assay was measured via ATP Determination kit as described in the manufacturer's description (#A22066, Life Technologies) and a standard curve from 5 nM to 1000 nM was applied in 96 well plates.

3.2.2.2 Hb detection

RBC pellet was lysed in 0.1% SDS/ 0.1 M NaOH and protein concentration was measured by Lowry assay (#5000116, Biorad) following the manufacturer's instructions. Hb content from the supernatant was determined by taking a UV-spectrum from 200-600 nm and absorbance at wavelengths of 416 and 540 nm were analyzed.

3.2.3 Flow cytometric analysis of RBCs

3.2.3.1 Detection of PS exposure

To analyze whether sGC signaling might play a key role in the regulation of membrane symmetry in RBCs, PS exposure was analyzed by flow cytometry. RBC pellets were diluted 1:1000 in the PS buffer (Table 9) and compounds were added depended on the experimental purpose (Table 10). The suspension was incubated for 1 hour at 37 °C. Afterwards, it was centrifuged at 300 x g for 10

minutes at 4°C and supernatant was discarded. The pellet was washed twice in the buffer containing 0.1% BSA. The pellet was resuspended 1:1000 in the buffer in presence of 100 µM calcium. 100 µl of the RBC suspension were transferred into FACS tubes and incubated 1:20 with Annexin-V-PE (#556422, BD) for 30 minutes in the dark. Samples were centrifuged at 300 x g for 10 minutes and buffer was removed. Pellets were resuspended in 500 µl PBS (+) and analyzed by FACS Verse (FACS Suite Software) and FlowJo.

Table 9: Formulation of PS buffer

Compound	Concentration (Millipore)
NaCl	55 mM
KCl	90 mM
Glucose	0,1%
Hepes	10 mM
add to pH=7,4 with NaOH	

Table 10: Chemicals for PS analysis

Compound	Endconcentration/diluent
NEM	10 mM/ Millipore water
Cal	4 µM/ DMSO
CaCl ₂	1 mM/ Millipore water
DEA/NO	0,5-1000 µM/ 10 mM NaOH
BAY-41	10 µM/ DMSO
8-CPT-cGMP	1-1000 µM/ Millipore water
ODQ	5 µM/ DMSO

3.2.3.2 Detection of NO-, ROS- and reduced thiols-levels

Heparinized whole blood was diluted 1:500 in PBS (+). Tubes were labeled as described in Figure 6 and 500 µl of the suspension was added to each tube. 3 mM nω-nitro-l-arginine methyl ester hydrochloride (L-NAME) was added in the provided tubes and all tubes were incubated for 30 minutes at 37°C.

Afterwards, the fluorochromes DAF-FM-DA (NO-level detection), DCF (ROS detection) and ThiolTracker® (TT®, reduced thiol detection) were diluted as

indicated in Table 11 and added to the blood suspensions. All tubes were incubated for another 30 minutes in the dark at RT. The tubes were centrifuged at 300 x g, 10 minutes at 4°C and buffer was removed. 500 µl PBS (+) were added to the tubes. H₂O₂ was diluted as indicated before and added to the tubes. All tubes were centrifuged in the dark for 15 minutes.

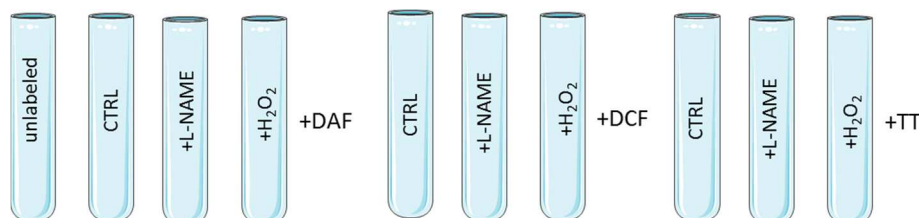


Figure 6: Treatments for flow cytometry of DAF-FM-DA, DCF and TT®

Table 11: Fluorochromes used in flow cytometric analysis

Compound	Concentration
DAF-FM-DA (NO detection)	10 µM
DCF (ROS detection)	6.67 µM
TT® (reduced thiol detection)	6.67 µM
Annexin V-PE (PS exposure)	5 µl of antibody in 100 µl suspension
H ₂ O ₂ (30 %)	3 (v/v%)

Afterwards, 500 µl of buffer was added to all tubes and analyzed via FACS verse (FACS Suite software) and FlowJo. Additionally, Annexin-V-PE detection was performed by using 100 µl of the blood suspension from the beginning. 5 µl of Annexin-V-PE (#556422, BD) was pipetted, incubated for 30 minutes in the dark and then centrifuged at 300 x g for 10 minutes at 4°C. The buffer was removed and 500 µl PBS (+) was added to the tubes. The samples were analyzed via FACS verse (FACS Suite software) and FlowJo.

3.2.4 Cell culture experiments

3.2.4.1 Cultivation of HUVECs

HUVECs of identical lot number were purchased by Promocell. The HUVEC vial was thawed in water bath and cultivated over night (o.n.) in endothelial cell

medium + supplements + 1% penicillin/streptomycin in a CO₂ incubator (37°C, 5% CO₂). The next day, medium was changed and cells were incubated for another 2 days. At the 4th day, cells were detached with Trypsin/EDTA. Reaction was stopped by adding DMEM medium + 2.5 % FCS followed by centrifugation at 500 x g at RT for 3 minutes. The supernatant was discarded and cell pellets were lysed as described in 3.2.4.2.

3.2.4.2 Cell lysis

HUVEC pellets were lysed in radioimmunoprecipitation assay (RIPA) buffer (Table 12) + 5% proteinase Inhibitor (#78445, Invitrogen) and alternately vortexed and sonicated for 30 seconds. This step was repeated three times. Samples were centrifuged at 13000 x g at 4°C for 10 minutes and supernatant was transferred to a new tube. Protein concentration of the lysate was determined by Lowry assay as described in 3.2.4.3

Table 12: Formulation of RIPA buffer

Compound	Concentration in PBS (+)
NP40	1 Vol.%
Sodium deoxycholate	1.2 mM
SDS (10%)	1 Vol.%

3.2.4.3 Protein determination

Protein concentration of lysates was determined by Lowry assay following the manufacturer's instructions (Biorad protein assay). A standard curve from 0.2 mg/ml to 2 mg/ml BSA was prepared. 5 µl of standards and samples were pipetted to a 96 well plate in duplicates in presence of the detection solutions of the kit. The plate was incubated for 15 minutes in the dark and analyzed photometrically at 740 nm with OMEGA software. Protein concentration was determined using Omega Mars software. 20 µg/µl aliquots of HUVEC lysates were diluted in 1 X lithium dodecyl sulfate (LDS) and frozen at -20°C until use.

3.2.5 Analysis of red cell eNOS expression

3.2.5.1 Cell lysis

RBC pellets were washed three times in PBS (+) as described in §3.2.1.1. 500 µl aliquots of the pellets were frozen in liquid nitrogen and stored in a -80 °C freezer. For analysis, samples were thawed by adding 2 ml H₂O including protease and phosphatase inhibitor (#5892953001, cOmplete Ultra Tablets, EDTA free, Roche) and 500 µl toluol to the samples. Samples were vortexed and centrifuged at 4000 x g 10 minutes at 4°C and the middle phase was transferred to a new eppendorf tube. The centrifugation step was repeated twice and the lysate was transferred to a new tube each time. Afterwards, the centrifugation step was repeated at 13000 x g. Finally, the protein content of the lysate was detected using Lowry assay. As protein standard, BSA was diluted in millipore water from concentrations of 0 mg/l to 2 mg/l. A standard curve from was applied in each experiment.

3.2.5.2 Protein determination

RBC lysates were diluted 1:50, 1:100 and 1:200 in millipore water. Protein content was analyzed by Lowry assay as described in 3.2.4.3. RBC lysates were immunoprecipitated using M-270 dynabeads coupled to an eNOS antibody (#624086, BD) as described in the following chapter.

3.2.5.3 Bead coupling and immunoprecipitation of red cell eNOS

For immunoprecipitation of red cell eNOS, magnetic beads were coupled to an eNOS antibody (#624086, BD). Therefore, dynabeads antibody coupling kit (#14311D, Invitrogen) was used following the manufacturer's instructions. 50 µl of the eNOS-antibody (1 mg/ml) and 10 mg of M-270 dynabeads were used in each tube. Coupled beads were stored at 4°C until usage.

For immunoprecipitation, PBS (10X), 70 µl bead-solution and 80 mg RBC lysate (from 3.2.5.1) were mixed and incubated under rotation o.n. at 4°C. The next day, beads were washed 4 times with 200 µl PBS (-). Finally, 22.5 µl LDS (1X) was added to the beads and samples were stored at -20°C until use.

3.2.5.4 Detection of red cell eNOS expression by western blot

A western blot modul was used by filling the outer chamber with 1X TA-buffer and the inner chamber with 1X TA-buffer + 0.1% Antioxidant. The measurement was performed using a 3-8 % TA-gel. Prepared bead-samples were thawed and 2.5 µl SRA (10X) was added. Tubes were incubated for 10 minutes at 70 °C and kept on ice. 10 µl Magic Marker (#LC5602, Invitrogen) and 25 µl of sample-solution were added to the pockets. As positive control, 5 µg of HUVECs stock lysate was used. Therefore 5µl of the stock solution were mixed with 13 µl LDS (1X) + 2.5 µl SRA (10X). SDS PAGE was run at 150 V for 1 hour.

Afterwards, the gel was removed from the blot system and protein was transferred on a methanol activated PVDR membrane. 3 wet whatman papers (in 1 X Transfer buffer + 1% MeOH) were placed to each side and transferred to the blot modul. The blot was run for one hour at 30 V. Afterwards, PVDR membrane was incubated for 5 minutes in Ponceau S and subsequently washed in millipore water until membrane was white again. The membrane was blocked for 1 hour at the shaker with 5% BSA in 1X TBS + 0.1% Tween-20 (TBS-T). Afterwards, blocking solution was removed and the membrane was incubated with eNOS antibody (#624086, BD) 1:250 in 5% BSA/TBS-T o.n. at 4°C. The next day, the membrane was washed three times for 10 minutes in 1X TBS-T and incubated with HRP goat anti-mouse 1:5000 in 5% BSA/TBS-T for one hour at R.T. Afterwards, membrane was washed three times for 10 minutes in TBS-T and analyzed with the West Femto Maximum Sensitivity Substrate kit (#34095, Invitrogen) according to the manufacturer's instructions. Detection was performed via ImageQuant LAS4000 and ImageJ.

3.2.6 RBC NO₂⁻ detection via chemiluminescence

50 µl RBC from patients with ACS, CAD or healthy age-matched controls was diluted in 333 µl preservation solution and samples were frozen at -80°C until usage. Additionally, an aliquot of preservation solution was frozen each day. Preservation solution was mixed as described in Table 13.

Table 13: Formulation of preservation solution

Compound	concentration
K ₃ Fe(CN) ₆	10 mM
NEM	20 mM
DTPA	10 μM
IGEPAL	1 (vol. %)
dest. water	ad. 20 ml

The samples were thawed at RT and diluted 1:2 in methanol. Afterwards, samples were centrifuged at 14000 x g for 10 minutes at 4°C. The supernatant was transferred for the measurement of NO₂⁻ levels. A NO₂⁻ standard curve was applied for each experiment from concentrations of 50 nM to 200 nM in PBS. A reduction solution was prepared in which the samples were injected during the experiment (Table 14). The reduction solution reduces NO₂⁻ to NO, which further reacts with O₃ to NO₂ and light. This light signal was analyzed by the chemiluminescence detector (CLD) representative for NO₂⁻ level of the RBC samples.

Table 14: Formulation of reduction solution

Compound	Amount (g,ml)
KJ	1.62 g
J ₂	0.57 g
Acetic acid	200 ml
HPLC-water	15 ml

The water bath was set at 60 °C and cooling bath at 4°C. The computer was and the NO analyzer was turned on. Afterwards, helium gas was turned on. The reaction vessel was cleaned with (1.) water then (2.) isopropanol and (3.) water. The glass container was cleaned the same way and filled with 1 M NaOH until the glass frit touched the solution. The solution was cooled on ice. The program Chromstar was started and set on: (1.) Acquisition: width 500 ms, run time 35 min and (2.) Integration: noise 50, threshold 500 mV, skim ratio 3.

The reaction vessel was filled with 40 ml of reduction solution with a syringe. Then, reaction vessel and NaOH-vessel were connected. The pressure measuring pipe was connected to the CLD. After this step, the pressure should be at 0 bars. A standard curve of NO_2^- was measured by adding 100 μl of NO_2^- standard to the system. The samples were measured in triplicates. Afterwards, samples were measured in the same way. After 6 samples, the reduction solution was changed. Data were analyzed via Chromstar software and Microsoft Excel.

3.2.7 Analysis of rheological properties of RBCs

RBCs deform in response to increasing shear stresses [14] and form aggregates in situations of low shear [177, 178]. Deformability and aggregability of RBCs was measured via ektacytometry using the Lorca system.

3.2.7.1 Aggregability measurement

RBC aggregability is analyzed in whole blood as backscattered light of a diode laser inside the inner cycle.

Aggregation of RBCs includes 4 stages:

1. Disaggregation stage
2. Shape-recovery stage (when motor is stopped)
3. Rouleaux formation
4. 3D-aggregate formation

RBC Aggregability is characterized by measurement of a syllectogram (Figure 7). Briefly, the motor of the system is stopped and aggregation behavior is measured by the back scattered light [205]. This is defined by usage of the aggregation index (AI), which is a value between 0 and 100% depending on extend (erythrocyte aggregation amplitude (AMP)) and kinetics ($t_{1/2}$) of the RBC aggregation [184, 206, 207]. For analysis of aggregability, the program was set to aggregation measurement and 1 ml whole blood was added. In Table 15, the program settings are listed.

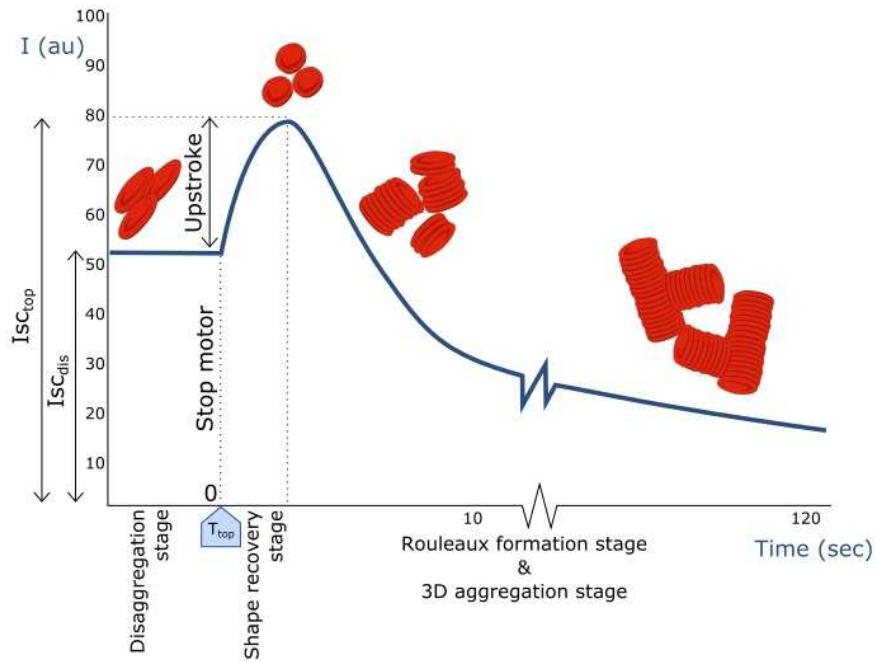


Figure 7: Sylllectogram of RBC aggregability [208]

RBC aggregation consists of 4 stages, which include disaggregation stage, shape-recovery stage (when motor is stopped), rouleaux formation and 3D-aggregate formation.

Table 15: Aggregation settings

Bob radius	15.660
Cup radius	16.020
Bob temperature	37.0
Fill/empty speed (rps)	1.0
Autostart if temperature is stable within (°C)	0.2
..for at least (s)	30
Perform iteration procedure	On
Inermediate disaggregation	On
Samples per shear rate	2.0
Maximum deviation (au)	0.5
Iteration timeout (s)	300
Binary search steps	2.0
Sort results	On
Disaggregation shear rate (1/s)	500
Disaggregation time (s)	3.0

3.2.7.2 Deformability measurement

To measure RBC deformability, increasing shear stresses were applied to a RBC suspension. A laser was led through the RBC suspension and the diffraction pattern was projected on a small screen. RBC deformability was analyzed by calculation of the elongation index (EI, Figure 8) [205]. This factor is defined as: $EI = \frac{A-B}{A+B}$, in which A represents the horizontal and B the vertical axis of the RBC [205].

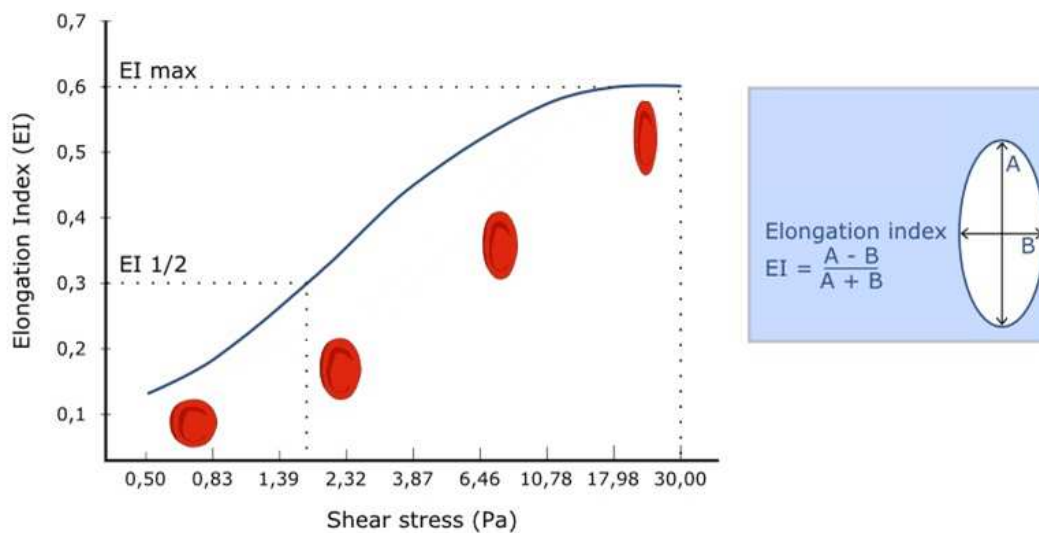


Figure 8: RBC deformability curve [208]

Deformability curve is defined by analysis of RBC shape calculated as EI in response to increasing shear stresses.

For deformability measurement, 25 μ l of whole blood was diluted in 5 ml pre-warmed PVP solution and gently homogenized. The Lorca system was turned on 30 minutes before usage. In the software, deformability curve was chosen and the system was started. 1 ml of the blood suspension was added to the Lorca and the measurement was started when temperature was stable at 37°C. In Table 16, the program settings are listed.

Table 16: Elongation settings

Bob radius	15.660
Cup radius	16.020
Bob temperature	37.0
Default medium viscosity (mPa*s)	dependent on PVP solution
Fill/empty speed (rps)	1.0
Shear stress for camera adjustment	10.0
Logarithmic shear stress axis	On
First shear stress (Pa)	0.3
Last shear stress (Pa)	10.0
Initial image stabilization time (s)	10000
Intermediate image stabilization time (s)	5000
Measuring points on curve	9
Valid determinations per shear stress	50

3.3 Study design: CVD

The present dissertation includes a patient study performed by the Department of Cardiology, Pulmonology and Angiology, Düsseldorf, Germany. The main aim of the study was to investigate, whether red cell eNOS/NO-mediated RBC dysfunctions might play a role in CVD. The study was separated into a main study indicated as case control and a follow up study described as longitudinal study (Figure 9). The main study was a cross-sectional, matched, 3-armed, parallel group design in patients with CAD, ACS and age-matched healthy controls. The follow-up study was a controlled, longitudinal, observational design in the cohort of ACS patients 1 day and 90 days after treatment of ACS. Male and female patients (aged 50-70 years) were recruited in the Department of Cardiology, Pulmonology and Angiology, Düsseldorf. The selection of study population was performed in the clinic via routine clinical parameters (e.g. troponin) as well as by coronary angiography and flow mediated-dilation. Patients with acute

inflammation (C-reactive protein (CRP) >1.0 mg/dl, blood leukocytes > 11000/ μ l), malignancies, or treatments with NOS/NO/sGC affecting drugs were excluded.

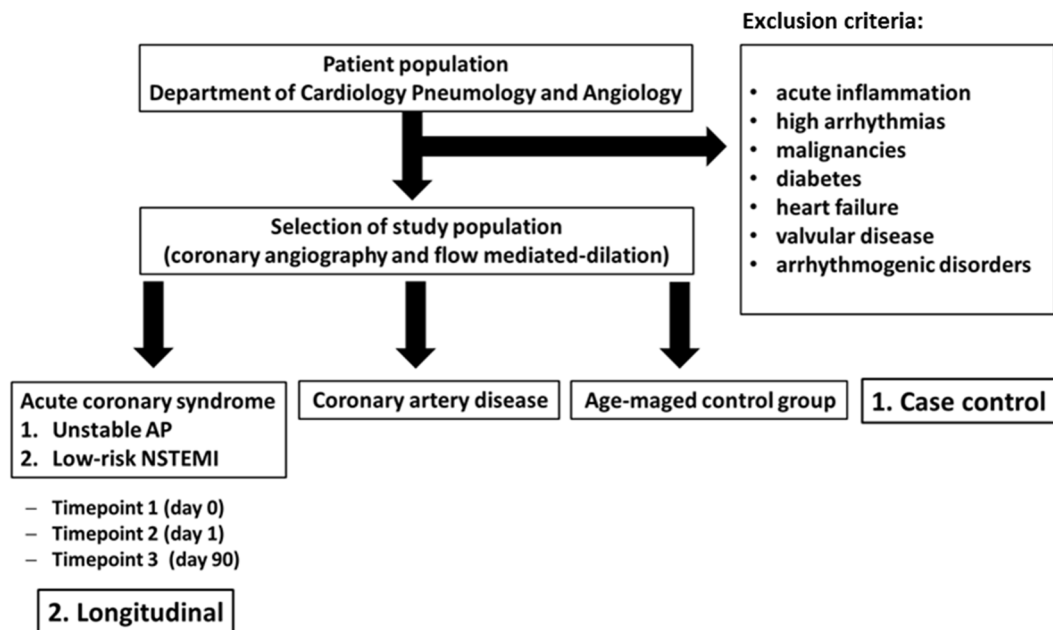


Figure 9: Study design of CAD and ACS study

To investigate, whether red cell eNOS/NO-mediated RBC dysfunctions might play a role in CVD, a patient study with patients from Department of Cardiology, Pulmonology and Angiology in Düsseldorf was performed. These included patients with ACS, CAD and age-matched controls. Exclusion criteria and study-characteristic are mentioned in the figure.

Group-specific inclusion-criteria were:

- Group 1: CAD (n=20)
 - Angiographic confirmed coronary heart disease
 - No ACS for at least 3 months
- Group 2: ACS (n=8)
 - Angiographic confirmed coronary heart disease
 - ACS
 - Instable angina pectoris with significant coronary stenose (troponin -, no significant ST increase) and Low-risk NSTEMI (troponin +, no significant ST increase)
- Group 3: control (n=25)
 - No angiographically confirmed atherosclerosis

Primary endpoint of the study was the analysis of red cell eNOS expression and activity. All other aims and the study protocol are listed in Figure 10. The patients were recruited in the department of Cardiology, Pulmonology and Angiology at the University Hospital in Düsseldorf. The study included biochemical, cell biological measurements as well as hemodynamic and cardiovascular analyses. In the clinic, flow mediated dilation was measured by Dr. med G. Wolff. In the next step, blood of the patients was taken by cubital venial puncture and heparinized [5000IU/ml]. Routine clinical blood parameters were elevated in the University hospital. The analysis of non-canonical functions (red cell eNOS/NO-pathway, membrane functions, NO metabolism) was analyzed in the lab of cardiology. As described in Figure 10, redox-state, levels of NO and PS exposure were measured via flow cytometry and red cell eNOS expression was analyzed via western blot. RBC deformability and aggregability was evaluated by usage of the Lorca system. Moreover, NO_2^- levels were examined by CLD.

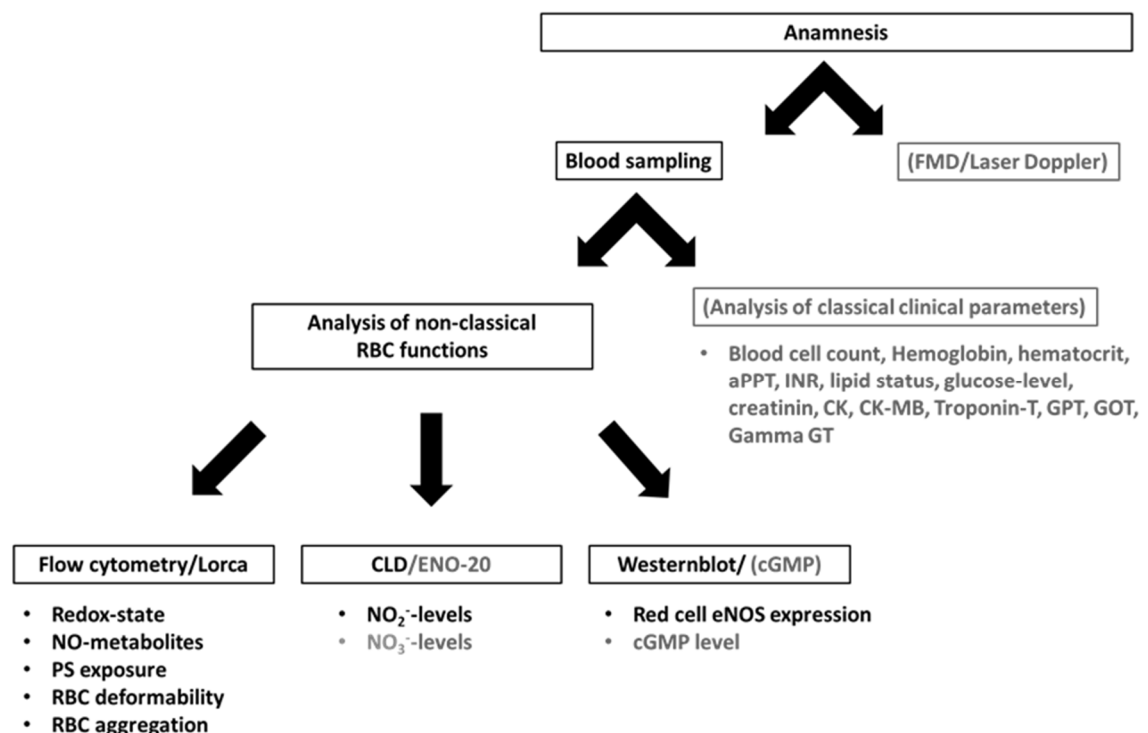


Figure 10: Study protocol of of CAD and ACS study

Parameters analyzed in the study following a defined protocol. These included physiological parameters (laser doppler, flow-mediated dilation (FMD) as well as analysis of biochemical parameters (red cell eNOS expression, NO_2^- -levels, redox-state, deformability...).

3.4 Study design: CKD

A clinical study with patients with CKD was performed by Di Pietro et al. from the Department of medical, oral and biotechnological sciences and the aging research center and translational medicine CeSI-MeT, Chieti, Italy. The general aim of the study was to evaluate, whether red cell eNOS/NO signaling plays a role in CKD.

In this study, red cell eNOS expression was analyzed in the laboratory of cardiology in Düsseldorf. All other parameters (routine clinical parameters, NO/cGMP levels, red cell eNOS Ser1177 phosphorylation level, multidrug resistance-associated protein 4 (MRP4) ATPase activity) were performed in the other departments (see publication Di Pietro et al.) [204].

The study included patients suffering from CKD and age- and gender-matched controls. The study population (age 18-75) was recruited at the dialysis center of the University Hospital of Chieti.

Exclusion criteria were: diabetes mellitus, uncontrolled hypertension, active infections, malignant or inflammatory disease, blood transfusion over the past 3 months, iron and folic acid deficiency, use of drugs that might interfere with erythropoiesis. Furthermore, the usage of NO pathway influencing drugs was avoided. Other exclusion criteria for the healthy controls were medications, abnormalities on routine physical examination, standard laboratory tests, electrocardiography (ECG), or chest x-ray [204].

3.5 Statistics

For statistical analysis GraphPad6 and SPSS V23 were used. Data are expressed as mean \pm standard error of the mean (SEM).

Multiple comparisons were calculated using one-way ANOVA or Kruskal-Wallis followed by an appropriate post hoc test as described in the figure legends in chapter 4. For comparison of two groups, paired or unpaired Student's T-test was performed. Outliers analysis was performed graphically by box & whiskers plots according to Tukey.

4 Results

4.1 Part 1: Measurement of ATP release from RBCs

4.1.1 Assay Optimization

4.1.1.1 Time-dependent decrease of ATP levels from RBCs

To analyze the concentrations of ATP in the supernatant of RBCs, the luciferin-luciferase assay was used. Briefly, ATP is used as a substrate for luciferase to convert D-luciferin into oxyluciferin and light, which was measured via luminescence. For verifying the stability of the assay, potentially interfering parameters were analyzed first. Murine RBCs were diluted 1:4 in KH buffer and incubated at RT for different time points to analyze steady state concentrations of ATP from the RBCs (Figure 11 (A)). After incubation, suspensions were centrifuged at 300 x g for 5 minutes at RT and the supernatant was analyzed for the presence of ATP.

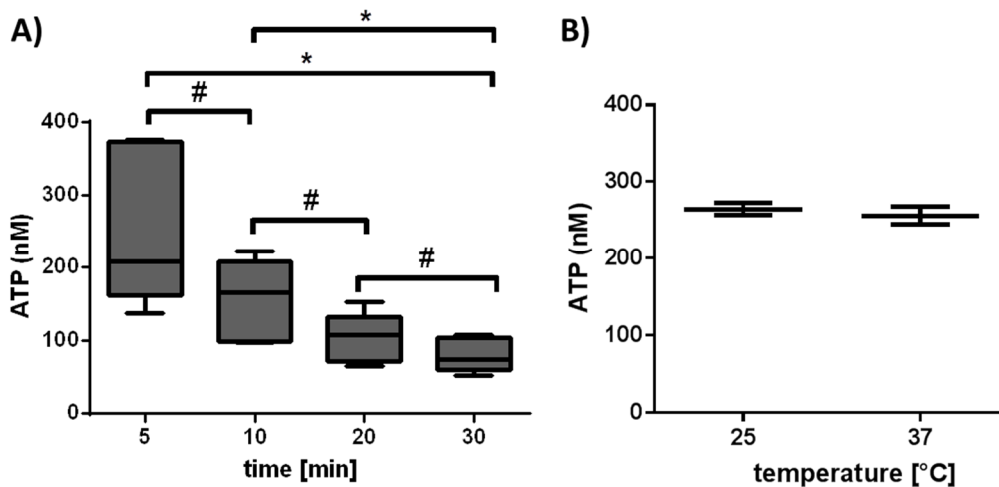


Figure 11: Basal ATP levels are decreasing with time in RBC suspensions

(A) Time-dependent decrease of ATP levels from RBC suspensions. RBCs of 25% Hct in total volume of 150 μ l were incubated at RT for different time points. Samples were analyzed via luciferin-luciferase assay, data are expressed as median in a Tukey distribution plot, $n=5$, paired one-way ANOVA against each treatment: post-hoc test Tukey (*) and paired T-test (#), #, * $p \leq 0.05$. (B) No differences of ATP release from RBCs after 20 minutes incubation time at 25°C (RT) and 37°C. RBCs of 25% Hct were incubated in a total volume of 500 μ l. After 20 minutes incubation time, samples were analyzed via luciferin-luciferase assay, data are expressed as median in a Tukey distribution plot, $n=2$.

Figure 11 (A) shows that levels of basal ATP are decreasing over time. In detail, the graph presents that the levels of ATP are already decreasing significantly within 5 (paired T-test between 5 minutes and 10 minutes) and 10 minutes (paired T-test 10 minutes against 20 minutes) of incubation. Furthermore, significant decrease of extracellular ATP levels was detected after 20 minutes incubation (time points 10 minutes against 30 minutes, one-way ANOVA).

In another setup, human RBCs were incubated for 20 minutes at 25°C and 37°C to analyze the effect of temperature on the steady state ATP release into the supernatant. Figure 11 (B) shows that there are no differences in ATP levels between the two treatments. This finding shows that temperature has no influence on steady state ATP levels. In conclusion, ATP decrease is time-dependent, but not temperature-dependent.

These data show that the assay should be performed within shorter incubation times and paired treatment analysis should be preferred because of sample to sample variability.

4.1.1.2 Hemolysis is a confounding parameter in ATP measurement

It was shown before that ATP release from RBCs may be regulated by intracellular signaling pathways within the RBCs [5, 6, 88, 99-101, 111, 125, 209-213]. PDE-dependent signaling as well as intracellular nucleotides (e.g. cAMP, cGMP) were proposed to participate in regulation of ATP [100, 119, 125-127, 209, 212, 214, 215]. In the present study, RBC suspensions of 20% Hct were incubated with the PDE 5 inhibitor Sil (100 μ M) at 37°C for different time points (Figure 12 (A)).

Figure 12 (A) shows that PDE 5 inhibition by Sil leads to significant increases in extracellular ATP levels in the supernatant after 15 minutes incubation time (see bars at 15 and 20 minutes).

In another setup, RBCs were incubated with Sil together with the NO-donor DEA/NO, the sGC stimulator BAY-41 or their combination for different time periods (Figure 12 (B)). The figure shows that stimulation with the different

pharmacological agents induces increase of ATP levels. Further analyses were performed by incubation with a stable and cell permeable derivate of cGMP CPT-cGMP (100 μ M) for various time points (data shown in Figure 12 (D)).

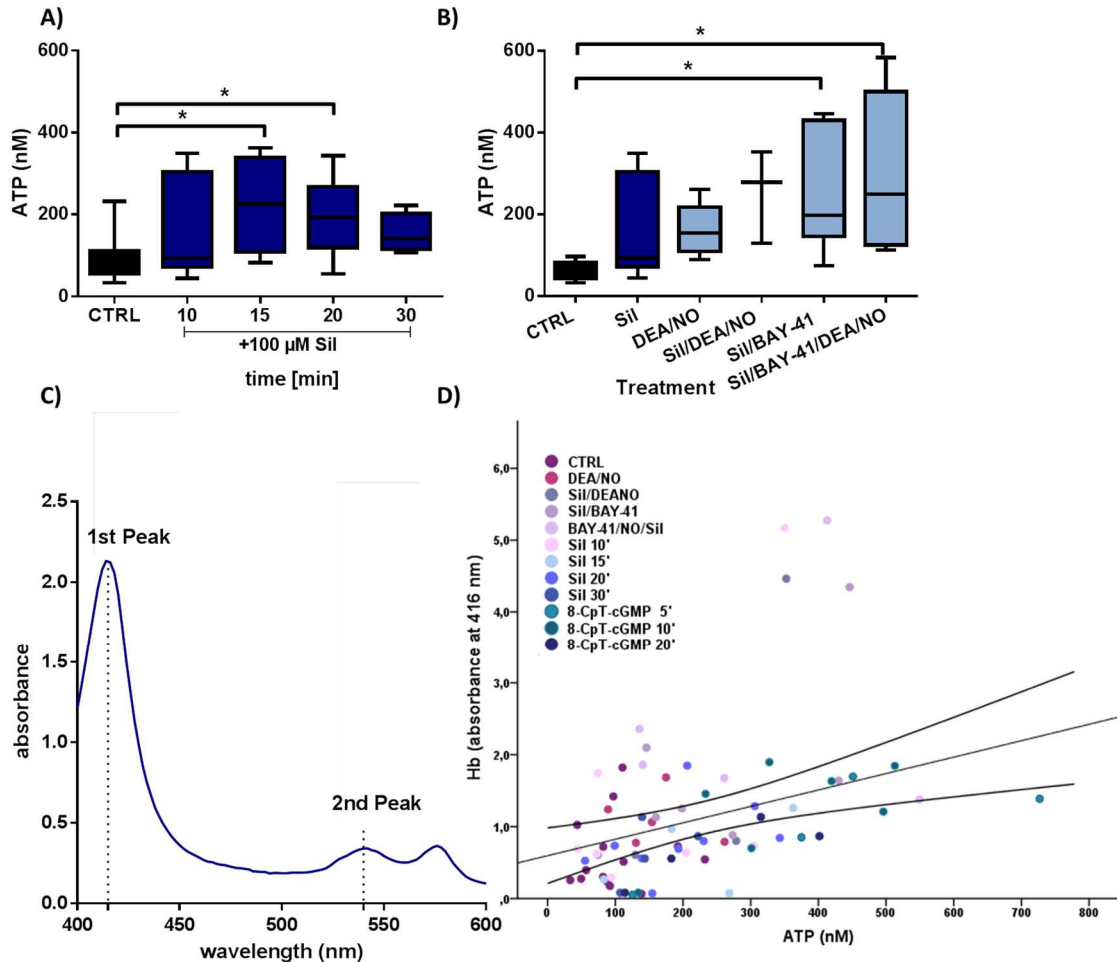


Figure 12: Hemolysis is a confounding parameter in ATP measurement

(A), (B) Extracellular ATP levels are increased by treatment with (A) PDE 5 inhibitor Sil or (B) sGC stimulator BAY-41 and NO-donor DEA/NO. Human RBCs of 20% Hct in total volume of 500 μ l were incubated at 37°C with (A) Sil (100 μ M, control (CTRL): n=16, 10 min: n=7, 15 min: n=4, 20 min: n=9, 30 min: n=4) for different time points and (B) BAY-41 and 200 μ M DEA/NO (CTRL: n=7, Sil: n=7, 200 μ M DEA/NO: n=5, Sil/BAY-41: n=7, Sil/BAY-41/DEA/NO: n=5, Sil/DEA/NO: n=3) for 10 minutes. Samples were analyzed via luciferin-luciferase assay. Data are expressed as median in a Tukey distribution plot, unpaired one-way ANOVA against CTRL: post-hoc test Dunnett (*), $p \leq 0.05$, ** $p \leq 0.01$. (C) Representative UV/VIS spectrum (400-600 nm) with marked Hb peaks. Supernatants of treated RBCs from (A), (B) and (D) were analyzed photometrically by full UV/VIS spectra for identification of free Hb. (D) Correlation of 1st Hb peak (416 nm) and ATP signal from the treatments of (A), (B) and 100 μ M CPT-cGMP for various time points. Data are expressed as scatter dot plots, two-tailed Pearson correlation analysis, $p=0.001$, $r=0.372$, $n=76$, ** $p \leq 0.01$.

The intracellular concentrations of ATP are 10-100 folds higher than the extracellular ATP concentrations [216]. Therefore, cell rupture of even few cells may be responsible for increases of ATP concentration in the supernatant. The concentration of Hb can be detected by absorbance in a full UV/VIS spectrum. To verify whether ATP increases in the supernatant are independent of hemolysis, an UV/VIS spectrum from 400 to 600 nm was recorded for each experiment. To assess Hb in the supernatant, 50 μ l of supernatant were analyzed in a 96 well UV-transparent plate.

Figure 12 (C) presents an absorbance spectrum from 400 to 600 nm. It shows the absorption spectrum of Hb, which is characterized by 2 main Hb peaks. The first peak maximum is at 416 nm (1st bigger peak) and the second one is at 540 nm (2nd smaller peak). To verify whether ATP levels in the supernatant correlate with the Hb levels, ATP levels were compared against absorbance at 416 nm (Figure 12 (D)) and 540 nm via two-tailed Pearson test (540 nm: $p=0,052$, $r=0,224$, $n =76$, n.s.). Although the results only correlate at 416 nm, but not at 540 nm, the present data demonstrate that measured ATP levels are related to the amount of free Hb in the supernatant. Due to this, the increase of ATP release may not be mediated by pharmacological agents, but rather by hemolysis of the RBCs induced by the treatment. To generate valid data, hemolysis should be minimized in the assay.

4.1.1.3 ATP measurement requires normalization

To analyze the effects of RBC concentration on extracellular ATP levels, human and murine RBC suspensions of increasing Hct (from 0.5% to 35%) were analyzed for ATP concentrations and Hb content (Figure 13 (A),(C)). Therefore, RBC suspensions were incubated for 10 minutes and analyzed for detection of ATP levels and Hb.

Figure 13 (A) shows that the concentrations of ATP in the supernatant were significantly higher in 0.5% Hct than in all other dilutions. Furthermore, ATP concentrations have a high variation from over 500 nM in the samples from 10 to 35% Hct. At 0.5% Hct the variation is smaller, but this is probably due to the small amount of RBCs in the sample. In conclusion, ATP release from RBCs is

dependent on cell concentration in the suspension. The levels of free Hb in the supernatant can indicate the grade of hemolysis of RBCs. To verify whether the measured ATP release is independent of hemolysis, a correlation of Hb and ATP was made for each experiment. The levels of Hb were defined as the amount of absorbance of the supernatant at 540 nm and 416 nm. Samples showing a positive correlation of either 416 nm or 540 nm were excluded. Furthermore, levels of absorbance at 540 nm were additionally compared with the ATP data (Figure 13 (B)). The figure shows that Hb levels are significantly decreased in samples corresponded to 0.5% Hct compared to 25% and 35% Hct. In contrast to ATP, the levels of Hb only have small variations ($0.1 \leq \lambda \leq 0.3$ at 540 nm), indicating that the release of steady state ATP levels is not related to hemolysis.

In conclusion, steady state ATP levels of human RBCs with increasing cell concentration (as % Hct) have high variations, but do not differ significantly at high concentrations (10% to 35% Hct). Moreover, the basal levels of hemolysis are relatively constant among 35% Hct.

Figure 13 (C) and (D) show the same experiment as (A) and (B) carried out with murine RBCs. In detail, also for murine RBCs low RBC concentrations (0.5% Hct) show significantly different (C) ATP release and (D) Hb levels as compared to higher concentrations. Moreover, the Hb levels are not different compared to human RBCs. Furthermore, the absorbance varies in the same range as in human RBCs (0.1 to 0.3). These results indicate that ATP release in murine RBCs also depends on Hct, but variability is smaller than in human samples.

For normalization of ATP levels, protein concentration of the RBC pellets was determined by Lowry assay. Figure 13 (E) shows that normalization of ATP per protein concentration minimizes the high variations in ATP release at higher RBC concentration (from 20% to 35% Hct). It shows that by normalization the differences of ATP release between 0.5% Hct and the other treatments become highly significant (****).

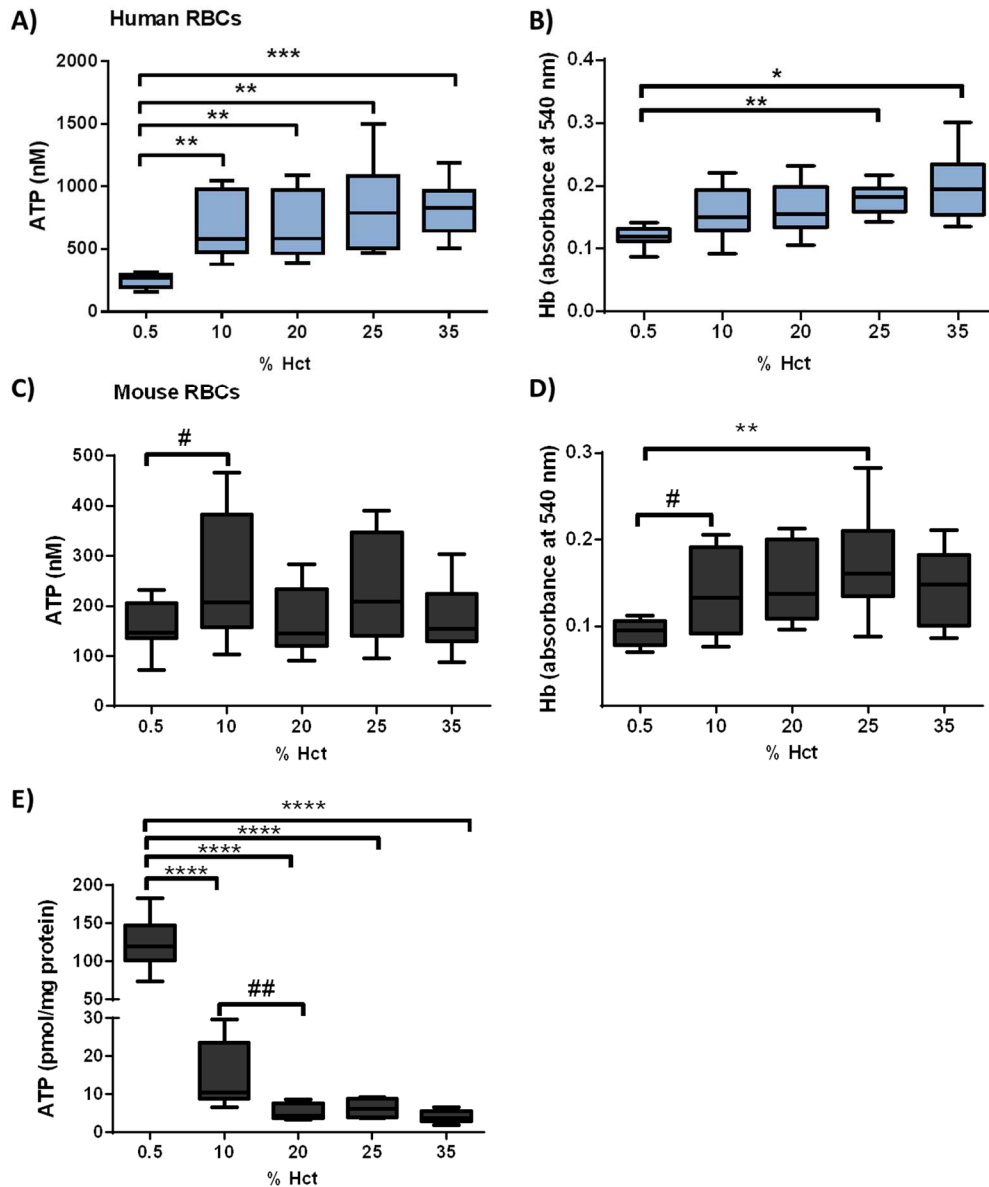


Figure 13: ATP measurement requires normalization

(A), (C) High variation of ATP levels of (A) human and (C) murine RBCs at increasing Hct. RBC suspensions (% Hct in total volume of 150 μ l) were incubated for 10 minutes at RT and analyzed via luciferin-luciferase assay. (B), (D) Low variation of absorbance of RBC supernatant at 2nd peak (540 nm) at increasing Hct. Supernatant of treated RBCs was analyzed photometrical by UV/VIS spectra for identification of free Hb. Data are expressed as median in a Tukey distribution plot. (B) paired one-way ANOVA against each treatment: post-hoc test Tukey (*, **, ***) $n=8$, (D) unpaired one-way ANOVA against each treatment: post-hoc test Tukey (*, **, ***, 0.5%: $n=9$, 10%, 20%, 25%: $n=10$, 35%: $n=8$), unpaired T-test of lower concentration against the next higher one (#). (E) Normalization of ATP signal against amount of RBCs minimizes high variation of ATP levels. Protein content of lysed RBCs were determined by Lowry assay, paired one-way ANOVA against each treatment: post-hoc test Tukey (****, 0.5%: $n=9$, 10%, 20%, 25%: $n=10$, 35%: $n=8$), unpaired T-test of lower concentration against the next higher one (#). (#), *, # $p \leq 0.05$, **, ## $p \leq 0.01$, *** $p \leq 0.001$, **** $p \leq 0.0001$.

In conclusion, steady state ATP release depends on Hct (RBC concentration) and has high variability and therefore requires normalization against protein concentration to decrease sample to sample variability. Furthermore, human RBCs show higher sample to sample variability than murine RBCs. The grade of hemolysis detected as Hb concentration in the supernatant (absorbance at 540 nm) did not affect the ATP measurement at high Hct range.

Therefore, further experiments were performed with murine RBCs of same Hct (25%) and ATP data was normalized against protein concentration.

4.1.1.4 Hypotonic stress induces ATP release in mouse RBCs independent of hemolysis

To verify assay functionality and to minimize treatment-dependent hemolysis, a positive control was established. It has been shown that hypotonic stress induces ATP release from RBCs [145]. Therefore, murine RBCs of 25% Hct were exposed to hypotonic stress conditions at RT for 30 seconds. Figure 14 (A) shows ATP levels after hypotonic treatment against control. The results demonstrate that hypotonic stress induces ATP release from murine RBCs.

Figure 14 (B) shows representative UV/VIS spectrum (n=8) of the treatments. To exclude the effects of hemolysis on ATP release, a threshold at wavelength of 540 nm was used as exclusion criteria. Figure 14 (B) shows that there is a variation of mean between 0.2 and 0.4 at the peak maximum independently of treatment (purple and blue lines are mixed). Based on these data, a threshold of absorbance of $\lambda=0.45$ was chosen (maximum + ~10% deviation).

Excluding data with Hb absorbance greater than the threshold, correlation analyses between ATP and Hb levels were made both with absorbance at 416 nm (Figure 14 (C)) and 540 nm. Pearson correlation analyses showed that there is no statistically relevant relationship (540 nm: $r=0.005$, $p=0.976$). Furthermore, Figure 14 (D) shows that there were no differences between Hb levels at 540 nm among the treatments (T-test).

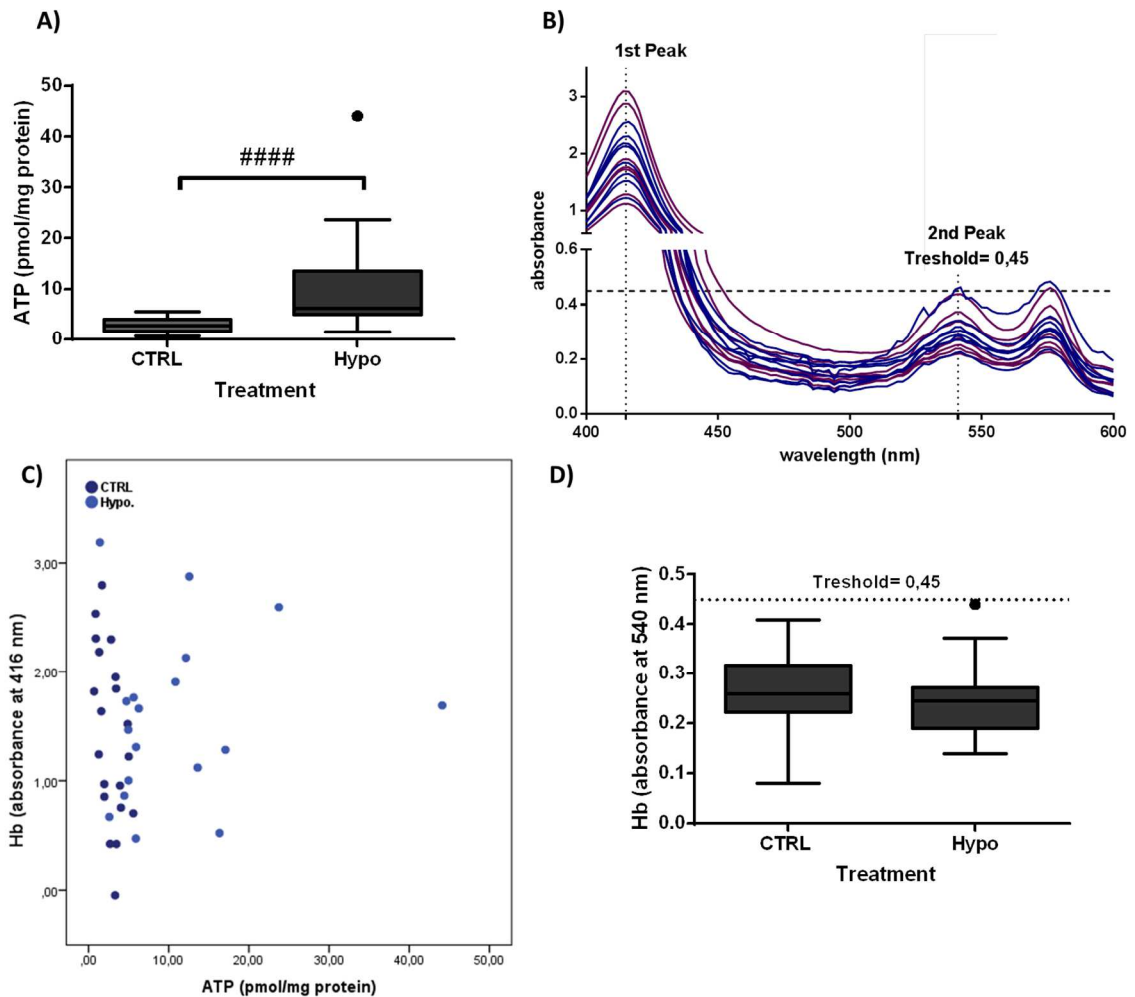


Figure 14: Hypotonic stress induces ATP release from RBCs independent of hemolysis

(A) Hypotonic stress induces ATP release from murine RBCs. Cell suspensions were incubated in with CTRL or hypotonic treatment. Samples were analyzed via luciferin-luciferase assay. For normalization, protein concentration of lysed RBCs was analyzed via Lowry assay, data are expressed as median in a Tukey distribution plot, paired T-test, $n=19$, #### $p \leq 0.0001$. (B) Representative UV/VIS spectrum (400-600 nm) with threshold definition of $\lambda=0.45$ at 2nd peak (absorbance at 540 nm). Supernatant of RBCs was analyzed photometrical by full UV/VIS spectra for identification of free Hb. blue: CTRL, purple: hypotonic treatment, $n=8$ C) No correlation of ATP levels and Hb at 1st peak (absorbance at 416 nm). Correlation calculation absorbance and ATP signal, two-tailed Pearson correlation analysis, $r= 0,069$, $p=0,680$, $n=38$. Data are expressed as scatter dot plots. D) No differences of absorbance of supernatant at 2nd peak (absorbance at 540 nm) between the treatments, data are expressed as median in a Tukey distribution plot, paired T-test, $n=19$.

In conclusion, hypotonic conditions induce ATP release from RBCs, which is independent of hemolysis. Furthermore, the effects of hemolysis can be excluded by definition of a threshold. For further experiments, hypotonic stress was used

as positive control. Therefore, correlation analyses of supernatant absorbance at 540 nm and 416 nm against ATP levels were performed in each experiment.

Data with absorbance which exceeded the threshold of 0.45 or which showed a positive correlation between ATP and Hb-absorbance were excluded.

4.1.2 Intracellular signaling of ATP release from murine RBCs

4.1.2.1 PDE-inhibition induces ATP release in RBCs

It is known that PDEs hydrolyze cAMP or cGMP to shut down cyclic nucleotide-dependent signaling pathways within the cell [119, 123] and different isoforms show different specificity [119]. The first aim was to test whether PDE 5 is involved in regulation of ATP release of RBCs.

Therefore, RBCs were incubated with various concentrations of the PDE 5 inhibitor Sil for 10 and 15 minutes and ATP- and Hb- levels were measured (Figure 15).

Figure 15 (A) shows that incubation of 100 μ M Sil for 10 minutes induces ATP release in RBCs. Furthermore, the incubation with 100 nM did not have any effect. Moreover, Figure 15 (A) shows that the vehicle control has no effect on ATP release. Figure 15 (B) shows that the vehicle control and 100 μ M Sil treatment both increase Hb-levels compared to control, but there were no significant differences between Sil and vehicle. Furthermore, there was no correlation at 540 nm and 416 nm between ATP levels and Hb.

In Figure 15 (C), the data obtained after 15 minutes treatment with 100 μ M Sil are presented paired to their respective control, and clearly demonstrate that ATP release is induced by Sil treatment. Figure 15 (D) shows that Hb levels (as absorbance at 540 nm) is unchanged between Sil and vehicle. This result indicates that the effect of Sil is independent of sample to sample variation.

In conclusion, Sil treatment induces ATP release independent of hemolysis. Thus, PDE 5 is involved in regulation of ATP release from RBCs. However, although Sil is a PDE 5 inhibitor at the high applied concentration of 100 μ M, we

cannot exclude that these results also depend on changes in cAMP levels induced by inhibition other isoforms of PDE.

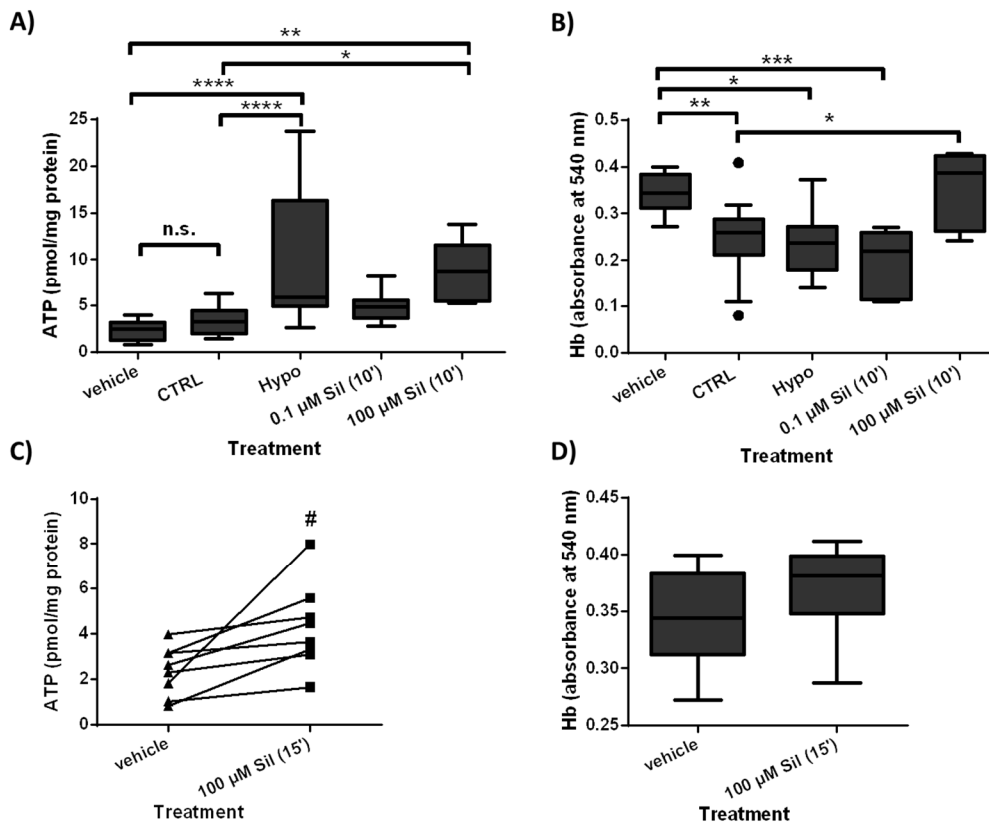


Figure 15: PDE 5 inhibition induces ATP release in murine RBCs

(A) Treatment of 100 μM Sil induces ATP release from murine RBCs. Cell suspensions were incubated with 0.1 and 100 μM of PDE 5 inhibitor Sil for 10 minutes at RT. Induction of hypotonic stress was used as positive- and water as vehicle- control. Samples were analyzed via luciferin-luciferase assay. For normalization, protein concentration of lysed RBCs was analyzed via Lowry assay. (B) No hemolysis in response to treatment of Sil. Supernatant of RBCs was analyzed photometrical by full UV/VIS spectra for identification of free Hb representative for amount of lysed RBCs. Absorbance of supernatant at 2nd peak at 540 nm including threshold definition of $\lambda=0.45$. (A), (B) data are expressed as median in a Tukey distribution plot, unpaired one-way ANOVA against CTRL or vehicle: post hoc test: Dunnett (CTRL: n=21, Hypo: n=11, 0.1 μM Sil: n=9, vehicle: n=8, 100 μM Sil: n=5). * $p \leq 0.05$, ** $p \leq 0.01$, *** $p \leq 0.001$, **** $p \leq 0.0001$. (C) Paired treatment of 100 μM Sil induces ATP release from murine RBCs. Cell suspensions were incubated with 0.1 and 100 μM of PDE 5 inhibitor Sil for 10 minutes at RT. (D) No hemolysis in response to paired treatment of 100 μM Sil. Supernatant of RBCs was analyzed photometrical by full UV/VIS spectra for identification of free Hb representative for amount of lysed RBCs. Absorbance of supernatant at 2nd peak at 540 nm including threshold definition of $\lambda=0.45$.

(C), (D) Paired T-test, n=8, # $p \leq 0.05$. Outlier analysis was performed graphically by box & whiskers plots according to Tukey.

4.1.2.2 No effect of extracellular cGMP on ATP release

Based on the result that PDE inhibition induces ATP release the next aim was to analyze whether cGMP and cAMP affect ATP release from RBCs (Fig. 16).

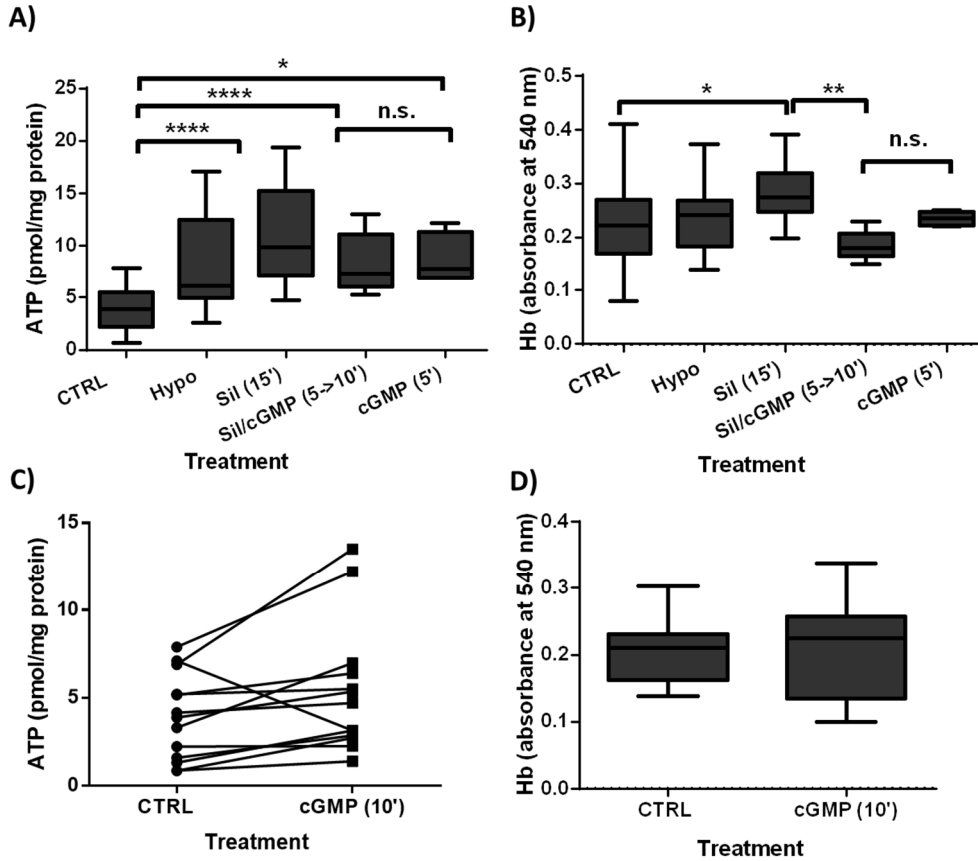


Figure 16: No effect of CPT-cGMP on ATP release from murine RBCs

(A) No effect of CPT-cGMP on ATP release from murine RBCs. Cell suspensions were incubated with 8-CPT-cGMP (100 μ M) for 10 minutes \pm 5 minutes preincubation with PDE 5 inhibitor Sil (100 μ M) at RT. Hypotonic stress or Sil treatment was used as positive control. Samples were analyzed via luciferin-luciferase assay. Samples were analyzed via luciferin-luciferase assay. For normalization, protein concentration of lysed RBCs was analyzed via Lowry assay. (B) Sil and cGMP treatment do not induce hemolysis in murine RBCs. Supernatant of RBCs was analyzed photometrical by full UV/VIS spectra for identification of free Hb representative for amount of lysed RBCs. Absorbance of supernatant at 2nd peak at 540 nm including threshold definition of $\lambda=0.45$. Data are expressed as median in a Tukey distribution plot, unpaired one-way ANOVA against CTRL, Sil: post hoc test: Dunnett (CTRL: n=35, Hypo: n=16, Sil: n=14, cGMP/Sil: n=6), * $p \leq 0.05$; ** $p \leq 0.01$, *** $p \leq 0.001$, **** $p \leq 0.0001$. C) No effect of paired treatment with CPT-cGMP on ATP release from murine RBCs. Cell suspensions were incubated with 8-CPT-cGMP (100 μ M) for 10 minutes against control. (D) Paired cGMP treatment does not induce hemolysis in murine RBCs. Supernatant of RBCs was analyzed photometrical by full UV/VIS spectra for identification of free Hb representative for amount of lysed RBCs. Absorbance of supernatant at 2nd peak at 540 nm including threshold definition of $\lambda=0.45$, (C), (D) Data are expressed as median in a Tukey distribution plot, paired T-test, n=13, n.s.

To investigate the role of extracellular cGMP, 100 μ M of CPT-cGMP was applied for 10 minutes with or without 5 minutes preincubation with Sil (Figure 16).

CPT-cGMP is a stable derivative of cGMP, which is able to cross the cell membrane and to activate cGMP specific downstream signaling.

Figure 16 (A) shows that the effect of Sil on ATP release is not affected by addition of cGMP (Sil/ Sil + cGMP not significant). Figure 16 (B) shows that cGMP treatment also has no effect on Hb-levels in the supernatant indicating no effects of hemolysis. Figure 16 (C) and (D) show that ATP and Hb-level in the supernatant are not affected by cGMP application in absence of Sil against control (paired measurements).

In conclusion, cGMP has no effects on ATP release or hemolysis in murine RBCs under the applied conditions.

4.1.2.3 No effect of extracellular cAMP on ATP release

To investigate the role of extracellular cAMP, a stable cell-permeable derivate of cAMP was used. As shown in Figure 17, CPT-cAMP was incubated for 5 minutes with or without a 10 minute preincubation with 100 μ M Sil.

Figure 17 (A) shows that the increase of ATP levels in the supernatant via Sil is not affected by cAMP application. Figure (B) shows that cAMP application also has no effect on Hb-levels in the supernatant indicating no effects of hemolysis. Furthermore, Figure 17 (C) shows that cAMP application alone does not influence on ATP release and Hb-levels in the supernatant (paired measurement).

In conclusion, the application of cGMP and cAMP (the downstream targets of PDEs) do not influence ATP release from RBCs.

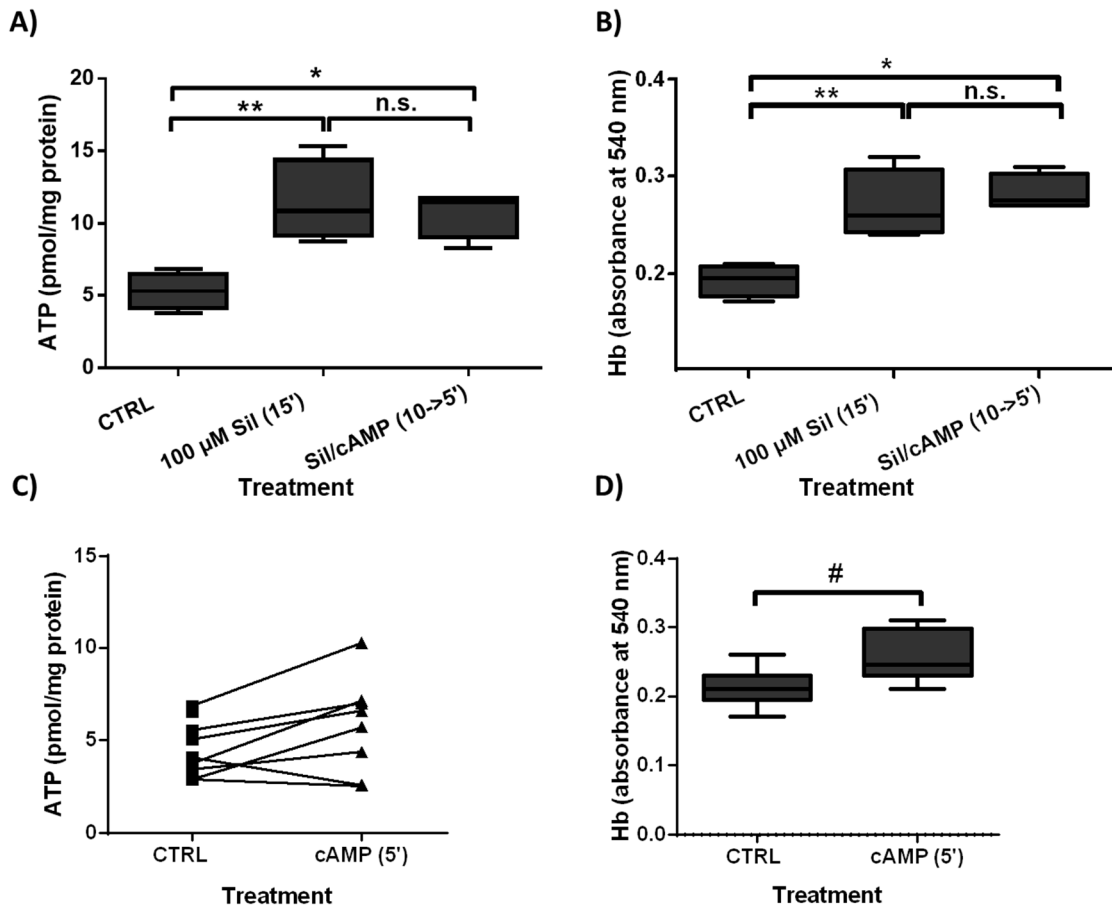


Figure 17: No effect of CPT-cAMP on ATP release in murine RBCs

A) No effect of CPT-cAMP on ATP release from murine RBCs. Cell suspensions were incubated with 8-CPT-cAMP (100 μ M) for 5 minutes \pm 10 minutes preincubation with PDE 5 inhibitor Sil (100 μ M) at RT. Sil was used as positive control. Samples were analyzed via luciferin-luciferase assay. For normalization, protein concentration of lysed RBCs was analyzed via Lowry assay. (B) Sil and cAMP treatment do not induce hemolysis in murine RBCs. Supernatant of RBCs was analyzed photometrical by full UV/VIS spectra for identification of free Hb representative for amount of lysed RBCs. Absorbance of supernatant at 2nd peak at 540 nm including threshold definition of $\lambda=0.45$. Data are expressed as median in a Tukey distribution plot, paired one-way ANOVA against CTRL, Sil: post hoc test: Dunnett (n=4), * $p \leq 0.05$; ** $p \leq 0.01$. (C) No effect of paired treatment with CPT-cAMP on ATP release from murine RBCs. Cell suspensions were incubated with 8-CPT-cAMP (100 μ M) for 5 minutes against control. (D) Paired cAMP treatment does not induce hemolysis in murine RBCs. Supernatant of RBCs was analyzed photometrical by full UV/VIS spectra for identification of free Hb representative for amount of lysed RBCs. Absorbance of supernatant at 2nd peak at 540 nm including threshold definition of $\lambda=0.45$. (C),(D) Data are expressed as median in a Tukey distribution plot, paired T-test, n=8, # $p \leq 0.05$.

4.1.3 No effect of sGC stimulation on ATP release

To verify whether sGC stimulation is involved in ATP release from RBCs, murine RBCs were treated with the heme-dependent sGC stimulator BAY-41 and DEA/NO in presence and absence of Sil.

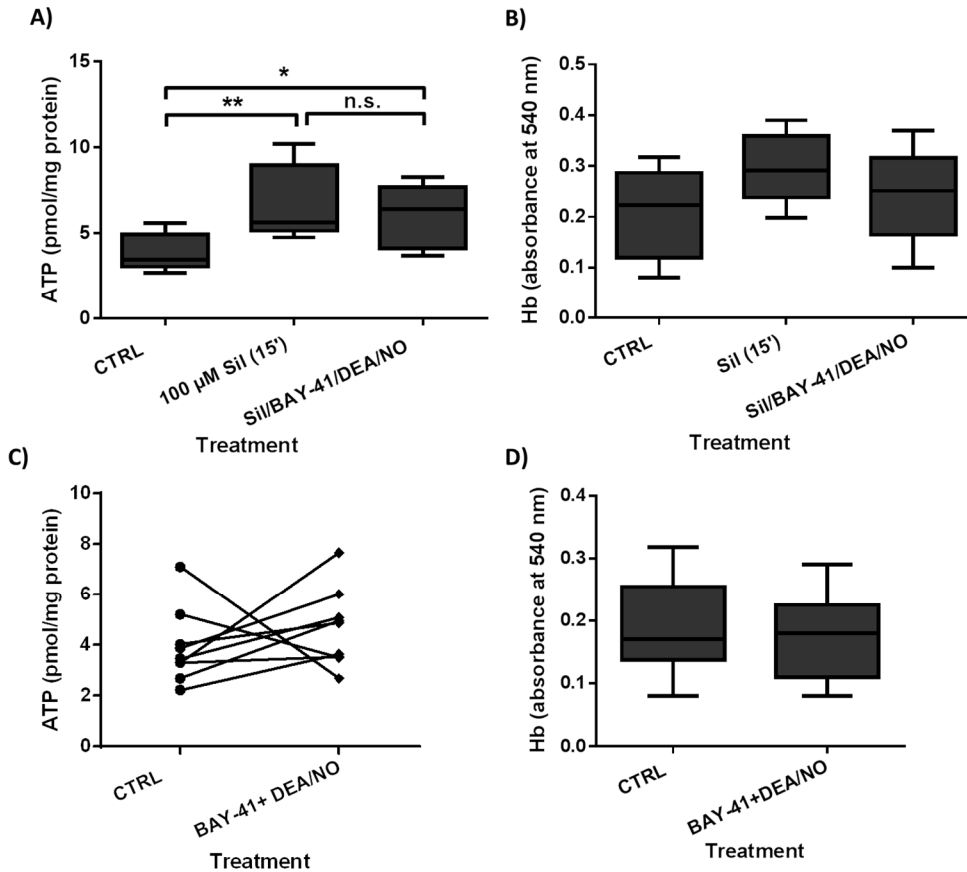


Figure 18: sGC stimulation has no impact on ATP release

A) No effect of sGC stimulation on ATP release from murine RBCs. Cell suspensions were incubated with sGC stimulator BAY-41 (1 µM), NO-donor DEA/NO (200 µM) and PDE 5 inhibitor Sil (100 µM) for 15 minutes at RT. Samples were analyzed via luciferin-luciferase assay. For normalization, protein concentration of lysed RBCs was analyzed via Lowry assay. (B) sGC stimulation does not induce hemolysis in murine RBCs. Supernatant of RBCs was analyzed photometrical by full UV/VIS spectra for identification of free Hb representative for amount of lysed RBCs. Absorbance of supernatant at 2nd peak at 540 nm including threshold definition of $\lambda=0.45$. (A), (B) data are expressed as median in a Tukey distribution plot, unpaired one-way ANOVA against CTRL, Sil; post hoc test: Dunnett (CTRL, Sil/BAY-41/DEA/NO: n=9, Sil: n=5), * $p \leq 0.05$; ** $p \leq 0.01$. (C) No effect of paired sGC stimulation on ATP release from murine RBCs. Cell suspensions were incubated with sGC stimulator BAY-41 (1 µM), NO-donor DEA/NO (200 µM) for 15 minutes at RT. (D) Paired sGC stimulation does not induce hemolysis in murine RBCs. Supernatant of RBCs was analyzed photometrical by full UV/VIS spectra for identification of free Hb representative for amount of lysed RBCs. Absorbance of supernatant at 2nd peak at 540 nm including threshold definition of $\lambda=0.45$. (C), (D) data are expressed as median in a Tukey distribution plot, paired T-test, n=9, n.s.

All treatments were added together for 15 minutes at RT and analyzed via luciferin-luciferase assay and UV/VIS spectrum (Figure 18).

Figure 18 (A) shows effects of treatments in presence of Sil. It shows that the increase of ATP levels in the supernatant via Sil is not further potentiated by sGC stimulation.

Figure 18 (B) shows that the stimulation also does not affect Hb-levels in the supernatant indicating lack of hemolysis. Figure 18 (C) and (D) show that sGC stimulation of BAY-41 and DEA/NO in absence of Sil also did not affect ATP release or hemolysis. Therefore, stimulation of sGC did not induce ATP release from RBCs.

To sum up, the presented data indicate that PDE inhibition with Sil induces ATP release from RBCs, but stimulation with cAMP and cGMP/sGC signaling does not have any effect.

4.1.4 Role of ion channels in ATP release

4.1.4.1 Hypotonic stress induces ATP release but is independent of Pnx-1

To verify whether hypotonic stress induced ATP release from RBCs is Pnx-1 dependent, RBCs from WT mice were induced to hypotonic conditions with or without pharmacological inhibitors of Pnx-1 (Figure 19).

As shown in Figure 19, RBC suspensions of WT mice were preincubated with the Pnx-1 inhibitors probenecid and carbenoxolone. Afterwards, hypotonic conditions were induced by buffer change and (A) ATP- and (B) Hb-levels were determined. Figure 19 (A) shows that incubation with both inhibitors did not affect the hypotonic stress induced ATP release from RBCs. Furthermore, as shown in (B) Hb levels were unchanged in all conditions excluding an effect of hemolysis. In conclusion, Pnx-1 is probably not involved in the transport of ATP out of the cell.

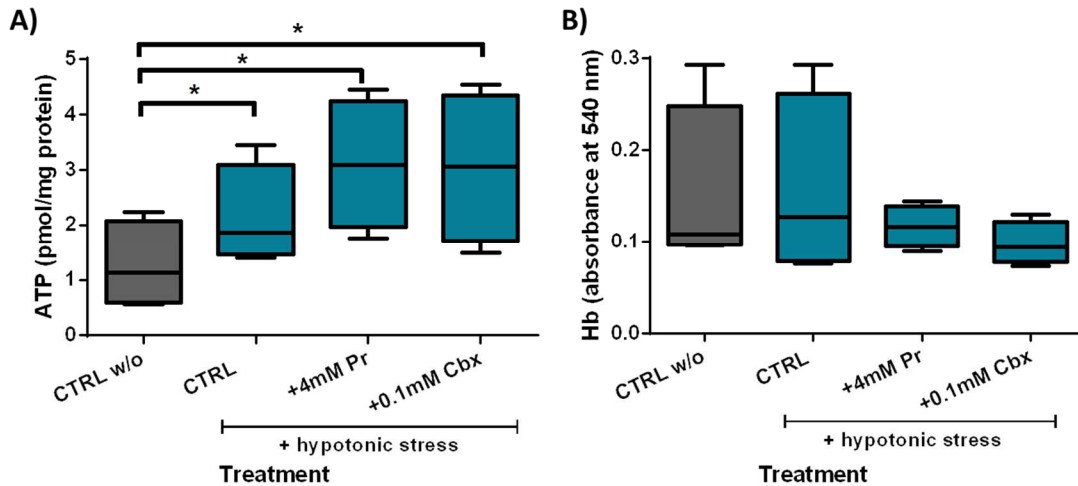


Figure 19: Hypotonic effect on ATP release is Pnx-1 independent

(A) No effect of Pnx-1 inhibition by probenecid and carbenoxolone on hypotonic induced ATP release from RBCs. Cell suspensions were preincubated with 4 mM probenecid and 0.1 mM carbenoxolone for 30 minutes. Afterwards, RBCs were induced to hypotonic stress. Samples were analyzed via luciferin-luciferase assay. For normalization, protein concentration of lysed RBCs was analyzed via Lowry assay. Data are expressed as median in a Tukey distribution plot, paired one-way ANOVA against CTRL w/o: post hoc test: Dunnett, $n=4$, $*p \leq 0.05$. (B) Pnx-1 inhibition does not induce hemolysis independent of hypotonic conditions. Supernatant of RBCs was analyzed photometrical by full UV/VIS spectra for identification of free Hb representative for amount of lysed RBCs. Absorbance of supernatant at 2nd peak at 540 nm including threshold definition of $\lambda=0.45$, data are expressed as median in a Tukey distribution plot, paired one-way ANOVA against CTRL w/o: post hoc test: Dunnett, $n=4$, n.s.

4.1.4.2 PDE 5 regulated ATP release is Pnx-1 independent

To verify whether Sil induced ATP release from RBCs is Pnx-1 dependent, RBCs of WT mice were preincubated with pharmacological inhibitors. RBC suspensions of WT mice were incubated with Pnx-1 inhibitors probenecid (4 mM) and carbenoxolone (100 μ M) before application of 100 μ M Sil for 15 minutes (Figure 20). Figure 20 (A) shows that pretreatment with Pnx-1 inhibitors does not influence the effect of Sil on ATP release from RBCs. As shown in Figure 20 (B), Hb-levels are increased in presence of the inhibitors indicating small amounts of hemolysis. However, there was no correlation between ATP- and Hb-levels in the supernatant.

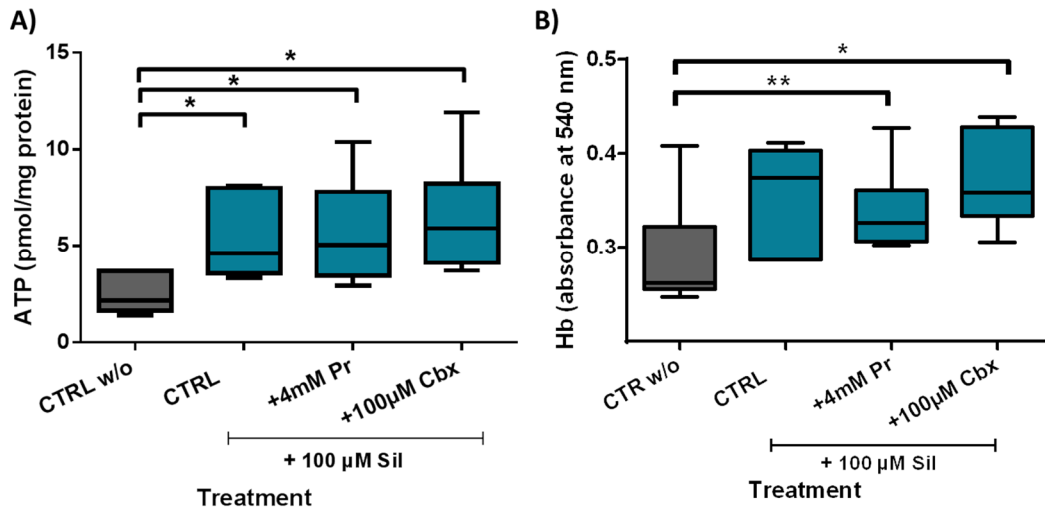


Figure 20: Pnx-1 is not involved in ATP release via phosphodiesterase 5 inhibition

(A) No effect of Pnx-1 inhibition by probenecid and carbenoxolone on Sil induced ATP release from RBCs. Cell suspensions were preincubated with 4 mM probenecid and 0.1 mM carbenoxolone for 30 minutes. Afterwards, RBCs were incubated with 100 µM of PDE 5 inhibitor Sil for 15 minutes. Samples were analyzed via luciferin-luciferase assay. For normalization, protein concentration of lysed RBCs was analyzed via Lowry assay. Data are expressed as median in a Tukey distribution plot, paired one-way ANOVA against CTRL w/o: post hoc test: Dunnett, $n=6$, $* p \leq 0.05$. (B) Pnx-1 inhibition does not induce hemolysis independent of Sil. Supernatant of RBCs was analyzed photometrical by full UV/VIS spectra for identification of free Hb representative for amount of lysed RBCs. Absorbance of supernatant at 2nd peak at 540 nm including threshold definition of $\lambda=0.45$, data are expressed as median in a Tukey distribution plot, paired one-way ANOVA against CTRL w/o: post hoc test: Dunnett, $n=6$, $* p \leq 0.05$, $** p \leq 0.01$.

In conclusion, the effect of Sil on ATP release from RBCs is independent of Pnx-1, but incubation with pharmacological inhibitors may lead to small amounts of hemolysis, however correlation was not significant.

4.1.4.3 Hypotonic stress induces hemolysis in RBCs from CFTR KO mice

Besides Pnx-1, the CFTR channel has been proposed to contribute to the transport of ATP from RBCs. CFTR is also known to be present in the RBC membrane and to be involved in shear-induced ATP release [137, 217]. To verify whether hypotonic stress induced ATP release from RBCs is CFTR-dependent, RBCs from CFTR KO mice and WT were treated with hypotonic buffer (Figure 21).

Figure 21 shows that induction of hypotonic stress with RBCs from CFTR KO mice leads to high levels of (A) ATP and (B) Hb in the supernatant indicating

strong hemolysis (absorbance>threshold). In conclusion, CFTR-dependency of hypotonic stress induced ATP release from RBCs cannot be verified in CFTR KO mice due to high amounts of hemolysis. Because there are no specific pharmacological CFTR inhibitors available, the role of CFTR in hypotonic-dependent ATP release was not further analyzed.

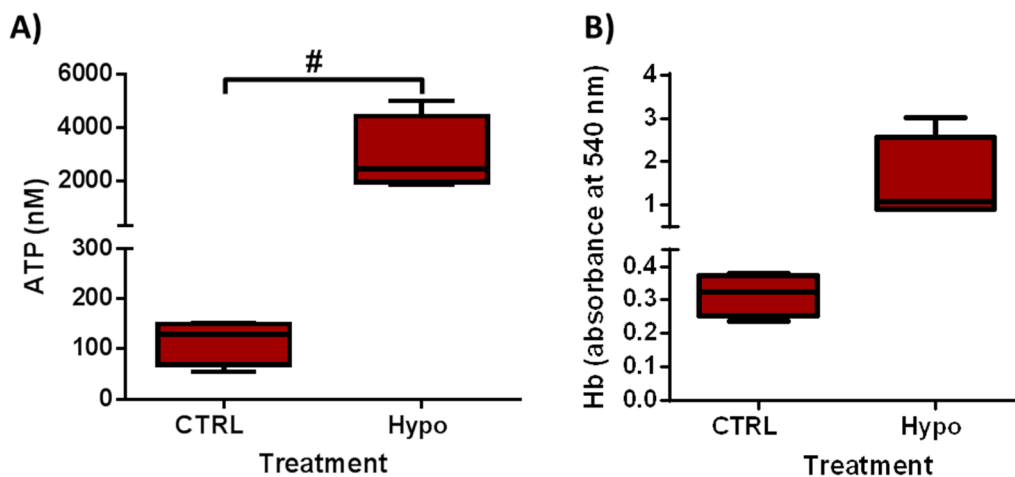


Figure 21: Hypotonic stress induces strong hemolysis in RBCs from CFTR KO mice

(A) Hypotonic stress induces ATP release from RBCs from CFTR KO mice. Cell suspensions from CFTR KO mice were induced to hypotonic stress. Samples were analyzed via luciferin-luciferase assay. For normalization, protein concentration of lysed RBCs was analyzed via Lowry assay. Data are expressed as median in a Tukey distribution plot, paired T-test, $n=4$, # $p \leq 0.05$. (B) Hypotonic stress induces strong hemolysis in RBCs from CFTR KO mice. Supernatant of RBCs was analyzed photometrical by full UV/VIS spectra for identification of free Hb representative for amount of lysed RBCs. Absorbance of supernatant at 2nd peak at 540 nm without threshold of $\lambda=0.45$, data are expressed as median in a Tukey distribution plot, paired T-test, $n=4$, *n.s.*

4.1.4.4 PDE 5 regulated ATP release is CFTR dependent

The next aim was to analyze whether Sil-dependent ATP release from RBCs is CFTR dependent. Therefore, RBC suspensions of CFTR KO and WT were incubated with 100 μ M Sil for 15 minutes and ATP concentration and Hb levels were measured from the supernatant (Figure 22).

Figure 22 (A) shows that steady state ATP concentrations (CTRL) are decreased in CFTR KO mice compared to WT. Furthermore, the figure shows that Sil treatment does not induce ATP release from CFTR KO RBCs. Instead, ATP levels of RBCs from WT mice are increased after Sil treatment. Moreover, levels

of ATP after Sil treatment are significantly decreased in WT versus KO. In conclusion, CFTR KO RBCs lack to release ATP in response to Sil treatment and have lower steady state ATP concentrations. Figure 22 (B) shows that Hb levels are significantly higher in CFTR KO than in WT mice since there are no differences in Hb-levels of CFTR KO between CTRL and Sil. These effects were independent of hemolysis.

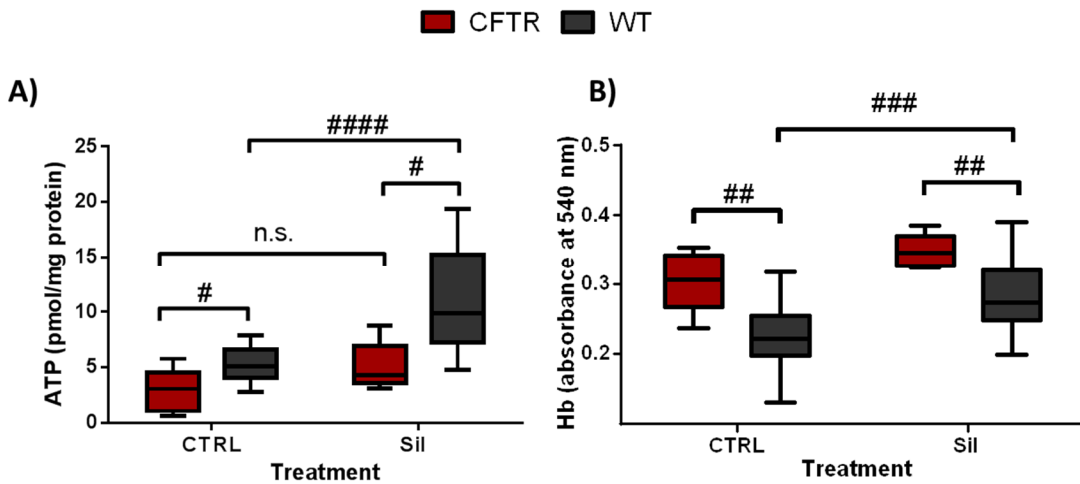


Figure 22: CFTR is participating in PDE 5 mediated ATP release

A) No effect of Sil on ATP release from CFTR KO RBCs. Cell suspensions of WT (grey) and CFTR KO mice (red) of 25% Hct were incubated with PDE 5 inhibitor Sil (100 μ M) for 15 minutes at RT. Samples were analyzed via luciferin-luciferase assay. For normalization, protein concentration of lysed RBCs was analyzed via Lowry assay. B) Levels of RBC hemolysis are higher in CFTR KO than in WT mice. Supernatant of RBCs was analyzed photometrical by full UV/VIS spectra for identification of free Hb representative for amount of lysed RBCs. Absorbance of supernatant at 2nd peak at 540 nm including threshold definition of $\lambda=0.45$. All data are expressed as median in a Tukey distribution plot, paired T-test within one strain, unpaired T-test for strain comparison, CFTR n=5, WT n=14, # $p \leq 0.05$, ## $p \leq 0.01$, ### $p \leq 0.001$, #### $p \leq 0.0001$.

In conclusion, the CFTR channel is involved in basal as well as Sil derived ATP release from mouse RBCs. Moreover, lacking of the CFTR channel is related to an increase of hemolysis on steady state, but not to treatment dependent hemolysis indicating that CFTR may be involved in the regulation of membrane stability of RBCs.

4.1.5 No Correlation of Hb levels and ATP

To ensure that hemolysis did not interfere the results of the experiments, Hb levels measured as absorbance at 416 nm and 540 nm were correlated against

ATP levels. Figure 23 shows that the total data set did not correlate and thus all effects can be assumed as ATP release induced by pharmacological treatment independent of hemolysis.

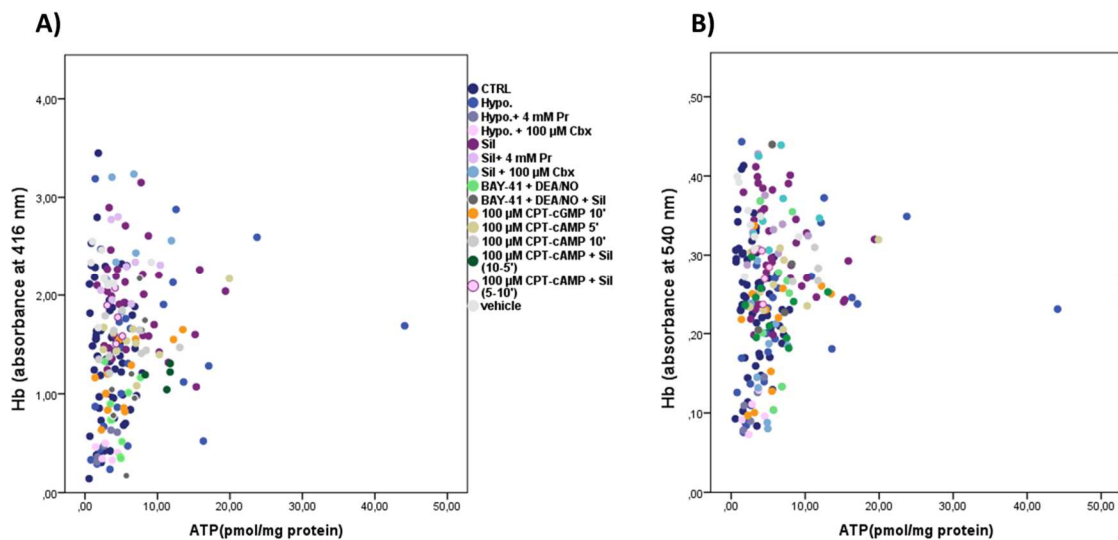


Figure 23: Hemolysis control of performed experiments

Correlation of Hb from (A) absorbance at 416 nm and (B) absorbance at 540 nm against ATP signal, two-tailed Pearson correlation analysis, (A) $p=0.147$, $r=0.145$, $n=102$, (B), $p=0.514$, $r=0.065$, $n=102$.

4.2 Part 2: Regulation of PS exposure in human RBCs

4.2.1 Induction of PS exposure in RBCs by NEM, CaCl₂ and Ca-I

PS is located in the inner leaflet of the membrane, but gets “flipped” to the outside in case of cardiac diseases and apoptosis [218]. Likewise RBCs carry PS, stimuli like glucose depletion or calcium influx increase PS on the surface of RBCs [17, 165, 219]. The aim of the second part of the study was to investigate the intracellular regulation mechanisms of PS exposure in RBCs.

Based on the protocol of Clossé et al. [220], increase of PS exposure from young and healthy RBCs was induced by treatment of RBC suspension with NEM (10 mM, Ca-I (4 μ M) and CaCl₂ (1 mM) for 1 hour at 37°C and exposure of PS was assessed as Annexin V positive cells in flow cytometric analysis (Figure 24).

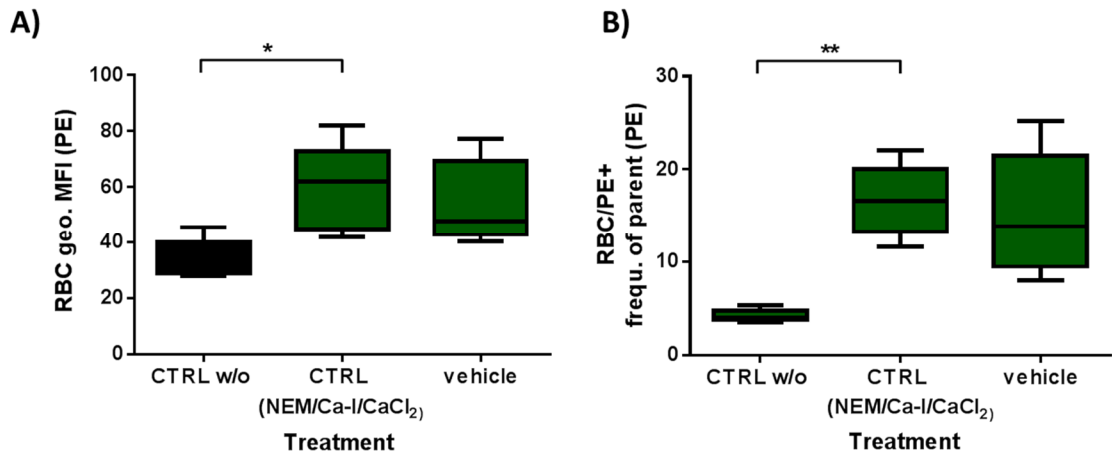


Figure 24: NEM/Ca-I/CaCl₂ increases phosphatidyserine exposure of human RBCs

Human RBCs were treated for 1 hour at 37°C with 10 mM NEM/ 4 μM Ca-I/ 1 mM CaCl₂ (CTRL) or DMSO (vehicle) and PS exposure was analyzed via Annexin V-PE with flow cytometry. Data are expressed as median in a Tukey distribution plot against (A) geo. MFI of RBC and (B) frequent of parent of RBC/PE+ cells, paired one-way ANOVA against CTRL: post hoc test: Dunnett, n=5, * p ≤ 0.05, ** p ≤ 0.01.

Figure 24 (A) shows that NEM/Ca-I/CaCl₂ (CTRL) treatment leads to a significant increase of PS exposure. Vehicle control (DMSO) had no effect on PS exposure. The figure shows that the treatment significantly increase the fluorescence intensity (FI) (assessed as geometric mean fluorescence intensity (geo. MFI)) and the % of positive cells. This demonstrates that both, percentage of PS exposing cells and the amount of total PS exposed are enhanced.

Besides the exposure of PS, also decrease in cell size in response to Ca-I treatment was demonstrated in the past [164]. To analyze whether changes in RBC morphology occur in response to the used treatment, RBCs were analyzed via light microscopy and flow cytometry (Figure 25). Figure 25 (A) and (B) show a representative flow cytometric experiment with (A) untreated RBCs (CTRL) and (B) RBCs treated with NEM/Ca-I/CaCl₂. The cell population was gated against RBC/PE+ (PS exposing cells) and results are shown as histograms against forward scatter (FSC) in Figure 25 (A) and (B). The result indicates that cell size assessed as FSC (frequent of parent) is increased in RBCs after treatment with NEM/Ca-I/CaCl₂.

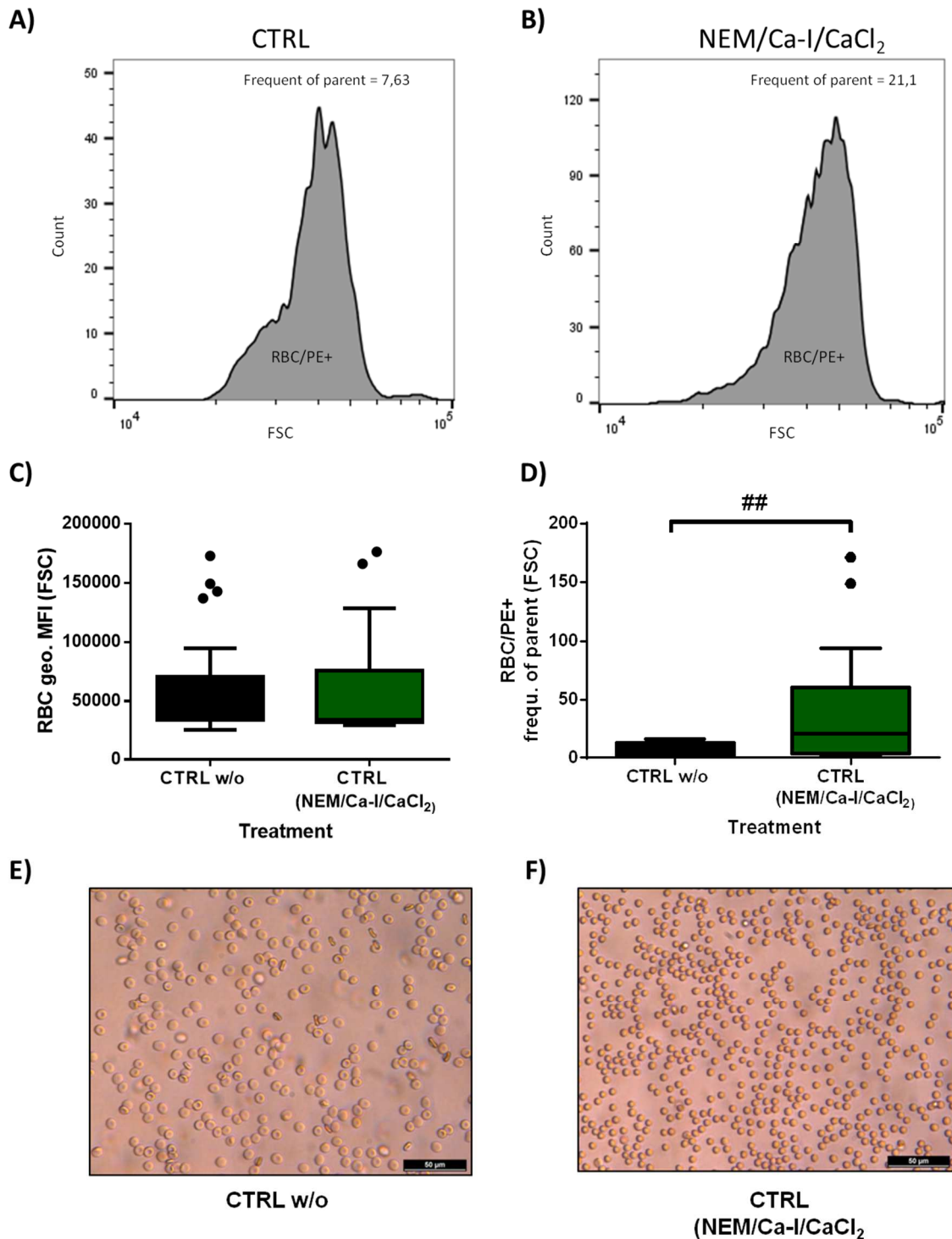


Figure 25: NEM/Ca-I/CaCl₂ treatment changes human RBC morphology

(A),(B) RBC/PE+ cell population of (A) CTRL versus (B) NEM/Ca-I/CaCl₂ treatment shown as FSC histogram with frequent of parent via flow cytometry. (C), (D) Increased RBC cell size by NEM/Ca-I/CaCl₂ treatment versus CTRL analyzed by FSC via flow cytometry. Data are expressed as median in a Tukey distribution plot against (E) geo. MFI of RBCs and (F) frequent of parent of RBC/PE+ cells, paired T-test, n=22, ## p ≤ 0.01. (E), (F) Changes of cell shape of human RBCs (A) before (CTRL w/o) and (B) after treatment with 10 mM NEM/ 4 μM Ca-I/ 1 mM CaCl₂ (CTRL) via light microscopy.

Figure (C) and (D) show the statistical analysis of the flow cytometric experiment from (A) and (B). These data demonstrate that cell size assessed as geometric mean of FSC of RBCs with flow cytometry is unchanged. Figure (D) demonstrated that FSC of RBC/PE+ cells is increased. In conclusion, the number of stained cells (RBC/PE+) PS exposing cells (PE+) increases cell size in response to NEM/Ca-I/CaCl₂ treatment.

Figure 25 (E) and (F) show that RBCs undergo changes in cell shape after treatment with NEM/Ca-I/CaCl₂ as assessed with light microscopy. The cells seem to change from their biconcave form to a more round form.

In conclusion, RBC cell size is increased in response to NEM/Ca-I/CaCl₂ treatment.

4.2.2 NO-donor DEA/NO inhibits NEM/ CaCl₂/ Ca-I mediated PS exposure

To analyze the effects of NO on the regulation of PS exposure, the effects of NO donor DEA/NO were assessed. Hence, a concentration-response curve of DEA/NO was measured in presence of NEM/Ca-I/CaCl₂ treatment (Figure 26).

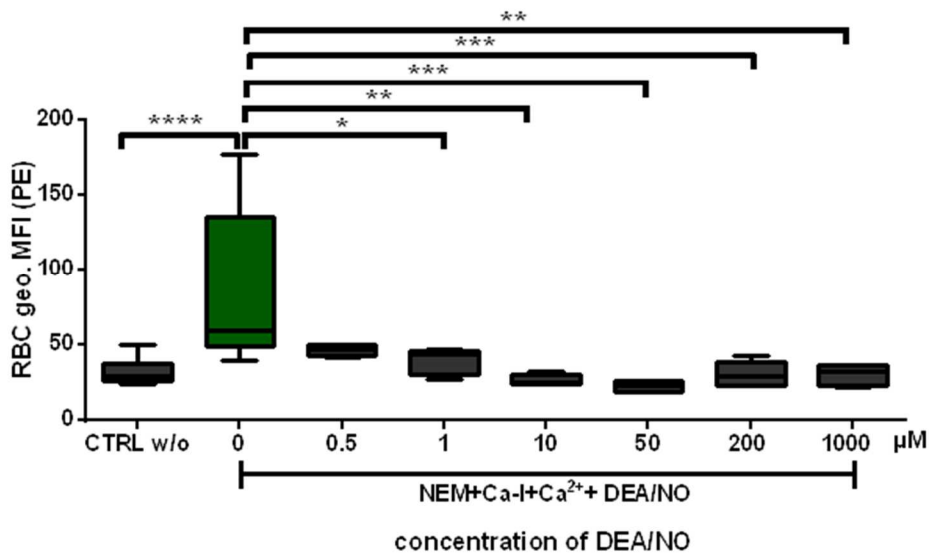


Figure 26: DEA/NO decreases NEM/Ca-I/CaCl₂ induced PS exposure

Concentration dependent effect of DEA/NO on NEM/Ca-I/CaCl₂ induced PS exposure. Human RBCs were treated for 1 hour at 37°C with 10 mM NEM/ 4 μM Ca-I/ 1 mM CaCl₂ ± increasing concentrations of DEA/NO (0-1000 μM). PS exposure was analyzed via Annexin V-PE with flow cytometry. Data are expressed as median in a Tukey distribution plot against geometric mean of RBC, unpaired one-way ANOVA against 0: post hoc test: Dunnett (CTRL w/o, 0: n= 15, 0.5, 10, 50 μM: n=4, 1.0, 1000 μM: n=5, 200 μM: n=7), * p ≤ 0.05; ** p ≤ 0.01, *** p ≤ 0.001, **** p ≤ 0.0001.

Figure 26 shows that NO treatment leads to a significant decrease of PS exposure at a range of concentrations from 1 to 1000 μM . Therefore, these results demonstrate that extracellular NO blocks PS exposure evoked by NEM, Ca-I and CaCl_2 .

4.2.3 PS exposure is sGC/cGMP independent

The next aim was to verify whether the effects of extracellular NO on PS exposure on activation of sGC and increase in cGMP levels. Therefore, PS exposure was induced by NEM, Ca-I and CaCl_2 and cells were additionally incubated with the sGC stimulator BAY-41 (10 μM) and DEA/NO (200 μM) \pm sGC inhibitor ODQ (5 μM) (Figure 27 (A)). ODQ was used as an sGC inhibitor, because it is able to inactivate sGC by oxidation of the heme from Fe^{2+} - to Fe^{3+} -form. In this state, sGC cannot be stimulated by NO and BAY-41.

The pharmacological agents were coincubated in different combinations as indicated in Figure 27 (B) with NEM, Ca-I and CaCl_2 for 1 hour at 37°C and affected RBCs were labeled with Annexin V-PE. Fluorescent data were analyzed as described above by determining RBC geo. MFI and % of PE+ RBCs. Because both analyses showed same results, only geometric mean is shown in the figures.

Figure 27 (A) shows that treatment of RBCs with DEA/NO \pm BAY-41 leads significant decreases of PS exposure compared to CTRL (NEM/Ca-I/ CaCl_2). Furthermore, there are no differences in PS exposure of RBCs between DEA/NO treatment alone and with BAY-41-2272. Moreover, BAY-41 alone has no effect on PS exposure. This means that BAY-41 has no effect on PS exposure.

The addition of ODQ doesn't change the effect of BAY-41+ DEA/NO, indicating that the effects of NO on PS exposure regulation are sGC independent.

As a control, RBCs were also treated with stable cell permeable cGMP derivate CPT-cGMP (Figure 27 (B)) at concentrations ranging from 1 μM to 1 mM. Similar to sGC stimulation, also cGMP did not affect PS exposure.

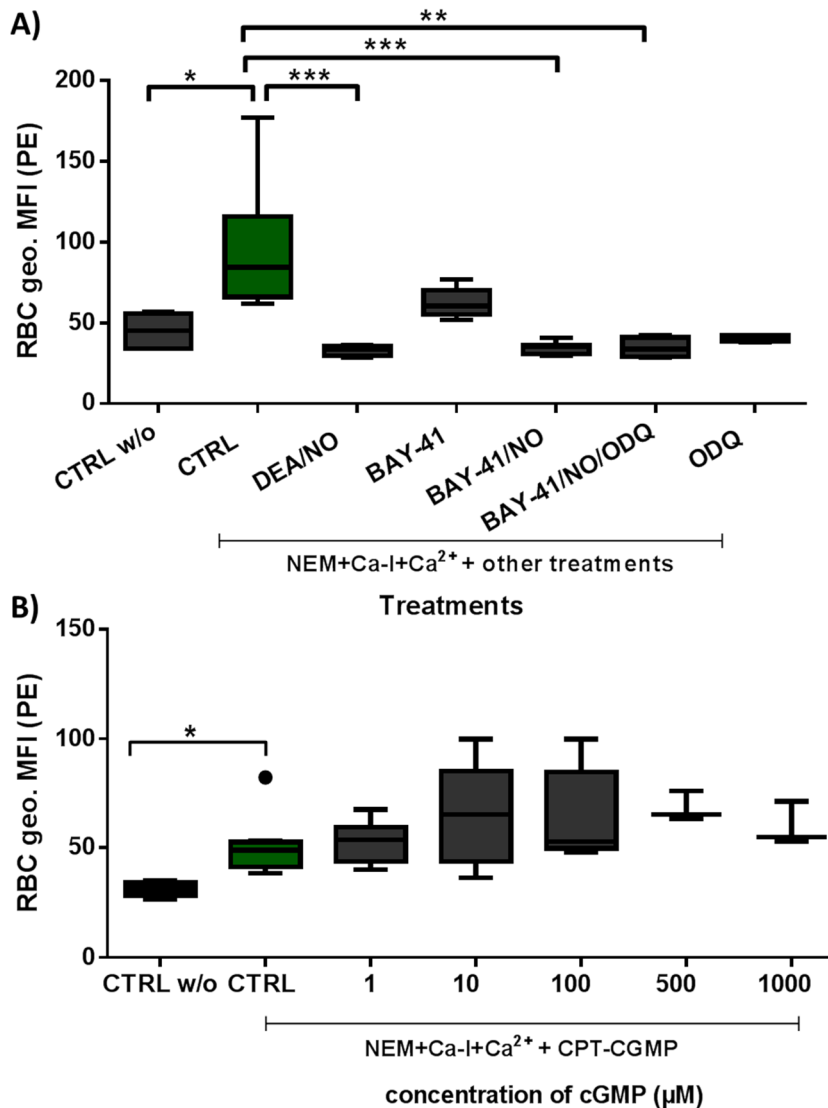


Figure 27: Effects of DEA/NO on PS exposure in RBCs are independent of sGC/cGMP signaling

(A) No effects of sGC stimulator BAY-41 (10 μM) and sGC inhibitor ODQ (5 μM) on PS exposure of RBCs in presence of NEM/Ca-I/CaCl₂ ± DEA/NO (NO, 200 μM). Human RBCs were incubated with the treatments for 1 hour at 37°C and samples were analyzed via Annexin V-PE with flow cytometry, Data are expressed as median in a Tukey distribution plot against geometric mean of RBC, Kruskal-Wallis against CTRL: post hoc test: Dunn's (CTRLw/o, CTRL: n=9, DEA/NO, BAY-41: n=5, BAY-41/NO: n=7, BAY-41/NO/ODQ, ODQ: n=4) * p ≤ 0.05, ** p ≤ 0.01, *** p ≤ 0.001. (B) No concentration dependent effects of 8-CPT-cGMP on NEM/Ca-I/CaCl₂ induced PS exposure. Human RBCs were treated for 1 hour at 37°C with 10 mM NEM/ 4 μM Ca-I/ 1 mM CaCl₂ (NEM) ± increasing concentrations of CPT-cGMP. PS exposure was analyzed via Annexin V-PE with flow cytometry. Data are expressed as median in a Tukey distribution plot against geometric mean of RBC, unpaired one-way ANOVA against CTRL: post hoc test: Dunnett (1000 μM: n=3, all other treatments: n=5), * p ≤ 0.05.

In conclusion, treatment with NO protects RBCs against Ca²⁺/Ca-I/NEM induced PS exposure, but these effects are not dependent on activation of sGC/cGMP pathway.

4.3 Part 3: Patient study I

The third aim of the study aimed to analyze whether non-canonical functions of RBCs are affected by pathological conditions like CKD and CAD. Therefore, 2 independent studies were performed.

4.3.1 Red cell eNOS expression is decreased in CKD

Di Pietro et al. from the Department of medical, oral and biotechnological sciences and the aging research center and translational medicine CeSI-MeT, Chieti, Italy, performed a clinical study with patients with CKD[204].

It has been proposed in the past, RBCs from CKD patients have impaired deformability or life span [221]. However, up to now little is known about the regulation of the red cell eNOS/NO pathway in CKD and CAD. The general aim of the study was to evaluate, whether red cell eNOS/NO signaling is affected in CKD.

Table 17 reports the demographic and clinical characteristics of the study population.

Table 17: Demographic and clinical characteristics of the study population (CKD) [204]

	Control (n = 18)	Hemodialysis (n = 27)	P-value
Gender (M/F)	(7/11)	(16/11)	
Age (years)	57.1 ± 9.4	65.3 ± 11.2	0.143
Systolic blood pressure (mmHg)	121.9 ± 11.4	118.5 ± 17.4	0.655
Diastolic blood pressure (mmHg)	74.1 ± 6.8	73.1 ± 10.4	0.413
Hb (g/dl)	13.6 ± 1.7	10.9 ± 2.1	<0.001
Creatinine (mg/dl)	1.0 ± 0.2	9.1 ± 2.5	<0.001
Body mass index	23.2 ± 1.4	22.5 ± 2.2	0.577

The study included patients suffering from CKD (n=27) and age- and gender-matched controls (n=18). The study population (age 18-75) was recruited at the dialysis center of the University Hospital of Chieti.

All patients have been treated with hemodialysis for more than 6 months. The CKD was caused by nephroangiosclerosis (n=13), chronic glomerulonephritis (n=7), chronic interstitial nephritis (n=4) or unknown (n=3). Patients with diabetes mellitus, uncontrolled hypertension, active infections, malignant or inflammatory disease, blood transfusion over the past 3 months, iron and folic acid deficiency, use of drugs that might interfere with erythropoiesis were excluded. Furthermore, patients who used NO donors were excluded from the study.

CKD patients were treated with erythropoietin dosage and got dialysis three times a week (4-h dialysis via bicarbonate dialysate and membranes of polysulphone (n = 12) or polyacrylonitrile (n=15). Other exclusion criteria for the healthy controls were medications, abnormalities on routine physical examination, standard laboratory tests, ECG, or chest x-ray. The study was approved by the Ethics Committee of the University of Chieti and was performed in accordance to the Declaration of Helsinki. Written informed consent was obtained from all subjects taking part in the study.

The data of Table 17 was observed by the Department of medical, oral and biotechnological sciences and the aging research center and translational medicine CeSI-MeT, Chieti, Italy [204]. The p-value was calculated by T-test.

To verify whether red cell eNOS expression is affected in CKD, frozen RBC pellets obtained by the described patient cohort were analyzed via immunoprecipitation and western blot. For normalization, an internal control (HUVECs) was used to generate comparable data. Figure 28 shows that red cell eNOS expression is decreased in CKD compared to healthy controls (135 kDa band).

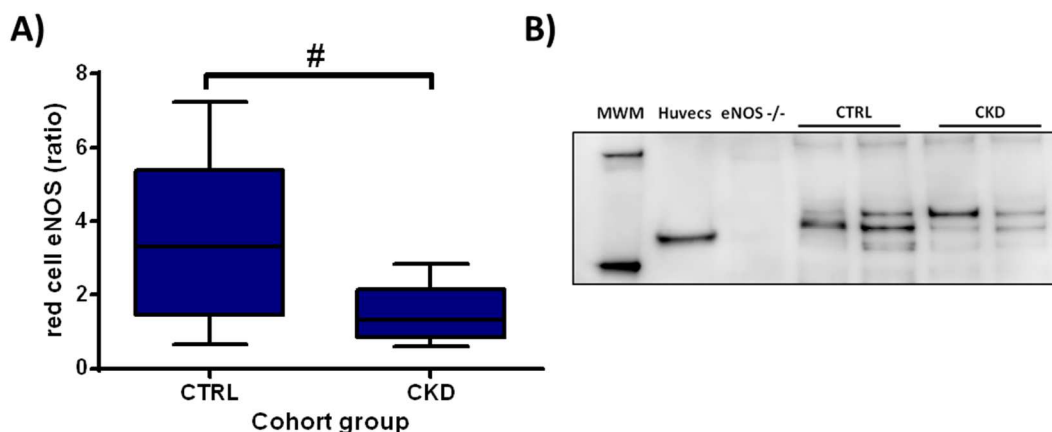


Figure 28: Red cell eNOS expression is decreased in CKD

Red cell eNOS expression of patients with CKD (CKD) compared to age-matched controls was measured from frozen RBC pellets after immunoprecipitation and western blot analysis. (A) Representative western blot gel modified by photoshop following the guidelines of good scientific practice. (B) Levels of red cell eNOS expression in CKD calculated against eNOS-expression of HUVECs (positive control) compared to healthy controls, data are expressed as median in a Tukey distribution plot, unpaired T-test, CTRL: n=8, CKD: n=10, # $p \leq 0.05$. Outlier analysis was performed graphically by box & whiskers plots according to Tukey.

4.3.2 Patient study II: Role of RBC functions in CAD and ACS

Here we aimed to verify whether red cell eNOS/NO signaling from RBC might play a role in CVD. Therefore, RBC functions of patients with CAD, ACS and healthy age-matched controls were characterized. This included the analysis of:

1. Red cell eNOS-expression
2. NO metabolism
3. Redox-state
4. PS exposure
5. Rheological parameters (deformability and aggregability)

For this aim, patients with CAD and ACS and healthy individuals without CAD and medication were recruited from the Department of Cardiology, Pulmonology and Angiology, Düsseldorf.

Figure 29 shows an overview of the study design. As described here, patients with acute inflammation (CRP >1.0 mg/dl, blood leukocytes >11000/ μ l), malignancies, pregnancy, or treatments with NOS/NO/sGC affecting drugs were excluded from the study.

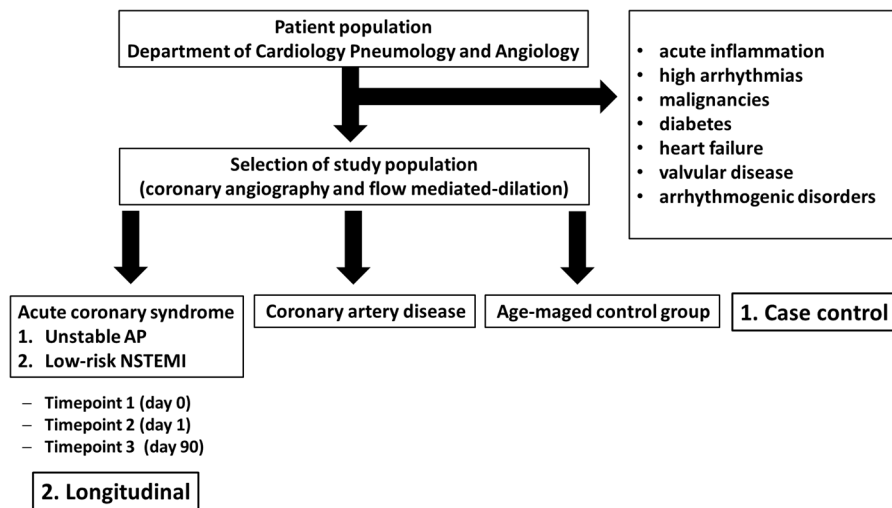


Figure 29: Study design of CAD and ACS study

To investigate, whether red cell eNOS/NO-mediated RBC dysfunctions might play a role in CVD, a patient study with patients from Department of Cardiology, Pulmonology and Angiology in Düsseldorf was performed. These included patients with ACS, CAD and age-matched controls. Exclusion criteria and study-characteristic are mentioned in the figure.

Figure 30 shows the study protocol including the used methods and analyzed parameters. Grayed parts of were part of the patient study, but described in this dissertation.

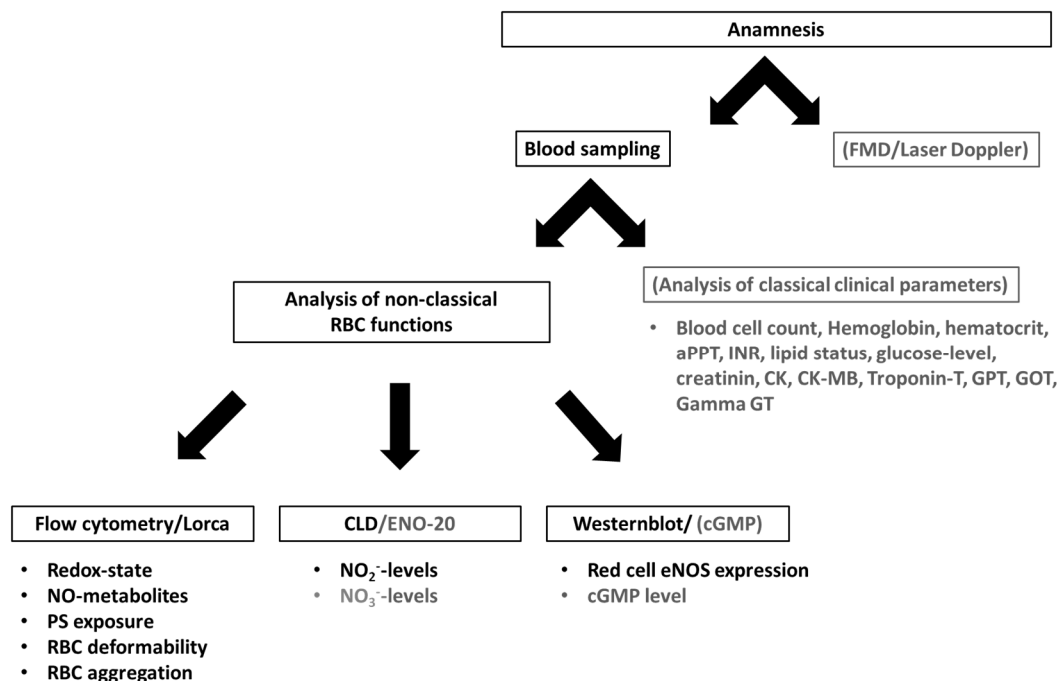


Figure 30: Overview of CAD and ACS study

The figure shows the parameters analyzed in the study following a defined protocol. These included physiological parameters (laser doppler, FMD as well as analysis of biochemical parameters (red cell eNOS expression, NO₂⁻-levels, redox-state, deformability...).

Demographic and clinical characteristics of CAD and ACS patients and healthy controls are reported in Table 18.

Table 18: Demographic and clinical characteristics of the study population (CAD, ACS)

	Stable CAD (n=20)			ACS (n=8)			Control (n=25)			P-value
Age (years)	59	±	10	51	±	10	54	±	6	ns
Weight (kg)	82	±	12	99	±	20	88	±	9	** (stable CAD vs. ACS)
Height (cm)	175	±	6	181	±	5	180	±	6	* (stable CAD vs. control)
Body mass index (kg/m ²)	26.8	±	4.1	30.3	±	5.4	27.2	±	2.8	ns
RRsystole (mmHg)	131	±	14	138	±	12	133	±	9	ns
RRdiastole (mmHg)	79	±	11	82	±	4	85	±	10	ns
Heart frequency (beats/sec)	63.2	±	8.7	64.4	±	10.3	67.9	±	7.5	ns
HbA1c (%)	5.5	±	0.4	5.5	±	0.2	5.4	±	0.3	ns
Creatinin (mg/dl)	1.0	±	0.2	1.0	±	0.1	1.0	±	0.1	ns
glomerular filtration rate (MDRD)	78.8	±	15.8	86.7	±	10.6	82.0	±	16.8	ns
Cholesterin (mg/dl)	164.0	±	32.4	188.5	±	28.2	210.7	±	42.8	*** (stable CAD vs. control)
low density lipoprotein (LDL) (mg/dl)	96.8	±	22.7	128.3	±	26.2	148.6	±	39.8	**** (stable CAD vs. control)
high density lipoprotein (mg/dl)	52.8	±	13.4	47.1	±	14.2	57.5	±	14.3	ns
CRP (mg/dl)	0.2	±	0.2	0.3	±	0.1	0.3	±	0.2	ns
Pack years (median)	30	range	0-100	20	range	0-40	10	range	0-50	** (stable CAD vs. control)
Risk factors (0-4; median)	3	range	1-4	3	range	1-4	1	range	0-3	*** (stable CAD/ACS vs. control)
RBC indices										
Hb (g/dl)	14.6	±	0.8	14.6	±	0.6	14.9	±	1.1	ns
RBC number (cells*10 ⁶ /μl)	4.7	±	0.4	4.8	±	0.3	4.9	±	0.4	ns
Hct (%)	43.1	±	2.6	43.5	±	1.9	43.8	±	3.0	ns
MCV (fl)	91.0	±	3.1	90.9	±	2.1	89.7	±	3.7	ns
MCH (pg)	30.8	±	1.2	30.5	±	0.9	30.4	±	1.3	ns
MCHC (g Hb/dl)	33.9	±	0.8	33.5	±	0.9	33.9	±	0.7	ns
RBC distribution width (%)	13.6	±	1.0	13.5	±	0.5	13.2	±	0.5	ns

Most patient data were in the same range. All patients were 50-60 years old, weighed about 80-100 kg and had a height from 170-180 cm. Moreover, CAD patients had higher cholesterol and LDL levels compared to controls. Furthermore, CAD and ACS patients had more risk factors than healthy volunteers. The p-value was calculated by one-way ANOVA against each group and post hoc test Bonferroni was chosen. All data were collected by Dr. med G. Wolff from the department of Cardiology, Pulmonology and Angiology, Düsseldorf, Germany.

4.3.2.1 Red cell eNOS expression is decreased in CAD

To verify whether NO synthesis of RBCs from patients with in CAD and ACS is changes, the levels of red cell eNOS expression was investigated. Figure 31 shows that red cell eNOS expression is decreased in CAD and ACS compared to healthy control (135 kDa band).

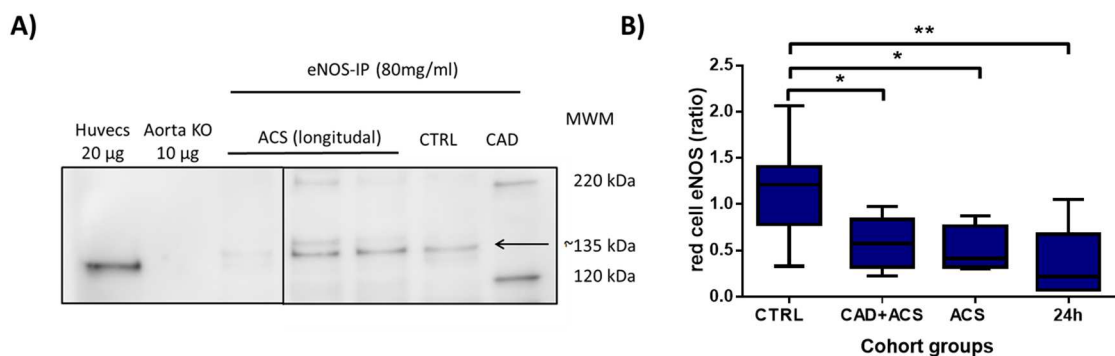


Figure 31: Red cell eNOS expression is decreased in CAD and ACS

Red cell eNOS expression of patients with CAD and ACS compared to age-matched controls was measured from frozen RBC pellets after immunoprecipitation and western blot analysis. (A) Representative western blot gel modified by photoshop following the guidelines of good scientific practice. (B) Levels of red cell eNOS expression in CAD and ACS calculated against eNOS-expression of HUVECs (positive control) compared to healthy controls, data are expressed as median in a Tukey distribution plot, unpaired one-way ANOVA against CTRL: post hoc test: Dunnetts, CTRL: n=10, CAD (+ACS): n=8, ACS (t=0; t=1): n=5, * p ≤ 0.05; ** p ≤ 0.01. Outlier analysis was performed graphically by box & whiskers plots according to Tukey.

4.3.2.2 Levels of NO and NO₂⁻ are unchanged in CAD

The next aim was to investigate whether levels of NO metabolites are effected in RBCs from patients with CAD and ACS. NO level were analyzed by loading RBCs with DAF-FM-DA and flow cytometry in presence and absence of NOS-Inhibitor

L-NAME (3 mM) for 30 minutes at 37°C (Figure 32 (A)). Moreover, the levels of NO_2^- of RBCs were measured by CLD.

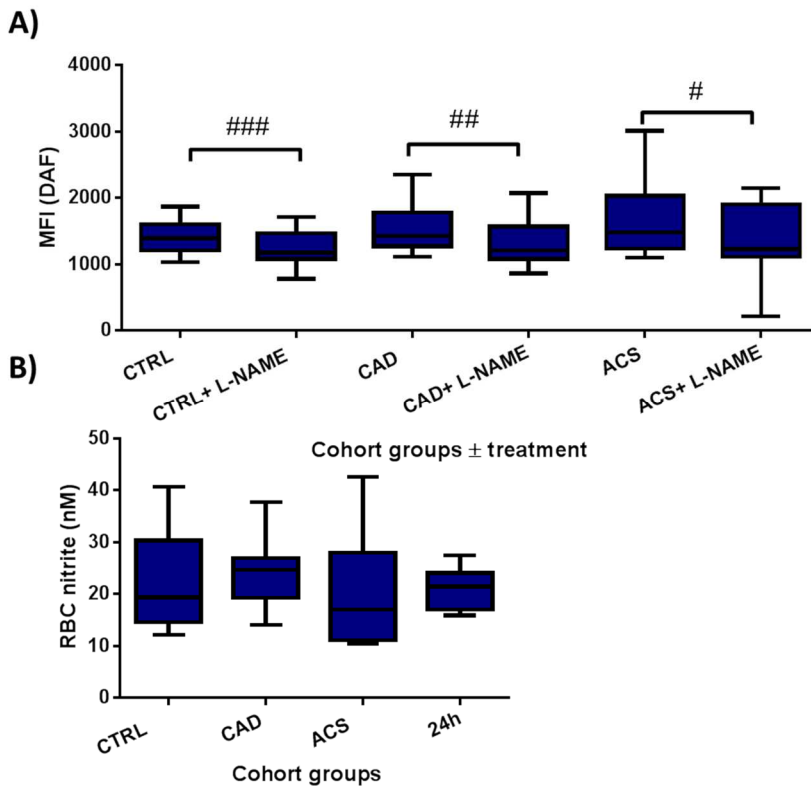


Figure 32: Levels of NO and NO_2^- are unchanged in CAD and ACS

(A) Levels of NO from human whole blood of all cohorts are decreased in presence of NOS inhibitor L-NAME, but basal levels of NO are unchanged. Whole blood samples were incubated in absence or presence of NOS inhibitor L-NAME (3 mM) and analyzed via DAF-FM-DA with flow cytometry, data are expressed as median in a Tukey distribution plot, unpaired one-way ANOVA against CTRL: Dunetts post hoc test, CTRL: $n=22$, CAD: $n=18$, ACS ($t=0$ - $t=3$): $n=19$, *n.s.*, paired T-test CTRL against L-NAME, # $p \leq 0.05$; ## $p \leq 0.01$, ### $p \leq 0.001$. Outlier analysis was performed graphically by box & whiskers plots according to Tukey, *n.s.*

(B) NO_2^- levels are unchanged in CAD and ACS. NO_2^- levels of frozen RBC pellets of all cohort groups were measured via CLD, data are expressed as median in a Tukey distribution plot, unpaired one-way ANOVA against CTRL: Dunetts post hoc test, CTRL: $n=14$, CAD: $n=12$, ACS ($t=0$): $n=6$, $t=1$ (24h): $n=7$, *n.s.* Outlier analysis was performed graphically by box & whiskers plots according to Tukey. The experiment was performed by medical student Claudio Parco from the department of Cardiology, Pulmonology and Angiology, Düsseldorf, Germany.

The figure shows that there are no differences in basal NO levels or between the cohort groups. The figure further shows that the levels of NO decrease in presence of NOS inhibitor, indicating red cell eNOS dependence of basal NO levels in RBCs. The figure shows that NO_2^- concentrations are unchanged in CAD

and ACS compared to healthy control. NO metabolite levels are NOS-dependent since levels are decreasing in presence of NOS inhibitor L-NAME, although basal NO metabolite- and NO_2^- - levels are unchanged in CAD and ACS. Furthermore, red cell eNOS expression is decreased in RBCs from CAD and ACS. In conclusion, although red cell eNOS expression is decreased, the levels of NO metabolites are preserved in CVD.

4.3.2.3 Redox-state is preserved in CAD and ACS

RBCs are equipped with highly effective antioxidant systems such as non-enzymatic, but also enzymatic anti-oxidative factors [159-162]. To analyze possible changes of RBC redox-state in CAD and ACS, ROS-levels and thiol-levels were evaluated (Figure 33).

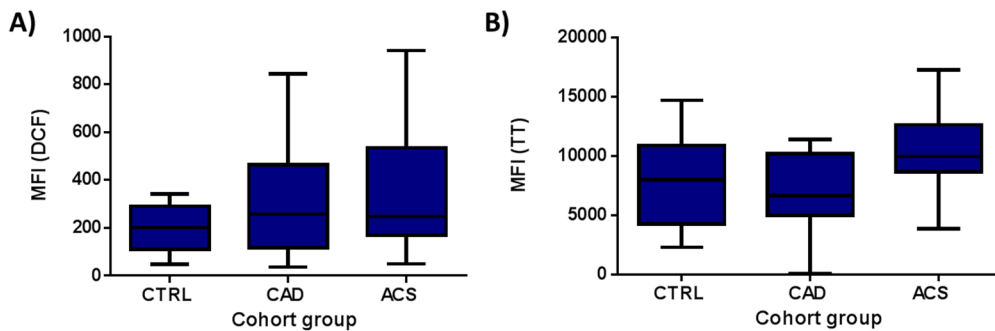


Figure 33: No differences of ROS- and thiol levels in CAD and ACS

(A) No changes of ROS levels in RBCs from patients with CAD and ACS versus age-matched controls. Human whole blood of all cohorts was analyzed via DCF with flow cytometry. Data are expressed as median in a Tukey distribution plot, unpaired one-way ANOVA against CTRL: Dunetts post hoc test, CTRL: n=25, CAD: n=19, ACS (t=0-t=3): n=20, n.s. Outlier analysis was performed graphically by box & whiskers plots according to Tukey. (B) No differences in free thiol levels in human RBCs from CAD and ACS compared to age-matched controls. Human whole blood of all cohorts was analyzed via ThiolTracker™ with flow cytometry. Data are expressed as median in a Tukey distribution plot, unpaired one-way ANOVA against CTRL: Dunetts post hoc test, CTRL: n=20, CAD: n=17, ACS (t=0-t=3): n=17, n.s. Outlier analysis was performed graphically by box & whiskers plots according to Tukey. The experiment was performed together with medical student Thirumakal Manokaran from the department of Cardiology, Pulmonology and Angiology, Düsseldorf, Germany.

Figure 33 (A) shows that ROS levels measured via loading with DCF with flow cytometry are unchanged in CAD and ACS. Furthermore, Figure 33 (B) shows that levels of reduced thiols detected by ThiolTracker™ are preserved in CAD compared to health matched controls.

To verify whether glutathione levels are changed in RBC in CAD and ACS, glutathione concentrations were analyzed. Therefore amount of GSH and tGSH, as well as GSSG was assessed by derivatization of GSH with fluorescence molecules in a glutathione reductase based assay (Figure 34).

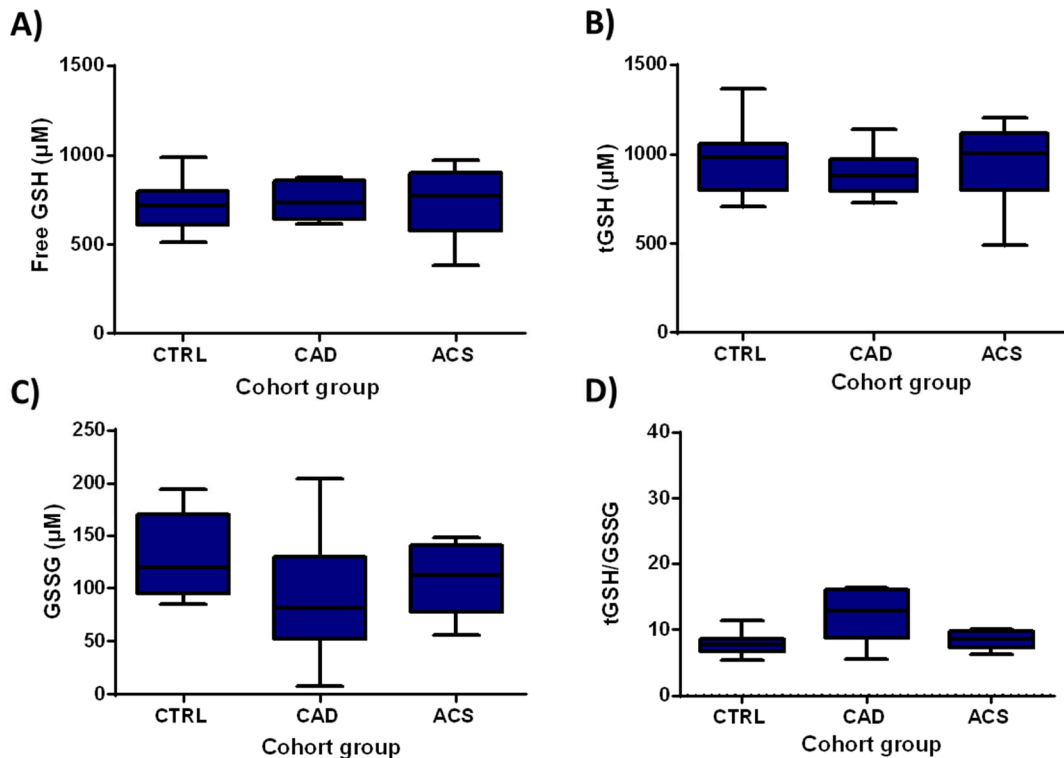


Figure 34: No changes of glutathione levels in CAD and ACS

Measurement of glutathione from frozen RBC pellets from patients with CAD and ACS compared to age-matched controls measured via glutathione detection kit (Arbor). No differences in (A) free GSH (B) total GSH (C) GSSG and (D) tGSH/GSSG. Data are expressed as median in a Tukey distribution plot, unpaired one-way ANOVA against CTRL: Dunetts post hoc test, CTRL: n=14, CAD: n=8, ACS (t=0-t=3): n=9, n.s. Outlier analysis was performed graphically by box & whiskers plots according to Tukey.

Figure 34 shows that GSH (A), tGSH (B)) as well as GSSG (C) and tGSH/GSSG ratio (D) are unchanged in CAD and ACS.

In conclusion, the results indicate that redox-state of RBCs is preserved in CAD and ACS.

4.3.2.4 PS exposure is unchanged in patients with CAD and ACS

The next aim was to reveal whether RBCs from patients with CAD and ACS show increased PS exposure. Therefore, PS exposure from RBCs was analyzed via flow cytometry.

Figure 35 shows that PS exposure is unchanged in CAD and ACS compared to age-matched controls.

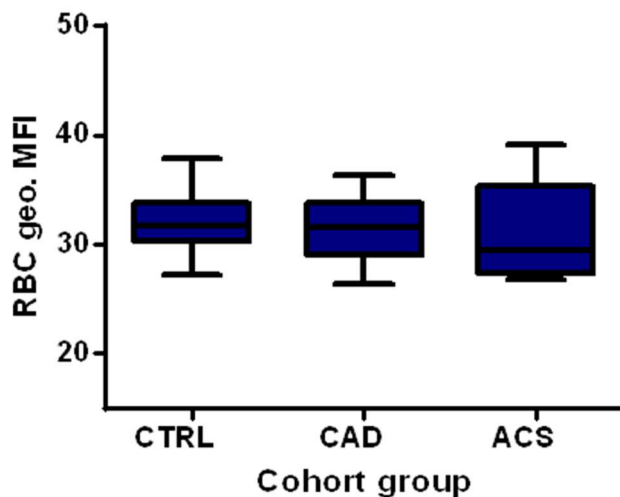


Figure 35: No changes in PS exposure in patients with CAD and ACS

PS exposure of human whole blood of patients with CAD and ACS compared to age-matched control group was analyzed via Annexin V-PE with flow cytometry. Data are expressed as median in a Tukey distribution plot against FI, unpaired one-way ANOVA against CTRL: Dunetts post hoc test, CTRL: n=19, CAD: n=11, ACS (t=0): n=8, n.s. Outlier analysis was performed by box & whiskers plots according to Tukey. Measurements were performed together with medical student Thirumakal Manokaran from the department of Cardiology, Pulmonology and Angiology, Düsseldorf, Germany.

In conclusion, RBCs compensate changes of membrane symmetry in CVD.

4.3.2.5 Rheological parameters

RBCs are a major determinant of blood viscosity, because of their high number and mechanical properties including deformation and aggregation. To verify changes in rheological parameters, deformability and aggregability of RBCs were analyzed by ectacytometry.

4.3.2.5.1 Aggregability is increased in ACS

Aggregability is displayed as AI. This index is calculated from $t_{1/2}$, the time, which RBCs take to aggregate and AMP, the amplitude, which defines the aggregation strength. For aggregability measurement, whole blood was measured against time (Figure 36).

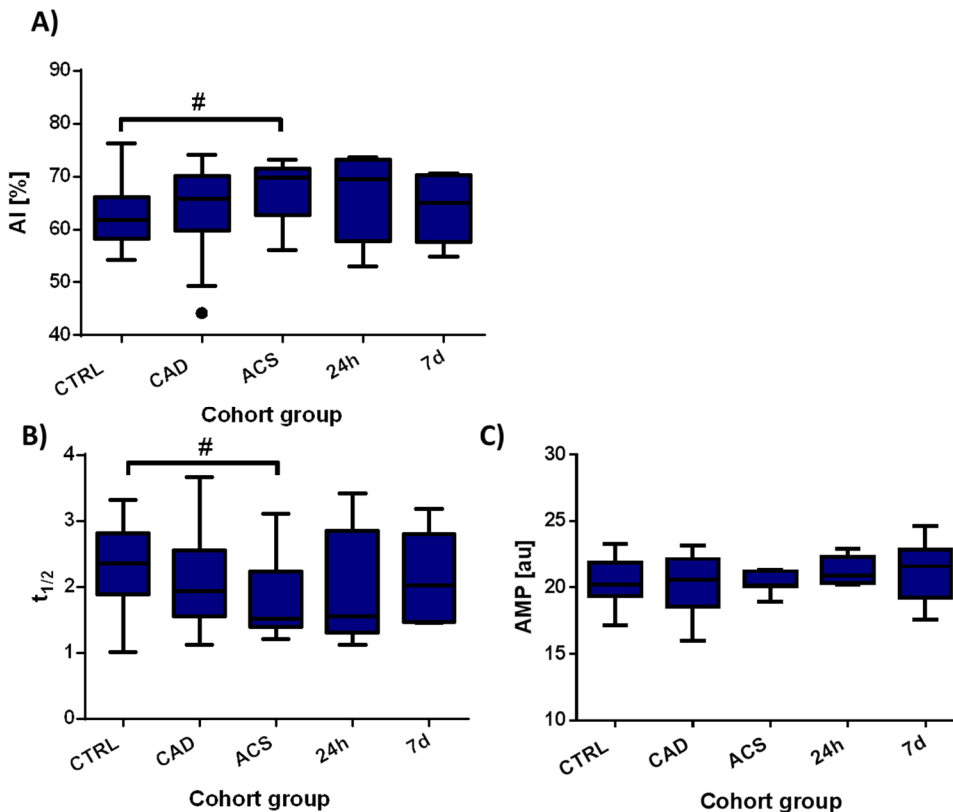


Figure 36: RBC Aggregability is increased in ACS

Measurement of RBC aggregability from whole blood of patients with CAD and ACS compared to age-matched controls via Lorca. (A) AI is increased in ACS ($t=0$), data are expressed as median in a Tukey distribution plot, unpaired T-test, CTRL: $n=25$, CAD: $n=21$, ACS ($t=0-t=3$): $n=7$ each, # $p \leq 0.05$. (B) $t_{1/2}$ is decreased in ACS ($t=0$), data are expressed as median in a Tukey distribution plot, unpaired T-test, CTRL: $n=25$, CAD: $n=19$, ACS ($t=0-t=3$): $n=7$ each, # $p \leq 0.05$. (C) AMP (au) is unchanged in ACS and CAD, data are expressed as median in a Tukey distribution plot, unpaired T-test, CTRL: $n=20$, CAD: $n=21$, ACS ($t=0-t=3$): $n=7$ each. Outlier analysis was performed graphically by box & whiskers plots according to Tukey. All aggregability experiments were performed by medical student Jonathan Schmith from the department of Cardiology, Pulmonology and Angiology, Düsseldorf, Germany. Outlier analysis was performed graphically by box & whiskers plots according to Tukey

Figure 36 (A) shows that aggregability (as AI) is increased in ACS ($t=0$), but not after 24 h and 7 days after ACS treatment. Figure 36 (B) and (C) indicate that $t_{1/2}$

is decreased in ACS whereas AMP (au) is unchanged. These data show that RBCs from patients with ACS have increased aggregability as compared to healthy controls.

4.3.2.5.2 Deformability is unchanged in CAD and ACS

RBC deformability was observed by ektacytometry. This method is based on the ability of RBCs to deform from their typically biconcave to an elliptic form in response of increasing shear stresses. For analysis, deformability was induced by stepwise increase of shear-stress and cell deformation was displayed as EI. This index is defined by the shape of the RBC to allow comparison of RBC deformability behavior from different cohort groups (Figure 37).

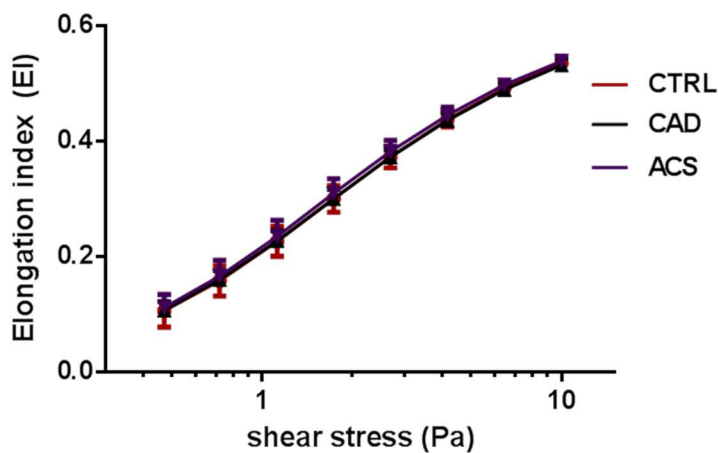


Figure 37: RBC deformability is unchanged in CAD and ACS

Measurement of RBC deformability from diluted whole blood of patients with CAD and ACS compared to age-matched controls via Lorca. Deformability (EI) of RBCs was measured against increasing shear stresses from 0,3 Pa to 10 Pa, data are expressed as mean \pm standard deviation of mean, two-way ANOVA, CTRL: $n=23$, CAD: $n=20$, ACS ($t=0$): $n=8$, n.s. Outlier analysis was performed graphically by box & whiskers plots according to Tukey. All deformability experiments were performed by medical student Jonathan Schmidh from the department of Cardiology, Pulmonology and Angiology, Düsseldorf, Germany.

Figure 37 shows that deformability is unchanged in RBCs from CAD and ACS patients. Taken together, the present data demonstrate that rheological parameters like aggregability are increased in ACS, but not in CAD. Moreover, deformability is preserved in both cohort groups.

5 Discussion

The main hypothesis of this study was that non-canonical functions of RBCs may be affected in CVD.

This study aimed to characterize non-canonical functions of RBCs from healthy young individuals and from patients with CAD and CKD, as compared to age-matched controls. The main goals were to analyze pathways regulating (1.) ATP release and (2.) PS exposure of RBCs, as well as (3.) to characterize non-canonical RBC functions in RBCs from CAD or CKD patients. Figure 38 describes the main goals of the present study.

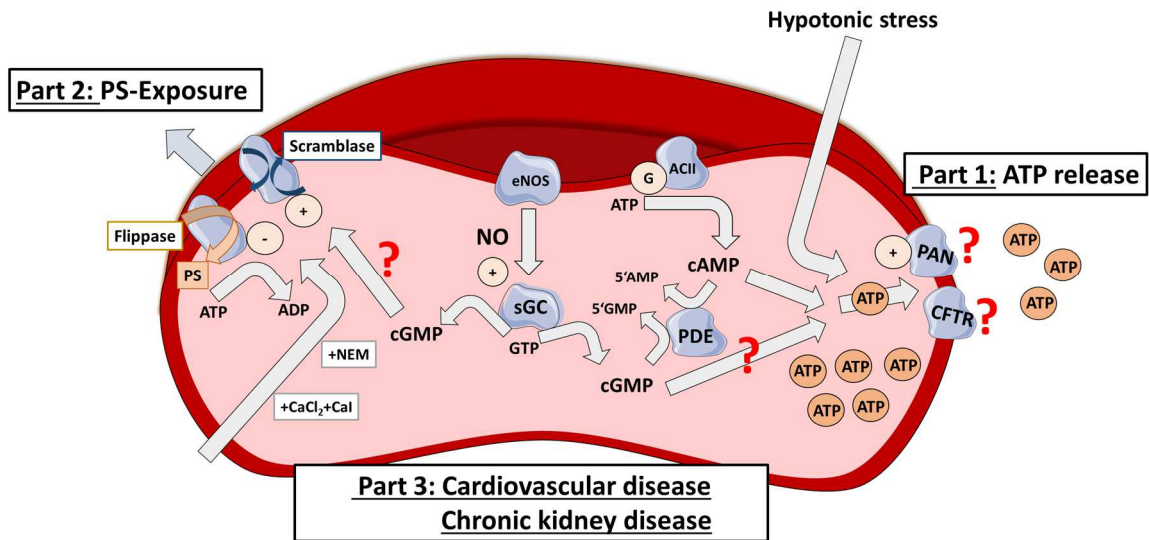


Figure 38: Aims and goals of the present study

The main findings of this study were the following:

(1.) The first goal (part 1) was to assess whether sGC/cGMP and cAMP signaling is involved in ATP release from RBCs. The present results show that sGC/cGMP as well as cAMP signaling do not regulate ATP release from RBCs.

(2.) Part 1 further aimed to investigate whether PDE inhibition or hypotonic stress induce ATP release and whether these are downstream dependent of Pnx-1 or CFTR. Data presented in this work demonstrate that ATP release is induced by hypotonic stress and PDE inhibition and that this release is not controlled via Pnx-1 channel, but that PDE mediated effects are downstream regulated via CFTR.

(3.) The second goal (part 2) was to analyze whether sGC/cGMP signaling might play a role in the NO-mediated regulation of PS exposure in RBCs. For these studies, ATP release and PS exposure were examined by pharmacological activation-and inhibition or direct incubation with stable derivatives of the second messengers. The data presented here show that treatment of RBCs with NO prevents $\text{Ca}^{2+}/\text{Ca-I}/\text{NEM}$ induced exposure of PS in RBCs, but the sGC/cGMP signaling is not involved in regulation of PS exposure.

(4.) The third goal (part 3) was to assess whether functional properties like redox-state, NO metabolism and membrane characteristics of RBCs are affected in patients with cardiovascular- and renal disease to identify possible changes of RBC functions under pathological conditions. The present results show that cellular redox-state, NO metabolites, RBC deformability and membrane symmetry are preserved in CVD indicating that RBCs are able to compensate in these pathological conditions.

5.1 Part 1: ATP release from RBCs

5.1.1 Technical hurdles of measurement of ATP release: Hemolysis

The present results demonstrate a positive correlation between ATP-concentration and Hb-levels (416 nm) in the supernatant. These data are in line with data of Sikora et al., who showed that hemolysis is a strong confounding parameter in the measurement of ATP release from RBCs [222]. They demonstrated that in most treatments (e.g. mechanical shear stress, hypoxia or pharmacological stimulation), there is a correlation between Hb- and ATP levels indicating presence of hemolysis. Because nM concentrations of ATP are measured in this assay and mM concentrations are present in the cell, a few destroyed cells may lead to increases of ATP in the supernatant. Therefore, it was important to optimize the assay concerning control of Hb levels to avoid systemic hemolysis. Thus, a threshold for Hb was established on the basis of measurement undertaken in untreated RBC suspensions from different donors. Furthermore, Hb levels were measured via UV/VIS spectrum for each sample and correlation curves were made for each experiment. By applying this method, many samples needed to be excluded because of the hemolysis.

As described in Figure 13, basal ATP levels show high variability in human and murine RBCs and thus, normalization was necessary (as done here). Ellsworth et al. [5, 6, 223] and other groups [90, 100, 111, 125, 126, 137, 212] used the same assay system, but measured ATP from RBC suspensions directly, not from the centrifuged supernatant. One advantage of usage of the supernatant is that ATP levels can directly be compared to Hb-levels from the same treatment and no further steps, which could interfere the result, were included. A further advantage of centrifugation is that extracellular ATP was separated from RBCs which are carrying membrane-bound ectonucleotidases [224].

Since Hb-levels were not reported in previous publications, data should be critically evaluated. The findings of the present study mainly support this by showing that cAMP application does not induce ATP release from RBCs which contradicts to previous published data [100]. However, the data which we observed by our study are in line with data of Sikora et al., who demonstrated that AC activation via forskolin does not affect ATP release from RBCs and further that its application induces hemolysis [222]. Taken together, the present study shows for the first time that hemolysis mediated ATP release can be minimized with adequate handling. For future studies, insertion of a threshold for Hb-levels (absorbance at 540 nm) should be taken into account for proper analysis of ATP signaling without side effects of hemolysis.

5.1.2 Hypotonic stress induces ATP release independent of hemolysis

The present study shows that hypotonic stress induces ATP release from murine WT RBCs independent of hemolysis. In contrast, Sikora et al. demonstrated that there is a correlation between Hb- and ATP-levels at hypotonic treatment in their setup [222]. A possible reason for the missing of reproducibility by Sikora et al. might be the incubation time of 5 and 15 minutes. In this study, the incubation time was 30 seconds followed by direct centrifugation and separation of the supernatant from the RBCs. This is supported by the data of the present study which shows that steady state ATP levels are decreasing with time. Moreover, these data are in line with results of Coade et al., who demonstrated that ATP is degraded to adenosine diphosphate (ADP) and adenosine monophosphate

(AMP) within 15 minutes in whole blood by ectonucleotidases [224]. In conclusion, the present data indicate that hypotonic stress induces ATP release from RBCs independent of hemolysis.

5.1.3 PDE inhibition induces ATP release

Phosphodiesterases have been proposed to play a main role in the regulation of ATP release [119]. The present findings indicate that PDE 5 inhibition by 100 μ M Sil induces ATP release from RBCs.

It has been reported previously that cGMP as well as cAMP specific PDEs are present in RBCs. Briefly, Sprague et al. verified the expression of different PDEs in the cytosol of RBCs; PDE4D, 3A and 5A [125]. However, Knebel et al. demonstrated that PDE 5 inhibition leads to a potentiation of ATP release in prostacyclin receptor activation [215]. Furthermore PDE3 inhibition has been proposed to function as ATP-release-restore in diabetes patients under hypoxia [212]. Indeed, our study is in line with these results that PDE regulation is involved in ATP release from RBCs.

A possible explanation of this is that the concentration of Sil applied here may lead to inactivation of other isoforms of PDE [225]. Lower concentrations of Sil (100 nM) did not lead to any differences in ATP levels suggesting that PDE 5 might not be alone involved in regulation of ATP release. In contrast to our own data with Sil, Sprague et al. found out that incubation with the unspecific PDE inhibitor 3-isobutyl-1-methylxanthine (IBMX) for 2 minutes does not induce ATP release from RBCs [100]. These contrasting results may be based on differences in incubation time (2 minutes IBMX vs 15 minutes Sil) and specificity, which might be solved by dose-response curves.

The present study demonstrates that application of CPT-cAMP or CPT-cGMP has no effect on ATP release in mouse RBCs. However, other groups showed that cAMP-application results in ATP release from RBCs [100]. Briefly, human and rabbit RBCs suspensions were incubated with 100 μ M of stable cAMP derivate sp-cAMP for 30 minutes [100]. Moreover, it was demonstrated that activation of G_i by mastoparan results in an increase of cAMP levels via ACII [104,

108-111] and induces ATP release from RBCs. A possible explanation for these contradictions might be lack of permeability of the synthetic cAMP and cGMP derivatives. Taken together, the present study shows that PDE inhibition induces ATP release from RBCs. However, the mechanisms of PDE inhibition were not clarified in this study since cAMP and cGMP both did not induce ATP release. Experiments analyzing the role of PDEs in ATP release should be carried out in future investigations.

5.1.4 ATP release is independent of sGC/cGMP signaling

Another aim of the study was to analyze the role of intracellular sGC/cGMP signaling in ATP release from RBCs. The results of this study demonstrate that neither activation of sGC by BAY-41 and NO nor cGMP application induces ATP release from RBCs suggesting that the sGC/cGMP pathway is not involved in ATP release from RBCs.

However, Adderley et al. demonstrated that sGC activation by YC-1 and NO increases cGMP levels in RBCs and further that cGMP application increases cAMP levels in RBCs [125]. Sprague et al. further investigated that hypoxia induced ATP release from RBCs is abolished in patients with diabetes mellitus [90] probably due to reduced levels of G_i [226]. Furthermore, it was shown that hypoxia induced ATP release is PDE3 dependent [212, 214]. In this context, C-peptide and insulin are able to restore this impairment via protein kinase C (PKC) and sGC signaling [101, 227]. In detail, it was demonstrated that coincubation of C-peptide and insulin in physiological ratios recovers hypoxia induced ATP release from RBCs from patients with diabetes mellitus [101]. Since C-peptide downstream activates PKC and sGC [227], C-peptide application leads to increase of intracellular cGMP levels [228, 229] and cGMP-mediated inhibition of PDE3. This results in inhibition of cAMP degradation [230]. Moreover, insulin inhibits hypoxia-induced ATP release in healthy volunteers and this effect is also abolished by C-peptide via PKC and sGC activation [227]. Similar to results of this study, it was shown that sGC inhibition itself by ODQ has no influence on hypoxia-derived ATP release from RBCs from healthy volunteers [101, 227].

Taken together, the data presented here and in the literature indicate that sGC/cGMP signaling is not involved in ATP release from healthy RBCs, but may play a role in situations of dysfunctions of the signaling pathway like decrease of RBC G_i levels in patients with diabetes mellitus [90].

5.1.5 Role of ion channels: Pnx-1 and CFTR

5.1.5.1 Hypotonic stress induced ATP release is Pnx-1 independent

The present study shows that hypotonic stress induced ATP release is not regulated via Pnx-1 as evident by channel blocking with carbenoxolone and probenecid. Furthermore, there is no correlation between Hb and ATP due to previous optimization of the assay. There is evidence that the Pnx-1 channel is expressed on the RBC membrane [145]. In the publication of Locovei et al, it is demonstrated that hypotonic stress induced ATP release is Pnx-1 dependent. This was shown by incubation of RBCs with carbenoxolone, which induced decrease of levels of extracellular ATP [194].

The data of the present study shows that no correlating hemolysis was induced in presence of hypotonic stress or the pharmacological inhibitors of Pnx-1, but also no Pnx-1 dependency of ATP release was present under these conditions suggesting that hypotonic stress induces ATP release from RBCs independent of Pnx-1.

The CFTR channel has been proposed to play a role in ATP release from RBC. The channel has been identified by Sterling et al. at the RBC surface [231]. It was demonstrated in the past that RBCs from CF patients have a reduced number of CFTR molecules at the membrane of RBCs [136]. It was further shown that CF-patients lack ATP release from RBCs in response to mechanical stress [137] suggesting an important role for CFTR in the regulation of ATP release from RBCs. In this study we observed that hypotonic stress induces high levels of hemolysis in RBCs from CFTR KO mice. Although the underlying mechanisms of increased hemolysis cannot be identified based on this study, a possible explanation might be that the CFTR controls the regulatory volume decrease of multiple cell types [232]. This is characterized by osmolyte and water efflux [233,

234] in response to autocrine activation of purinergic receptors via ATP [235, 236]. Therefore, lack of CFTR in RBCs might result in impairment of RBC cell volume regulation in response to hypotonic stress conditions and thus to swelling-mediated hemolysis.

In conclusion, the present data indicate that hypotonic stress induces ATP release from RBCs independent of hemolysis, but the involvement of Pnx-1 or CFTR could not be confirmed in this study.

5.1.5.2 PDE mediated ATP release is CFTR dependent, but Pnx-1 independent

The data of the present study show that PDE 5-dependent ATP release is independent of Pnx-1 demonstrated by channel blocking with carbenoxolone and probenecid, but dependent of CFTR as assessed by usage of RBCs from WT and CFTR KO mice. The present study shows that PDE-mediated ATP release is blunted in CFTR KO mouse RBCs. Furthermore, this study demonstrated that basal ATP levels are decreased in these mice and that basal hemolysis assessed as concentration in the supernatant was significantly higher in CFTR KO RBCs compared to WT. A possible explanation might be that lack of CFTR results in impairment of salt and fluid balance in RBCs as it occurs in epithelial cells [237-240]. This might lead to RBC cell membrane instability and increased cell lysis.

The decrease of steady state ATP release from RBCs from CFTR KO mice contradicts to published data, which shows an increase in basal ATP levels in CFTR KO mice [241]. In both data sets, the same CFTR KO strains (UNC CFTR KO, Jackson Laboratory, see §3.2) were used. Therefore, a possible explanation might be that in the present results, CFTR KO mice of different ages were used. This was performed because of low survival rates of the mice induced by CF. Stumpf et al. showed that basal levels of hemolysis are unchanged in RBCs from CF patients compared to healthy volunteers [242]. A possible explanation for the contradicting results might be compensatory effects of RBCs for lower levels of CFTR in CF [136].

In conclusion, the present data indicate that CFTR is involved in the regulation of steady state ATP release and cell membrane integrity of RBCs, and that this channel contributes to PDE mediated ATP release.

5.1.6 Limitations and perspectives

Since ATP was measured as steady state level, no information about release and degradation rates was identified in the present study. Kinetics and regulatory aspects of ATP release from RBCs should be examined in future investigations. A possibility might be usage of HPLC/MS-techniques, which are able to detect ATP and its degradation products like ADP, AMP or adenosine. This might may a more detailed view into the kinetics and metabolism of ATP in RBCs.

Furthermore, alternative methods used in the literature might be more effective to analyze ATP. For instance, usage of fluorescence microscopy in a luciferase solution might investigate effects of stimulation on ATP release directly from single RBCs. It may further be more precise to visually exclude hemolytic cells by microscopy as used by Locovei et al. [145]. In detail, Locovei et al. established a protocol, in which RBCs were incubated with non-permeable fluorescent dye 5,6-carboxyfluorescein. Pnx-1 dependent dye uptake was measured by fluorescence microscopy and hemolytic cells were visually excluded [145]. It might be more effective not to use 5,6-carboxyfluorescein, but rather the principle of the luciferase-luciferin assay as used by Cinar et al [4]. They established a protocol in, ATP is measured in a microfluidic chamber filled with RBCs in a luciferase assay solution and detected ATP release by using a photon-counting photomultiplier tube [4]. The investigation of new alternative methods might open new perspectives to clarify intracellular signaling of ATP release from RBCs.

5.2 Part 2: Regulation of PS exposure

The aim of the second part of this study was to investigate whether sGC/cGMP signaling is involved in regulation of PS exposure in RBCs. Incubation with NEM and induced calcium-influx treated with Ca-I evoke PS exposure in healthy human RBCs. The protocol applied was first established by Closse et al[220]. RBC suspensions were incubated for 1 hour at 37°C in presence and absence of

Ca-I and NEM and analyzed via flow cytometry [220]. Compared to the protocol of Nicolay et al. [164], in which RBCs were incubated for 4 hours in presence and absence of Ca-I alone, the first protocol was shown to be more time-effective. The shorter incubation time probably is the result of additional inhibition of the flippase by the alkylating agent NEM.

The present results show that treatment with NEM/Ca-I increases the size of RBCs assessed as FSC. In contrast, in RBCs treated with the protocol of Nicolay et al. cell size is decreased. This might be due to the higher concentrations of KCl in the buffer used in present study as also proposed before by Clossé et al. In the present study 90 mM KCl instead of 5 mM as in the protocol of Nicolay et al. were used. It has been demonstrated in previous investigations that K-efflux is induced by increasing concentrations of Ca^{2+}_i in RBCs via activation of calcium-dependent-potassium channels (gardos-channels) followed by RBC shrinkage [171]. This efflux might be blunted by high potassium concentrations outside the cell due to lacking of concentration gradients.

The present study shows that treatment with the NO-donor DEA/NO (1 μ M-1000 μ M) decreases PS exposure in a concentration dependent manner in presence of NEM, Ca-I and $CaCl_2$. This finding is in line with other findings, which show that application of NO-donors such as 1 μ M SNP and 100 μ M PAPA/NONOate decrease PS exposure evoked by Ca-I or glucose depletion [164]. In conclusion, these results demonstrate that NO plays a protective role in NEM/Ca-I induced PS exposure and that NO may protect RBC membrane symmetry. According to our results, sGC/cGMP signaling is not involved in regulation of PS exposure, since sGC inhibition by ODQ did not affect PS exposure in presence of BAY-41 and DEA/NO. Furthermore, cGMP did also have no effect on NEM/Ca-I evoked PS exposure.

In contrast to our data, Nicolay et al. showed that 1 mM cGMP application decreases PS exposure in presence of Ca-I [164]. The used cGMP (db-cGMP) lacks potency and selectivity, as it is a poor activator of cGMP- dependent protein kinase and additionally releases butyrate a derivate, which could lead to off-target effects. The effect of butyrate itself on PS exposure was not investigated in the

publication by Nicolay et al. Furthermore, the usage of 1 mM cGMP is not physiologic as evidenced by previous publications which show that intracellular cGMP concentrations in 10^8 RBCs were measured to be 14.4 fmol/l [164, 243]. Moreover, variations in method specificity could also be the reason for these contrasting results. Based on the fact that sGC is not involved in the regulation of PS exposure, other possible mechanisms should be considered in the future.

The effect of NO could be explained by S-nitrosation of scramblase and/or flippase. It is known that the main function of NEM is the SH-alkylation. Together with the knowledge that scramblase activity is increased via calcium influx or modifications via protein-SH groups or oxidation [157-160], modifications of SH-groups by NO might be involved in the regulation of PS exposure. This is in agreement with the finding that also flippase activity is controlled via sulfhydryl modifications and leads to a decrease in enzyme activity [159, 161]. Considering that there is still a disagreement about the existence of scramblases and flippases in RBCs [147] and that the exact molecular mechanisms and distribution have not been described in detail yet [162], research remains further investigations. S-nitrosation status of flippase and scramblase should be determined via biotin-switch assay. Taken together, the present data show that NO regulates PS exposure in human RBCs independent of sGC/cGMP signaling.

5.3 Part 3: Analysis of RBC functions in CAD and CKD

The third part of this study aimed to investigate whether NO metabolism and/or rheology changes of RBCs are affected in disease conditions like CAD or CKD. Therefore, 2 independent patient studies were performed.

5.3.1 Red cell eNOS expression is decreased in CKD

In the CKD study, red cell eNOS expression was analyzed in the Department of Cardiology, Pulmonology and Angiology, Düsseldorf. All other data were investigated by Di Pietro et al. from the Department of medical, oral and biotechnological sciences and the aging research center and translational medicine CeSI-MeT, Chieti. A clinical cohort study with patients with CKD was performed and routine clinical parameters as well as NO content, phosphorylation

level of red cell eNOS, red cell eNOS signaling complex activation, NO production, cGMP levels, cGMP transporter expression, nitration and/or nitrosation levels and activity of RBCs were investigated [204].

The data presented here show that red cell eNOS expression is decreased in patients with CKD. Our cooperation partner further demonstrated that basal NO as well as cGMP levels were increased in RBCs from CKD patients [204]. Moreover, they could show that the increase of NO and cGMP levels in response to insulin and ionomycin treatment was significantly lower in RBCs from patients with CKD and that this increase is red cell eNOS dependent [204].

As previously described, PS-exposure of RBCs is increased in CKD resulting in higher adhesion to endothelial cells [244-246]. Furthermore, RBCs show decrease in deformability, shape and life span [247]. It has been proposed that CKD development is connected to the development of endothelial dysfunction [247-251]. In detail, CKD is associated with increased cardiovascular risk factors like hypertension, elevated LDL levels and diabetes [249]. Moreover, incident dialysis patients have been demonstrated to have higher potential for hospitalized stroke [251].

5.3.2 Non-canonical RBC functions are preserved in CAD and ACS

The second study aimed to assess whether red cell eNOS/NO signaling from RBC might play a role in CVD. Therefore, RBC functions of patients with CAD, ACS and healthy age-matched controls were characterized in the Department of Cardiology, Pulmonology and Angiology, Düsseldorf. Routine clinical parameters as well as non-canonical RBC functions were analyzed. These included the analysis of red cell eNOS-expression and NO metabolism, redox-state, PS exposure and rheological parameters.

The data presented here demonstrates that red cell eNOS expression is decreased in CAD and ACS. This result is in line with published data, which shows that decreased red cell eNOS expression is correlating to endothelial function assessed as flow mediated dilation in CAD patients [252]. These results were also confirmed by immunofluorescence staining performed by Eligini et al.

[11]. It was further investigated that not only expression, but also red cell eNOS activity is reduced in CAD [11].

The present results further demonstrated that basal levels of NO metabolites are unchanged in CAD and ACS by assessment of nitrosative chemistry by labeling RBCs with DAF-FM-DA in flow cytometry [253] and by measuring intracellular NO_2^- levels by CLD. Both NO levels assessed by loading RBCs with DAF-FM-DA and NO_2^- levels are unchanged in RBCs from patients with CAD and ACS compared to healthy controls. It was further shown that levels of NO were decreased when incubated with the NOS-inhibitor L-NAME, indicating a red cell NOS dependency of basal NO-levels in RBCs from healthy volunteers and patients with CAD. DAF-FM in the presence of an oxidant reacts with NO and/or nitrosating species. Therefore, FI depends on presence of oxidants (e.g. ascorbate, ROS). Furthermore, the reaction with NO leads to generation of fluorescent triazole derivate DAF-FM-T [253]. Furthermore, it has been demonstrated that the majority of whole blood NO_2^- is present in RBCs [65]. Moreover, it has been proposed that NO_2^- might function as a main marker for NO bioavailability [64]. To sum up, our data indicate that although red cell eNOS expression is decreased in CAD, NO metabolism is preserved suggesting that RBCs compensate lack of NO bioavailability.

The present results show no differences in redox-state in CAD and ACS indicated as ROS- and glutathione levels measured as DCF and enzymatic assay for total glutathione. These results agree with data of Pytel et al., who showed that glutathione peroxidase-1 activity is unchanged in CAD [254]. In contrast, Blankenberg et al. showed that decreasing levels of glutathione peroxidase-1 activity are associated with cardiovascular events in patients with CAD [255]. In other disease states like sickle cell disease, RBC glutathione levels were decreased [84]. Pytel et al. demonstrated that in in CAD, RBC catalase- and superoxide dismutase- activity is downregulated [254]. The present study shows that thiol- and ROS levels are not changed in CAD, but other important anti-oxidative enzyme like catalase and superoxide-dismutase are decreased as shown in previous publications [254]. Therefore, this should be further investigated in the future.

In the present study membrane properties of RBCs in patients with CAD and ACS were characterized by analysis of PS exposure. The main result of the study was that PS exposure is unchanged in CAD and ACS. However, it was investigated in other studies that increased levels of PS are linked to other diseases like sickle cell disease, anemia or acute cardiac failure [150, 218, 256]. Moreover, these changes are believed to be involved in the development of anemia, which has been proposed as an independent risk factor in various diseases like myocardial infarction [257]. In conclusion, regulation of PS exposure is unchanged in CAD suggesting that RBC membrane symmetry is preserved.

Changes in deformability as well as increase of aggregability have been linked to pathophysiological conditions such as myocardial infarction, inflammation, sickle cell anemia or diabetes [258]. In other studies, increased RBCs aggregation has been proposed to function as an indicator of bad clinical outcome in angina pectoris [185]. However, this study shows that aggregability is increased in ACS. Arbel et al. showed that RBCs aggregability of ACS patients is increased due to changes of plasma factors. In detail, it was shown that high level of fibrinogen in ACS correlate to RBC aggregability strength under low stress conditions [259]. Therefore, the increase of aggregability measured in the present study might also be related to increased concentrations of plasma proteins. Thus, besides the characteristics of the RBCs like e.g. membrane composition or viscosity also other environmental parameters like plasma factors or platelet aggregability should be analyzed.

The present study shows that deformability is unchanged in CAD and ACS and therefore might not be associated to the clinical outcome. It was further demonstrated by Pytel et al. that RBCs have decreased membrane fluidity in CAD [254]. Taken together, although parameters like RBC membrane fluidity are impaired, RBC deformability is unchanged in CAD.

In conclusion, the present study shows that RBCs are able to compensate pathological conditions like CAD resulting in preservation of non-canonical functions like cellular NO metabolism, redox-state, membrane symmetry and deformability.

6 Summary and Conclusion

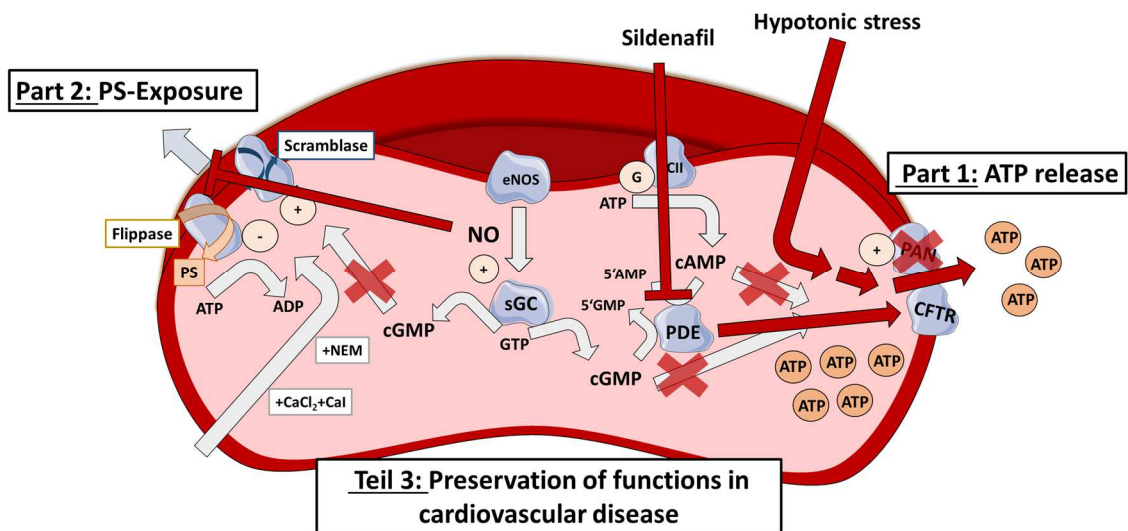


Figure 39: Main findings of the present study

There is evidence that RBCs, beside their role as O₂ and CO₂ transporters and as regulators of the physiological acid/ base equilibrium, might have additional non-canonical functions, which include the release of vasoactive metabolites like ATP [4-7] and NO [8-11], regulation of membrane functions like deformability, aggregation [13-15] and PS exposure [16, 17] as well as redox regulation [18, 19]. These non-canonical functions have been proposed to play an important role in human physiology, for instance in the regulation of vascular homeostasis and integrity [3, 10], but are not well understood.

However, there are many contradicting results concerning the underlying mechanisms of RBC non-canonical functions in the literature. One of the biggest challenges to characterize RBCs is their high fragility compared to other cell types [10]. Membrane rupture leads to uncontrolled release of free Hb and ATP from the cells. This represents a strong methodological issue in the analysis of regulation of ATP release from RBCs, which may lead to controversial results. There is one study showing that ATP levels measured after stimulation of RBCs with pharmacological and mechanical stimuli correlate to concentration of free Hb found in the supernatant [222], the authors of this study proposed that cell lysis is the only mechanism leading to ATP release from RBCs.

The results of the present study demonstrate that cell instability is a strong confounding parameter in RBC measurement, but may be kept under control by carefully optimizing assay conditions as well as by defining a threshold for Hb concentration in the supernatant. Under these optimized conditions, the results presented here show that sGC/cGMP as well as cAMP signaling are not involved in ATP release from RBCs. In addition, the present study shows that hypotonic stress induces ATP release from RBCs independently of Pnx-1. Moreover, the present study demonstrates that PDE inhibition induces ATP release in a Pnx-1-independent, but CFTR-dependent manner. However, the underlying mechanisms remain to be clarified since cAMP and cGMP treatment did not have an effect on ATP release.

The second part of the present study is in line with results of Nicolay et.al., who show that NO treatments inhibits PS exposure from RBCs in presence of $Ca^{2+}/Ca-I/NEM$, but as we show here, sGC/cGMP signaling is not involved in this regulation. Moreover, the present results indicate that in contrast to published data [164], cGMP has no effect on PS exposure evoked by $Ca^{2+}/Ca-I/NEM$ treatment.

There is accumulating evidence that RBCs may contribute to the regulation of vascular homeostasis and integrity [3, 10]. Several studies indicate that anemia is associated to cardiovascular complications [194-196, 260-262] and to increase of mortality in CKD [263, 264]. The data presented here show for the first time that RBC non-canonical functions like cellular NO metabolism, redox-state, membrane symmetry and deformability are unchanged in CVD suggesting that RBCs are compensating in pathological conditions.

Further investigations will reveal the role of RBC signaling in control of their non-canonical functions and will allow to characterize their changes under pathological conditions.

7 References

1. Gothoskar, A.V., *Resealed erythrocytes: a review*. Pharmaceutical Technology, 2004. **28**(3): p. 140-155.
2. Schmidt, R.F., F. Lang, and M. Heckmann, *Physiologie des Menschen: mit Pathophysiologie*. 2010: Springer-Verlag.
3. Kuhn, V., L. Diederich, T.S. Keller IV, C.M. Kramer, W. Lückstädt, C. Panknin, T. Suvorava, B. Isakson, M. Kelm, and M.M. Cortese-Krott, *Red Blood Cell Function and Dysfunction: Redox Regulation, Nitric Oxide Metabolism, Anemia*. Antioxidants and Redox Signaling, 2016(ja).
4. Cinar, E., S. Zhou, J. DeCoursey, Y. Wang, R.E. Waugh, and J. Wan, *Piezo1 regulates mechanotransductive release of ATP from human RBCs*. Proceedings of the National Academy of Sciences, 2015. **112**(38): p. 11783-8.
5. Ellsworth, M.L., C.G. Ellis, D. Goldman, A.H. Stephenson, H.H. Dietrich, and R.S. Sprague, *Erythrocytes: oxygen sensors and modulators of vascular tone*. Physiology (Bethesda), 2009. **24**: p. 107-16.
6. Ellsworth, M.L., C.G. Ellis, and R.S. Sprague, *Role of erythrocyte-released ATP in the regulation of microvascular oxygen supply in skeletal muscle*. Acta Physiologica (Oxford, England), 2016. **216**(3): p. 265-76.
7. Sridharan, M., S.P. Adderley, E.A. Bowles, T.M. Egan, A.H. Stephenson, M.L. Ellsworth, and R.S. Sprague, *Pannexin 1 is the conduit for low oxygen tension-induced ATP release from human erythrocytes*. American journal of physiology. Heart and circulatory physiology, 2010. **299**(4): p. H1146-52.
8. Helms, C. and D.B. Kim-Shapiro, *Hemoglobin-mediated nitric oxide signaling*. Free Radical Biology and Medicine, 2013. **61**: p. 464-472.
9. Kleinbongard, P., R. Schulz, T. Rassaf, T. Lauer, A. Dejam, T. Jax, I. Kumara, P. Gharini, S. Kabanova, and B. Özüyan, *Red blood cells express a functional endothelial nitric oxide synthase*. Blood, 2006. **107**(7): p. 2943-2951.
10. Cortese-Krott, M.M. and M. Kelm, *Endothelial nitric oxide synthase in red blood cells: key to a new erythrocrine function?* Redox Biology, 2014. **2**: p. 251-8.
11. Eligini, S., B. Porro, A. Lualdi, I. Squellerio, F. Veglia, E. Chiorino, M. Crisci, A. Garlasche, M. Giovannardi, J.P. Werba, E. Tremoli, and V. Cavalca, *Nitric oxide synthetic pathway in red blood cells is impaired in coronary artery disease*. PLoS One, 2013. **8**(8): p. e66945.

12. Crawford, J.H., B.K. Chacko, C.G. Kevil, and R.P. Patel, *The red blood cell and vascular function in health and disease*. Antioxidants and Redox Signaling, 2004. **6**(6): p. 992-9.
13. Chien, S., *Biophysical behavior of red cells in suspensions*. The red blood cell, 1975. **2**(4): p. 1031-1133.
14. Chien, S., *Red cell deformability and its relevance to blood flow*. Annual review of physiology, 1987. **49**(1): p. 177-192.
15. Baskurt, O.K. and H.J. Meiselman, *Cellular determinants of low-shear blood viscosity*. Biorheology, 1997. **34**(3): p. 235-247.
16. Lang, E., S.M. Qadri, and F. Lang, *Killing me softly—suicidal erythrocyte death*. The international journal of biochemistry & cell biology, 2012. **44**(8): p. 1236-1243.
17. Lang, K.S., P.A. Lang, C. Bauer, C. Duranton, T. Wieder, S. Huber, and F. Lang, *Mechanisms of suicidal erythrocyte death*. Cellular Physiology and Biochemistry, 2005. **15**(5): p. 195-202.
18. Buehler, P.W. and A.I. Alayash, *Oxygen sensing in the circulation: "cross talk" between red blood cells and the vasculature*. Antioxidants & redox signaling, 2004. **6**(6): p. 1000-1010.
19. Minetti, M. and W. Malorni, *Redox control of red blood cell biology: the red blood cell as a target and source of prooxidant species*. Antioxidants & redox signaling, 2006. **8**(7-8): p. 1165-1169.
20. Gallis, B., G.L. Corthals, D.R. Goodlett, H. Ueba, F. Kim, S.R. Presnell, D. Figeys, D.G. Harrison, B.C. Berk, and R. Aebersold, *Identification of flow-dependent endothelial nitric-oxide synthase phosphorylation sites by mass spectrometry and regulation of phosphorylation and nitric oxide production by the phosphatidylinositol 3-kinase inhibitor LY294002*. Journal of Biological Chemistry, 1999. **274**(42): p. 30101-30108.
21. Fleming, I. and R. Busse, *Molecular mechanisms involved in the regulation of the endothelial nitric oxide synthase*. American Journal of Physiology-Regulatory, Integrative and Comparative Physiology, 2003. **284**(1): p. R1-R12.
22. Garcia, C.E., C.M. Kilcoyne, C. Cardillo, R.O. Cannon, A.A. Quyyumi, and J.A. Panza, *Evidence that endothelial dysfunction in patients with hypercholesterolemia is not due to increased extracellular nitric oxide breakdown by superoxide anions*. The American journal of cardiology, 1995. **76**(16): p. 1157-1161.
23. Alderton, W.K., C.E. Cooper, and R.G. Knowles, *Nitric oxide synthases: structure, function and inhibition*. Biochemical Journal, 2001. **357**(3): p. 593-615.

24. Fulton, D., J.-P. Gratton, and W.C. Sessa, *Post-translational control of endothelial nitric oxide synthase: why isn't calcium/calmodulin enough?* Journal of Pharmacology and Experimental Therapeutics, 2001. **299**(3): p. 818-824.
25. Fulton, D., J.-P. Gratton, T.J. McCabe, J. Fontana, Y. Fujio, K. Walsh, T.F. Franke, A. Papapetropoulos, and W.C. Sessa, *Regulation of endothelium-derived nitric oxide production by the protein kinase Akt.* Nature, 1999. **399**(6736): p. 597-601.
26. Dimmeler, S., I. Fleming, B. Fisslthaler, C. Hermann, R. Busse, and A.M. Zeiher, *Activation of nitric oxide synthase in endothelial cells by Akt-dependent phosphorylation.* Nature, 1999. **399**(6736): p. 601-605.
27. Igarashi, J., H.S. Thattai, P. Prabhakar, D.E. Golan, and T. Michel, *Calcium-independent activation of endothelial nitric oxide synthase by ceramide.* Proceedings of the National Academy of Sciences, 1999. **96**(22): p. 12583-12588.
28. Lefer, D.J., S.P. Jones, W.G. Girod, A. Baines, M.B. Grisham, A.S. Cockrell, P.L. Huang, and R. Scalia, *Leukocyte-endothelial cell interactions in nitric oxide synthase-deficient mice.* American Journal of Physiology-Heart and Circulatory Physiology, 1999. **276**(6): p. H1943-H1950.
29. Marletta, M.A., *Nitric oxide synthase: aspects concerning structure and catalysis.* Cell, 1994. **78**(6): p. 927-930.
30. Kuchan, M. and J. Frangos, *Role of calcium and calmodulin in flow-induced nitric oxide production in endothelial cells.* American Journal of Physiology-Cell Physiology, 1994. **266**(3): p. C628-C636.
31. Michell, B., J. Griffiths, K. Mitchell, I. Rodriguez-Crespo, T. Tiganis, S. Bozinovski, P.O. de Montellano, B. Kemp, and R. Pearson, *The Akt kinase signals directly to endothelial nitric oxide synthase.* Current biology, 1999. **9**(15): p. 845-S1.
32. Michel, T., G.K. Li, and L. Busconi, *Phosphorylation and subcellular translocation of endothelial nitric oxide synthase.* Proceedings of the National Academy of Sciences, 1993. **90**(13): p. 6252-6256.
33. Corson, M.A., N.L. James, S.E. Latta, R.M. Nerem, B.C. Berk, and D.G. Harrison, *Phosphorylation of endothelial nitric oxide synthase in response to fluid shear stress.* Circulation research, 1996. **79**(5): p. 984-991.
34. García-Cardena, G., R. Fan, D.F. Stern, J. Liu, and W.C. Sessa, *Endothelial nitric oxide synthase is regulated by tyrosine phosphorylation and interacts with caveolin-1.* Journal of Biological Chemistry, 1996. **271**(44): p. 27237-27240.

35. Raj, U. and L. Shimoda, *Oxygen-dependent signaling in pulmonary vascular smooth muscle*. American Journal of Physiology-Lung Cellular and Molecular Physiology, 2002. **283**(4): p. L671-L677.
36. Gerzer, R., E.W. Radany, and D.L. Garbers, *The separation of the heme and apoheme forms of soluble guanylate cyclase*. Biochemical and biophysical research communications, 1982. **108**(2): p. 678-686.
37. Gerzer, R., F. Hofmann, and G. Schultz, *Purification of a Soluble, Sodium-Nitroprusside-Stimulated Guanylate Cyclase from Bovine Lung*. European Journal of Biochemistry, 1981. **116**(3): p. 479-486.
38. Ohlstein, E.H., K.S. Wood, and L.J. Ignarro, *Purification and properties of heme-deficient hepatic soluble guanylate cyclase: effects of heme and other factors on enzyme activation by NO, NO-heme, and protoporphyrin IX*. Archives of biochemistry and biophysics, 1982. **218**(1): p. 187-198.
39. Poulos, T.L., *Soluble guanylate cyclase*. Current opinion in structural biology, 2006. **16**(6): p. 736-743.
40. Löffler, G., *Basiswissen Biochemie: mit Pathobiochemie*. 2013: Springer-Verlag.
41. Zabel, U., M. Weeger, L. Mylinh, and H.H. Schmidt, *Human soluble guanylate cyclase: functional expression and revised isoenzyme family*. Biochemical Journal, 1998. **335**(1): p. 51-57.
42. Zabel, U., C. Häusler, M. Weeger, and H.H. Schmidt, *Homodimerization of Soluble Guanylyl Cyclase Subunits dimerization analysis using glutathiones-transferase tag* Journal of Biological Chemistry, 1999. **274**(26): p. 18149-18152.
43. Evgenov, O.V., P. Pacher, P.M. Schmidt, G. Hasko, H.H. Schmidt, and J.P. Stasch, *NO-independent stimulators and activators of soluble guanylate cyclase: discovery and therapeutic potential*. Nature Reviews Drug Discovery, 2006. **5**(9): p. 755-68.
44. Russwurm, M. and D. Koesling, *NO activation of guanylyl cyclase*. The EMBO journal, 2004. **23**(22): p. 4443-4450.
45. Ignarro, L.J., K.S. Wood, and M.S. Wolin, *Activation of purified soluble guanylate cyclase by protoporphyrin IX*. Proceedings of the National Academy of Sciences, 1982. **79**(9): p. 2870-2873.
46. Foerster, J., C. Harteneck, J. Malkewitz, G. Schultz, and D. Koesling, *A Functional Heme-Binding Site of Soluble Guanylyl Cyclase Requires Intact N-Termini of $\alpha 1$ and $\beta 1$ Subunits*. European Journal of Biochemistry, 1996. **240**(2): p. 380-386.

47. Ignarro, L., J. Adams, P. Horwitz, and K. Wood, *Activation of soluble guanylate cyclase by NO-hemoproteins involves NO-heme exchange. Comparison of heme-containing and heme-deficient enzyme forms.* Journal of Biological Chemistry, 1986. **261**(11): p. 4997-5002.
48. Hwang, T.L., C.C. Wu, and C.M. Teng, *Comparison of two soluble guanylyl cyclase inhibitors, methylene blue and ODQ, on sodium nitroprusside-induced relaxation in guinea-pig trachea.* British journal of pharmacology, 1998. **125**(6): p. 1158-1163.
49. Zhao, Y., P.E. Brandish, M. DiValentin, J.P. Schelvis, G.T. Babcock, and M.A. Marletta, *Inhibition of soluble guanylate cyclase by ODQ.* Biochemistry, 2000. **39**(35): p. 10848-10854.
50. Stasch, J.-P., P.M. Schmidt, P.I. Nedvetsky, T.Y. Nedvetskaya, A.K. HS, S. Meurer, M. Deile, A. Taye, A. Knorr, and H. Lapp, *Targeting the heme-oxidized nitric oxide receptor for selective vasodilatation of diseased blood vessels.* The Journal of clinical investigation, 2006. **116**(9): p. 2552-2561.
51. Rapoport, R.M., M.B. Draznin, and F. Murad, *Endothelium-dependent relaxation in rat aorta may be mediated through cyclic GMP-dependent protein phosphorylation.* Nature 1983. **306**: p. 174 - 176.
52. Kolluru, G.K., J.H. Siamwala, and S. Chatterjee, *eNOS phosphorylation in health and disease.* Biochimie, 2010. **92**(9): p. 1186-1198.
53. Jialal, I., S. Devaraj, and S.K. Venugopal, *C-reactive protein: risk marker or mediator in atherothrombosis?* Hypertension, 2004. **44**(1): p. 6-11.
54. Venugopal, S.K., S. Devaraj, I. Yuhanna, P. Shaul, and I. Jialal, *Demonstration that C-reactive protein decreases eNOS expression and bioactivity in human aortic endothelial cells.* Circulation, 2002. **106**(12): p. 1439-1441.
55. Laight, D., M. Carrier, and E. Änggård, *Antioxidants, diabetes and endothelial dysfunction.* Cardiovascular research, 2000. **47**(3): p. 457-464.
56. May, J.M., Z.-C. Qu, L. Xia, and C.E. Cobb, *Nitrite uptake and metabolism and oxidant stress in human erythrocytes.* American Journal of Physiology-Cell Physiology, 2000. **279**(6): p. C1946-C1954.
57. Lancaster, J.R., *Simulation of the diffusion and reaction of endogenously produced nitric oxide.* Proceedings of the National Academy of Sciences, 1994. **91**(17): p. 8137-8141.
58. Kelm, M., *Nitric oxide metabolism and breakdown.* Biochimica et Biophysica Acta (BBA)-Bioenergetics, 1999. **1411**(2): p. 273-289.

59. Wang, X., J.E. Tanus-Santos, C.D. Reiter, A. Dejam, S. Shiva, R.D. Smith, N. Hogg, and M.T. Gladwin, *Biological activity of nitric oxide in the plasmatic compartment*. Proceedings of the National Academy of Sciences of the United States of America, 2004. **101**(31): p. 11477-11482.
60. Ignarro, L.J., J.M. Fukuto, J.M. Griscavage, N.E. Rogers, and R.E. Byrns, *Oxidation of nitric oxide in aqueous solution to nitrite but not nitrate: comparison with enzymatically formed nitric oxide from L-arginine*. Proceedings of the National Academy of Sciences, 1993. **90**(17): p. 8103-8107.
61. Rhodes, P., A. Leone, P. Francis, A. Struthers, and S. Moncada, *The L-arginine: nitric oxide pathway is the major source of plasma nitrite in fasted humans*. Biochemical and biophysical research communications, 1995. **209**(2): p. 590-596.
62. Owusu, B.Y., R. Stapley, J. Honavar, and R.P. Patel, *Effects of erythrocyte aging on nitric oxide and nitrite metabolism*. Antioxidants & redox signaling, 2013. **19**(11): p. 1198-1208.
63. Stapley, R., B.Y. Owusu, A. Brandon, M. Cusick, C. Rodriguez, M.B. Marques, J.D. Kerby, S.R. Barnum, J.A. Weinberg, and J.R. Lancaster, *Erythrocyte storage increases rates of NO and nitrite scavenging: implications for transfusion-related toxicity*. Biochemical Journal, 2012. **446**(3): p. 499-508.
64. Cosby, K., K.S. Partovi, J.H. Crawford, R.P. Patel, C.D. Reiter, S. Martyr, B.K. Yang, M.A. Waclawiw, G. Zalos, and X. Xu, *Nitrite reduction to nitric oxide by deoxyhemoglobin vasodilates the human circulation*. Nature medicine, 2003. **9**(12): p. 1498-1505.
65. Dejam, A., C.J. Hunter, M.M. Pelletier, L.L. Hsu, R.F. Machado, S. Shiva, G.G. Power, M. Kelm, M.T. Gladwin, and A.N. Schechter, *Erythrocytes are the major intravascular storage sites of nitrite in human blood*. Blood, 2005. **106**(2): p. 734-739.
66. Crawford, J.H., T.S. Isbell, Z. Huang, S. Shiva, B.K. Chacko, A.N. Schechter, V.M. Darley-Usmar, J.D. Kerby, J.D. Lang, and D. Kraus, *Hypoxia, red blood cells, and nitrite regulate NO-dependent hypoxic vasodilation*. Blood, 2006. **107**(2): p. 566-574.
67. Doyle, M.P., R.A. Pickering, T.M. DeWeert, J.W. Hoekstra, and D. Pater, *Kinetics and mechanism of the oxidation of human deoxyhemoglobin by nitrites*. Journal of Biological Chemistry, 1981. **256**(23): p. 12393-12398.
68. Hunter, C.J., A. Dejam, A.B. Blood, H. Shields, D.B. Kim-Shapiro, R.F. Machado, S. Tarekegn, N. Mulla, A.O. Hopper, and A.N. Schechter, *Inhaled nebulized nitrite is a hypoxia-sensitive NO-dependent selective pulmonary vasodilator*. Nature medicine, 2004. **10**(10): p. 1122-1127.

69. Cortese-Krott, M.M., A. Rodriguez-Mateos, R. Sansone, G.G. Kuhnle, S. Thasian-Sivarajah, T. Krenz, P. Horn, C. Krisp, D. Wolters, and C. Hei, *Human red blood cells at work: identification and visualization of erythrocytic eNOS activity in health and disease*. *Blood*, 2012. **120**(20): p. 4229-4237.
70. Wood, K.C., M.M. Cortese-Krott, J.C. Kovacic, A. Noguchi, V.B. Liu, X. Wang, N. Raghavachari, M. Boehm, G.J. Kato, and M. Kelm, *Circulating blood endothelial nitric oxide synthase contributes to the regulation of systemic blood pressure and nitrite homeostasis*. *Arteriosclerosis, thrombosis, and vascular biology*, 2013. **33**(8): p. 1861-1871.
71. Betteridge, D.J., *What is oxidative stress?* *Metabolism*, 2000. **49**(2): p. 3-8.
72. Johnson, R.M., G. Goyette, Jr., Y. Ravindranath, and Y.S. Ho, *Hemoglobin autoxidation and regulation of endogenous H₂O₂ levels in erythrocytes*. *Free Radic Biol Med*, 2005. **39**(11): p. 1407-17.
73. Minetti, M., L. Agati, and W. Malorni, *The microenvironment can shift erythrocytes from a friendly to a harmful behavior: pathogenetic implications for vascular diseases*. *Cardiovascular Research*, 2007. **75**(1): p. 21-8.
74. Martin, F.M., G. Bydlon, and J.S. Friedman, *SOD2-deficiency sideroblastic anemia and red blood cell oxidative stress*. *Antioxidants & redox signaling*, 2006. **8**(7-8): p. 1217-1225.
75. Nickel, C., S. Rahlfs, M. Deponete, S. Koncarevic, and K. Becker, *Thioredoxin networks in the malarial parasite Plasmodium falciparum*. *Antioxidants & redox signaling*, 2006. **8**(7-8): p. 1227-1239.
76. Kennett, E.C. and P.W. Kuchel, *Plasma membrane oxidoreductases: effects on erythrocyte metabolism and redox homeostasis*. *Antioxidants & redox signaling*, 2006. **8**(7-8): p. 1241-1247.
77. Griffith, O.W., *Glutathione turnover in human erythrocytes. Inhibition by buthionine sulfoximine and incorporation of glycine by exchange*. *Journal of Biological Chemistry*, 1981. **256**(10): p. 4900-4904.
78. Lunn, G., G. Dale, and E. Beutler, *Transport accounts for glutathione turnover in human erythrocytes*. *Blood*, 1979. **54**(1): p. 238-244.
79. Lyons, J., A. Rauh-Pfeiffer, Y. Yu, X.-M. Lu, D. Zurakowski, R. Tompkins, A. Ajami, V. Young, and L. Castillo, *Blood glutathione synthesis rates in healthy adults receiving a sulfur amino acid-free diet*. *Proceedings of the National Academy of Sciences*, 2000. **97**(10): p. 5071-5076.

80. Reid, M., A. Badaloo, T. Forrester, J.F. Morlese, M. Frazer, W.C. Heird, and F. Jahoor, *In vivo rates of erythrocyte glutathione synthesis in children with severe protein-energy malnutrition*. American Journal of Physiology-Endocrinology And Metabolism, 2000. **278**(3): p. E405-E412.
81. Reid, M. and F. Jahoor, *Glutathione in disease*. Current Opinion in Clinical Nutrition & Metabolic Care, 2001. **4**(1): p. 65-71.
82. Jones, D.P., [11] *Redox potential of GSH/GSSG couple: Assay and biological significance*. Methods in enzymology, 2002. **348**: p. 93-112.
83. Townsend, D.M., K.D. Tew, and H. Tapiero, *The importance of glutathione in human disease*. Biomedicine & Pharmacotherapy, 2003. **57**(3): p. 145-155.
84. Morris, C.R., J.H. Suh, W. Hagar, S. Larkin, D.A. Bland, M.H. Steinberg, E.P. Vichinsky, M. Shigenaga, B. Ames, F.A. Kuypers, and E.S. Klings, *Erythrocyte glutamine depletion, altered redox environment, and pulmonary hypertension in sickle cell disease*. Blood, 2008. **111**(1): p. 402-10.
85. Harrison, D., K.K. Griendling, U. Landmesser, B. Hornig, and H. Drexler, *Role of oxidative stress in atherosclerosis*. The American journal of cardiology, 2003. **91**(3): p. 7-11.
86. Opara, E.C., *Role of oxidative stress in the etiology of type 2 diabetes and the effect of antioxidant supplementation on glycemic control*. Journal of investigative medicine, 2004. **52**(1): p. 19-23.
87. Kojda, G. and D. Harrison, *Interactions between NO and reactive oxygen species: pathophysiological importance in atherosclerosis, hypertension, diabetes and heart failure*. Cardiovascular research, 1999. **43**(3): p. 652-671.
88. Ramdani, G. and G. Langsley, *ATP, an extracellular signaling molecule in red blood cells: A messenger for malaria?* Biomedical journal, 2014. **37**(5): p. 284.
89. Dietrich, H.H., M.L. Ellsworth, R.S. Sprague, and R.G. Dacey, *Red blood cell regulation of microvascular tone through adenosine triphosphate*. American Journal of Physiology-Heart and Circulatory Physiology, 2000. **278**(4): p. H1294-H1298.
90. Sprague, R.S., D. Goldman, E.A. Bowles, D. Achilleus, A.H. Stephenson, C.G. Ellis, and M.L. Ellsworth, *Divergent effects of low-O₂ tension and iloprost on ATP release from erythrocytes of humans with type 2 diabetes: implications for O₂ supply to skeletal muscle*. American Journal of Physiology-Heart and Circulatory Physiology, 2010. **299**(2): p. H566-H573.

91. Horiuchi, T., H.H. Dietrich, K. Hongo, and R.G. Dacey, *Comparison of P2 receptor subtypes producing dilation in rat intracerebral arterioles*. *Stroke*, 2003. **34**(6): p. 1473-1478.
92. Horiuchi, T., H.H. Dietrich, S. Tsugane, and R.G. Dacey, *Analysis of purine-and pyrimidine-induced vascular responses in the isolated rat cerebral arteriole*. *American Journal of Physiology-Heart and Circulatory Physiology*, 2001. **280**(2): p. H767-H776.
93. You, J., T.D. Johnson, W.F. Childres, and R. Bryan, *Endothelial-mediated dilations of rat middle cerebral arteries by ATP and ADP*. *American Journal of Physiology-Heart and Circulatory Physiology*, 1997. **273**(3): p. H1472-H1477.
94. Busse, R., G. Trogisch, and E. Bassenge, *The role of endothelium in the control of vascular tone*. *Basic research in cardiology*, 1985. **80**(5): p. 475-490.
95. Furchgott, R.F. and J.V. Zawadzki, *The obligatory role of endothelial cells in the relaxation of arterial smooth muscle by acetylcholine*. *Nature*, 1980. **288**(5789): p. 373-376.
96. Malmjö, M., D. Erlinge, E.D. Högestätt, and P.M. Zygmunt, *Endothelial P2Y receptors induce hyperpolarisation of vascular smooth muscle by release of endothelium-derived hyperpolarising factor*. *European journal of pharmacology*, 1999. **364**(2): p. 169-173.
97. Bergfeld, G. and T. Forrester, *Release of ATP from human erythrocytes in response to a brief period of hypoxia and hypercapnia*. *Cardiovascular research*, 1992. **26**(1): p. 40-47.
98. Sprague, R.S., M.L. Ellsworth, A.H. Stephenson, and A.J. Lonigro, *ATP: the red blood cell link to NO and local control of the pulmonary circulation*. *American Journal of Physiology-Heart and Circulatory Physiology*, 1996. **271**(6): p. H2717-H2722.
99. Olearczyk, J.J., A.H. Stephenson, A.J. Lonigro, and R.S. Sprague, *Receptor-mediated activation of the heterotrimeric G-protein Gs results in ATP release from erythrocytes*. *Medical Science Monitor*, 2001. **7**(4): p. 669-674.
100. Sprague, R.S., M.L. Ellsworth, A.H. Stephenson, and A.J. Lonigro, *Participation of cAMP in a signal-transduction pathway relating erythrocyte deformation to ATP release*. *American journal of cell physiology*, 2001. **281**(4): p. C1158-64.

101. Richards, J.P., G.L. Yosten, G.R. Kolar, C.W. Jones, A.H. Stephenson, M.L. Ellsworth, and R.S. Sprague, *Low O₂-induced ATP release from erythrocytes of humans with type 2 diabetes is restored by physiological ratios of C-peptide and insulin*. *Regulatory, Integrative and Comparative Physiology*, 2014. **307**(7): p. R862-8.
102. Schaub, M.C., M.A. Hefti, and M. Zaugg, *Integration of calcium with the signaling network in cardiac myocytes*. *Journal of molecular and cellular cardiology*, 2006. **41**(2): p. 183-214.
103. Bos, J.L., *Epac proteins: multi-purpose cAMP targets*. *Trends in biochemical sciences*, 2006. **31**(12): p. 680-686.
104. Sunahara, R.K., C.W. Dessauer, and A.G. Gilman, *Complexity and diversity of mammalian adenylyl cyclases*. *Annual review of pharmacology and toxicology*, 1996. **36**(1): p. 461-480.
105. Simonds, W.F., *G protein regulation of adenylate cyclase*. *Trends in pharmacological sciences*, 1999. **20**(2): p. 66-73.
106. Tang, W.-J. and A.G. Gilman, *Adenylyl cyclases*. *Cell*, 1992. **70**(6): p. 869-872.
107. Choi, E.-J., Z. Xia, E.C. Villacres, and D.R. Storm, *The regulatory diversity of the mammalian adenylyl cyclases*. *Current opinion in cell biology*, 1993. **5**(2): p. 269-273.
108. Sprague, R., E. Bowles, M. Stumpf, G. Ricketts, A. Freidman, W. Hou, A. Stephenson, and A. Lonigro, *Rabbit erythrocytes possess adenylyl cyclase type II that is activated by the heterotrimeric G proteins G_s and G_i*. *Pharmacological Reports*, 2005. **57**: p. 222.
109. Bayewitch, M.L., T. Avidor-Reiss, R. Levy, T. Pfeuffer, I. Nevo, W.F. Simonds, and Z. Vogel, *Differential modulation of adenylyl cyclases I and II by various G β subunits*. *Journal of Biological Chemistry*, 1998. **273**(4): p. 2273-2276.
110. Federman, A.D., B.R. Conklin, K.A. Schrader, R.R. Reed, and H.R. Bourne, *Hormonal stimulation of adenylyl cyclase through Gi-protein $\beta\gamma$ subunits*. *Nature*, 1992. **356**(6365): p. 159-161.
111. Olearczyk, J.J., A.H. Stephenson, A.J. Lonigro, and R.S. Sprague, *Heterotrimeric G protein Gi is involved in a signal transduction pathway for ATP release from erythrocytes*. *American Journal of Physiology-Heart and Circulatory Physiology*, 2004. **286**(3): p. H940-H945.
112. Sridharan, M., R.S. Sprague, S.P. Adderley, E.A. Bowles, M.L. Ellsworth, and A.H. Stephenson, *Diamide decreases deformability of rabbit erythrocytes and attenuates low oxygen tension-induced ATP release*. *Experimental biology and medicine*, 2010. **235**(9): p. 1142-1148.

113. Nobles, M., A. Benians, and A. Tinker, *Heterotrimeric G proteins precouple with G protein-coupled receptors in living cells*. Proceedings of the National Academy of Sciences of the United States of America, 2005. **102**(51): p. 18706-18711.
114. Chachisvilis, M., Y.-L. Zhang, and J.A. Frangos, *G protein-coupled receptors sense fluid shear stress in endothelial cells*. Proceedings of the National Academy of Sciences, 2006. **103**(42): p. 15463-15468.
115. Ngai, C. and X. Yao, *Vascular responses to shear stress: the involvement of mechanosensors in endothelial cells*. The Open Circulation And Vascular Journal, 2010. **3**: p. 85-94.
116. Chen, J. and R. Iyengar, *Inhibition of cloned adenylyl cyclases by mutant-activated Gi-alpha and specific suppression of type 2 adenylyl cyclase inhibition by phorbol ester treatment*. Journal of Biological Chemistry, 1993. **268**(17): p. 12253-12256.
117. Taussig, R., W.-J. Tang, J.R. Hepler, and A.G. Gilman, *Distinct patterns of bidirectional regulation of mammalian adenylyl cyclases*. Journal of Biological Chemistry, 1994. **269**(8): p. 6093-6100.
118. Kuhn, M., *Structure, regulation, and function of mammalian membrane guanylyl cyclase receptors, with a focus on guanylyl cyclase-A*. Circulation research, 2003. **93**(8): p. 700-709.
119. Adderley, S.P., R.S. Sprague, A.H. Stephenson, and M.S. Hanson, *Regulation of cAMP by phosphodiesterases in erythrocytes*. Pharmacological reports, 2010. **62**(3): p. 475-482.
120. Zaccolo, M., G. Di Benedetto, V. Lissandron, L. Mancuso, A. Terrin, and I. Zamparo, *Restricted diffusion of a freely diffusible second messenger: mechanisms underlying compartmentalized cAMP signalling*. Biochemical Society Transactions, 2006. **34**(4): p. 495-497.
121. Baillie, G.S., *Compartmentalized signalling: spatial regulation of cAMP by the action of compartmentalized phosphodiesterases*. FEBS Journal, 2009. **276**(7): p. 1790-9.
122. Bender, A.T. and J.A. Beavo, *Cyclic nucleotide phosphodiesterases: molecular regulation to clinical use*. Pharmacological reviews, 2006. **58**(3): p. 488-520.
123. Zaccolo, M. and M.A. Movsesian, *cAMP and cGMP signaling cross-talk role of phosphodiesterases and implications for cardiac pathophysiology*. Circulation Research, 2007. **100**(11): p. 1569-1578.
124. Degerman, E., P. Belfrage, and V.C. Manganiello, *Structure, localization, and regulation of cGMP-inhibited phosphodiesterase (PDE3)*. Journal of Biological Chemistry, 1997. **272**(11): p. 6823-6826.

125. Adderley, S.P., K.M. Thuet, M. Sridharan, E.A. Bowles, A.H. Stephenson, M.L. Ellsworth, and R.S. Sprague, *Identification of cytosolic phosphodiesterases in the erythrocyte: a possible role for PDE5*. Medical Science Monitor, 2011. **17**(5): p. CR241-7.
126. Adderley, S.P., E.A. Dufaux, M. Sridharan, E.A. Bowles, M.S. Hanson, A.H. Stephenson, M.L. Ellsworth, and R.S. Sprague, *Iloprost-and isoproterenol-induced increases in cAMP are regulated by different phosphodiesterases in erythrocytes of both rabbits and humans*. American Journal of Physiology-Heart and Circulatory Physiology, 2009. **296**(5): p. H1617-H1624.
127. Hanson, M.S., A.H. Stephenson, E.A. Bowles, M. Sridharan, S. Adderley, and R.S. Sprague, *Phosphodiesterase 3 is present in rabbit and human erythrocytes and its inhibition potentiates iloprost-induced increases in cAMP*. American journal of physiology. Heart and circulatory physiology, 2008. **295**(2): p. H786-93.
128. Amaral, M.D. and K. Kunzelmann, *Molecular targeting of CFTR as a therapeutic approach to cystic fibrosis*. Trends in pharmacological sciences, 2007. **28**(7): p. 334-341.
129. Jentsch, T.J., V. Stein, F. Weinreich, and A.A. Zdebik, *Molecular structure and physiological function of chloride channels*. Physiological reviews, 2002. **82**(2): p. 503-568.
130. Rommens, J.M., M.C. Iannuzzi, B.-s. Kerem, M.L. Drumm, G. Melmer, M. Dean, R. Rozmahel, J.L. Cole, D. Kennedy, and N. Hidaka, *Identification of the cystic fibrosis gene: chromosome walking and jumping*. Science, 1989. **245**(4922): p. 1059-1065.
131. Cheng, S.H., D.P. Rich, J. Marshall, R.J. Gregory, M.J. Welsh, and A.E. Smith, *Phosphorylation of the R domain by cAMP-dependent protein kinase regulates the CFTR chloride channel*. Cell, 1991. **66**(5): p. 1027-1036.
132. Sheppard, D.N. and M.J. Welsh, *Structure and function of the CFTR chloride channel*. Physiological reviews, 1999. **79**(1): p. S23-S45.
133. Gadsby, D.C., P. Vergani, and L. Csanády, *The ABC protein turned chloride channel whose failure causes cystic fibrosis*. Nature, 2006. **440**(7083): p. 477-483.
134. Dalemans, W., P. Barbry, G. Champigny, S. Jallat, S. Jallat, K. Dott, D. Dreyer, R.G. Crystal, A. Pavirani, and J.-P. Lecocq, *Altered chloride ion channel kinetics associated with the $\Delta F508$ cystic fibrosis mutation*. Nature, 1991. **354**(6354): p. 526-528.

135. Morral, N., J. Bertranpetit, X. Estivill, V. Nunes, T. Casals, J. Gimenez, A. Reis, R. Varon-Mateeva, M. Macek Jr, and L. Kalaydjieva, *The origin of the major cystic fibrosis mutation (DF508) in European populations*. Nature genetics, 1994. **7**(2): p. 169-175.
136. Lange, T., P. Jungmann, J. Haberle, S. Falk, A. Duebbers, R. Bruns, A. Ebner, P. Hinterdorfer, H. Oberleithner, and H. Schillers, *Reduced number of CFTR molecules in erythrocyte plasma membrane of cystic fibrosis patients*. Molecular membrane biology, 2006. **23**(4): p. 317-323.
137. Sprague, R.S., M.L. Ellsworth, A.H. Stephenson, M.E. Kleinhenz, and A.J. Lonigro, *Deformation-induced ATP release from red blood cells requires CFTR activity*. American Journal of Physiology, 1998. **275**(5 Pt 2): p. H1726-32.
138. Boassa, D., C. Ambrosi, F. Qiu, G. Dahl, G. Gaietta, and G. Sosinsky, *Pannexin1 channels contain a glycosylation site that targets the hexamer to the plasma membrane*. Journal of Biological Chemistry, 2007. **282**(43): p. 31733-31743.
139. Baranova, A., D. Ivanov, N. Petrash, A. Pestova, M. Skoblov, I. Kelmanson, D. Shagin, S. Nazarenko, E. Geraymovych, and O. Litvin, *The mammalian pannexin family is homologous to the invertebrate innexin gap junction proteins*. Genomics, 2004. **83**(4): p. 706-716.
140. Bao, L., S. Locovei, and G. Dahl, *Pannexin membrane channels are mechanosensitive conduits for ATP*. FEBS letters, 2004. **572**(1-3): p. 65-68.
141. Sandilos, J.K., Y.-H. Chiu, F.B. Chekeni, A.J. Armstrong, S.F. Walk, K.S. Ravichandran, and D.A. Bayliss, *Pannexin 1, an ATP release channel, is activated by caspase cleavage of its pore-associated C-terminal autoinhibitory region*. Journal of Biological Chemistry, 2012. **287**(14): p. 11303-11311.
142. Qiu, F. and G. Dahl, *A permeant regulating its permeation pore: inhibition of pannexin 1 channels by ATP*. American Journal of Physiology-Cell Physiology, 2009. **296**(2): p. C250-C255.
143. Barbe, M.T., H. Monyer, and R. Bruzzone, *Cell-cell communication beyond connexins: the pannexin channels*. Physiology, 2006. **21**(2): p. 103-114.
144. Dando, R. and S.D. Roper, *Cell-to-cell communication in intact taste buds through ATP signalling from pannexin 1 gap junction hemichannels*. The Journal of physiology, 2009. **587**(24): p. 5899-5906.
145. Locovei, S., L. Bao, and G. Dahl, *Pannexin 1 in erythrocytes: function without a gap*. Proceedings of the National Academy of Sciences, 2006. **103**(20): p. 7655-9.

146. Mohandas, N. and E. Evans, *Mechanical properties of the red cell membrane in relation to molecular structure and genetic defects*. Annual review of biophysics and biomolecular structure, 1994. **23**(1): p. 787-818.
147. Mohandas, N. and P.G. Gallagher, *Red cell membrane: past, present, and future*. Blood, 2008. **112**(10): p. 3939-3948.
148. Verkleij, A., R. Zwaal, B. Roelofsen, P. Comfurius, D. Kastelijn, and L. Van Deenen, *The asymmetric distribution of phospholipids in the human red cell membrane. A combined study using phospholipases and freeze-etch electron microscopy*. Biochimica et Biophysica Acta (BBA)-Biomembranes, 1973. **323**(2): p. 178-193.
149. Zwaal, R.F. and A.J. Schroit, *Pathophysiologic implications of membrane phospholipid asymmetry in blood cells*. Blood, 1997. **89**(4): p. 1121-1132.
150. Wood, B.L., D.F. Gibson, and J.F. Tait, *Increased erythrocyte phosphatidylserine exposure in sickle cell disease: flow-cytometric measurement and clinical associations*. Blood, 1996. **88**(5): p. 1873-80.
151. Yasin, Z., S. Witting, M.B. Palascak, C.H. Joiner, D.L. Rucknagel, and R.S. Franco, *Phosphatidylserine externalization in sickle red blood cells: associations with cell age, density, and hemoglobin F*. Blood, 2003. **102**(1): p. 365-370.
152. Kuypers, F.A., J. Yuan, R.A. Lewis, L.M. Snyder, C.R. Kiefer, A. Bunyaratvej, S. Fucharoen, L. Ma, L. Styles, and K. de Jong, *Membrane phospholipid asymmetry in human thalassemia*. Blood, 1998. **91**(8): p. 3044-3051.
153. Zachowski, A., *Phospholipids in animal eukaryotic membranes: transverse asymmetry and movement*. Biochemical Journal, 1993. **294**(Pt 1): p. 1.
154. Pomorski, T., J.C. Holthuis, A. Herrmann, and G. van Meer, *Tracking down lipid flippases and their biological functions*. Journal of cell science, 2004. **117**(6): p. 805-813.
155. Bevers, E., P. Comfurius, D. Dekkers, M. Harmsma, and R. Zwaal, *Transmembrane phospholipid distribution in blood cells: control mechanisms and pathophysiological significance*. Biological chemistry, 1997. **379**(8-9): p. 973-986.
156. Sahu, S.K., S.N. Gummadi, N. Manoj, and G.K. Aradhyam, *Phospholipid scramblases: an overview*. Archives of biochemistry and biophysics, 2007. **462**(1): p. 103-114.
157. Williamson, P., E.M. Bevers, E.F. Smeets, P. Comfurius, R.A. Schlegel, and R.F. Zwaal, *Continuous analysis of the mechanism of activated transbilayer lipid movement in platelets*. Biochemistry, 1995. **34**(33): p. 10448-10455.

158. Kamp, D., T. Sieberg, and C.W. Haest, *Inhibition and stimulation of phospholipid scrambling activity. Consequences for lipid asymmetry, echinocytosis, and microvesiculation of erythrocytes*. *Biochemistry*, 2001. **40**(31): p. 9438-9446.
159. de Jong, K., D. Geldwerth, and F.A. Kuypers, *Oxidative damage does not alter membrane phospholipid asymmetry in human erythrocytes*. *Biochemistry*, 1997. **36**(22): p. 6768-6776.
160. Martin, D.W. and J. Jesty, *Calcium Stimulation of Procoagulant Activity in Human Erythrocytes ATP Dependence and The Effects of Modifiers of Stimulation and Recovery*. *Journal of Biological Chemistry*, 1995. **270**(18): p. 10468-10474.
161. Devaux, P.F. and A. Zachowski, *Maintenance and consequences of membrane phospholipid asymmetry*. *Chemistry and Physics of Lipids*, 1994. **73**(1): p. 107-120.
162. Orrenius, S., B. Zhivotovsky, and P. Nicotera, *Regulation of cell death: the calcium-apoptosis link*. *Nature reviews Molecular cell biology*, 2003. **4**(7): p. 552-565.
163. Mandal, D., P.K. Moitra, S. Saha, and J. Basu, *Caspase 3 regulates phosphatidylserine externalization and phagocytosis of oxidatively stressed erythrocytes*. *FEBS letters*, 2002. **513**(2-3): p. 184-188.
164. Nicolay, J.P., G. Liebig, O.M. Niemoeller, S. Koka, M. Ghashghaieina, T. Wieder, J. Haendeler, R. Busse, and F. Lang, *Inhibition of suicidal erythrocyte death by nitric oxide*. *Pfluegers Archive - European Journal of Physiology*, 2008. **456**(2): p. 293-305.
165. Lang, K., C. Duranton, H. Poehlmann, S. Myssina, C. Bauer, F. Lang, T. Wieder, and S. Huber, *Cation channels trigger apoptotic death of erythrocytes*. *Cell Death & Differentiation*, 2003. **10**(2): p. 249-256.
166. Duranton, C., S.M. Huber, and F. Lang, *Oxidation induces a Cl⁻-dependent cation conductance in human red blood cells*. *The Journal of physiology*, 2002. **539**(3): p. 847-855.
167. Dekkers, D.W., P. Comfurius, E.M. Bevers, and R.F. Zwaal, *Comparison between Ca²⁺-induced scrambling of various fluorescently labelled lipid analogues in red blood cells*. *Biochemical Journal*, 2002. **362**(3): p. 741-747.
168. Woon, L., J. Holland, E. Kable, and B. Roufogalis, *Ca²⁺ sensitivity of phospholipid scrambling in human red cell ghosts*. *Cell calcium*, 1999. **25**(4): p. 313-320.

169. Zhou, Q., J. Zhao, T. Wiedmer, and P.J. Sims, *Normal hemostasis but defective hematopoietic response to growth factors in mice deficient in phospholipid scramblase 1*. *Blood*, 2002. **99**(11): p. 4030-4038.
170. Seigneuret, M. and P.F. Devaux, *ATP-dependent asymmetric distribution of spin-labeled phospholipids in the erythrocyte membrane: relation to shape changes*. *Proceedings of the National Academy of Sciences*, 1984. **81**(12): p. 3751-3755.
171. Lang, P.A., S. Kaiser, S. Myssina, T. Wieder, F. Lang, and S.M. Huber, *Role of Ca²⁺-activated K⁺ channels in human erythrocyte apoptosis*. *American Journal of Physiology-Cell Physiology*, 2003. **285**(6): p. C1553-C1560.
172. Mahmud, H., W.P. Ruifrok, B.D. Westenbrink, M.V. Cannon, I. Vreeswijk-Baudoin, W.H. van Gilst, H.H. Silljé, and R.A. de Boer, *Suicidal erythrocyte death, eryptosis, as a novel mechanism in heart failure-associated anaemia*. *Cardiovascular research*, 2013: p. cvt010.
173. Banerjee, D., S. Saha, S. Basu, and A. Chakrabarti, *Porous red cell ultrastructure and loss of membrane asymmetry in a novel case of hemolytic anemia*. *European journal of haematology*, 2008. **81**(5): p. 399-402.
174. Cokelet, G. *Hemorheology and hemodynamics*. in *Colloquium Series on Integrated Systems Physiology: From Molecule to Function*. 2011. Morgan & Claypool Life Sciences.
175. Baskurt, O.K. and H.J. Meiselman, *Blood Rheology and Hemodynamics*. *Seminars in Thrombosis and Hemostasis*, 2003. **29**(05): p. 435-450.
176. Chasis, J.A. and S.B. Shohet, *Red cell biochemical anatomy and membrane properties*. *Annual review of physiology*, 1987. **49**(1): p. 237-248.
177. Simmonds, M.J., H.J. Meiselman, and O.K. Baskurt, *Blood rheology and aging*. *Journal of Geriatric Cardiology*, 2013. **10**(3): p. 291-301.
178. Rampling, M., *Red cell aggregation and yield stress*. *Clinical blood rheology*, 1988. **1**: p. 45-64.
179. Rampling, M., H. Meiselman, B. Neu, and O. Baskurt, *Influence of cell-specific factors on red blood cell aggregation*. *Biorheology*, 2004. **41**(2): p. 91-112.
180. Baskurt, O.K., *Mechanisms of blood rheology alterations*. *Biomedical and Health Research - IOS Press*, 2007. **69**: p. 170.
181. Baskurt, O., *Clinical significance of hemorheological alterations*. *Handbook of hemorheology and hemodynamics*, 2007. **69**: p. 392.

182. Somer, T. and H.J. Meiselman, *Disorders of blood viscosity*. Annals of medicine, 1993. **25**(1): p. 31-39.
183. Baskurt, O.K., T.C. Fisher, and H.J. Meiselman, *Sensitivity of the cell transit analyzer (CTA) to alterations of red blood cell deformability: role of cell size-pore size ratio and sample preparation*. Clinical Hemorheology and Microcirculation, 1996. **16**(6): p. 753-765.
184. Hardeman, M. and P. Goedhart, *Laser-assisted optical rotational cell analyser (LORCA); a new instrument for measurement of various structural hemorheological parameters*. Biorheology, 1995. **32**(2): p. 121-121.
185. Neumann, F., H. Katus, E. Hoberg, P. Roebruck, M. Braun, H. Haupt, H. Tillmanns, and W. Kübler, *Increased plasma viscosity and erythrocyte aggregation: indicators of an unfavourable clinical outcome in patients with unstable angina pectoris*. British heart journal, 1991. **66**(6): p. 425-430.
186. Baskurt, O.K., A. Temiz, and H.J. Meiselman, *Effect of superoxide anions on red blood cell rheologic properties*. Free Radical Biology and Medicine, 1998. **24**(1): p. 102-110.
187. Goldsmith, H.L., G.R. Cokelet, and P. Gaetgens, *Robin Fahraeus: evolution of his concepts in cardiovascular physiology*. American Journal of Physiology-Heart and Circulatory Physiology, 1989. **257**(3): p. H1005-H1015.
188. McKay, C.B. and H.J. Meiselman, *Osmolality-mediated Fahraeus and Fahraeus-Lindqvist effects for human RBC suspensions*. American Journal of Physiology-Heart and Circulatory Physiology, 1988. **254**(2): p. H238-H249.
189. Parthasarathi, K. and H.H. Lipowsky, *Capillary recruitment in response to tissue hypoxia and its dependence on red blood cell deformability*. American Journal of Physiology-Heart and Circulatory Physiology, 1999. **277**(6): p. H2145-H2157.
190. Secomb, T.W. and R. Hsu, *Resistance to blood flow in nonuniform capillaries*. Microcirculation, 1997. **4**(4): p. 421-427.
191. Organization, W.H., *Haemoglobin concentrations for the diagnosis of anaemia and assessment of severity*. 2011.
192. Wintrobe, M., *Anemia: classification and treatment on the basis of differences in the average volume and hemoglobin content of the red corpuscles*. Archives of internal medicine, 1934. **54**(2): p. 256-280.
193. Rodak, B.F., G.A. Fritsma, and E. Keohane, *Hematology: clinical principles and applications*. 2013: Elsevier Health Sciences.

194. Jolicœur, E.M., W.W. O'Neill, A. Hellkamp, C.W. Hamm, D.R. Holmes, H.R. Al-Khalidi, M.R. Patel, F.J. Van de Werf, K. Pieper, and P.W. Armstrong, *Transfusion and mortality in patients with ST-segment elevation myocardial infarction treated with primary percutaneous coronary intervention*. *European heart journal*, 2009. **30**(21): p. 2575-2583.
195. Ducrocq, G., E. Puymirat, P.G. Steg, P. Henry, M. Martelet, C. Karam, F. Schiele, T. Simon, and N. Danchin, *Blood transfusion, bleeding, anemia, and survival in patients with acute myocardial infarction: FAST-MI registry*. *American heart journal*, 2015. **170**(4): p. 726-734. e2.
196. Jani, S.M., D.E. Smith, D. Share, E. Kline-Rogers, S. Khanal, M.J. O'Donnell, J. Gardin, and M. Moscucci, *Blood Transfusion and In-hospital Outcomes in Anemic Patients with Myocardial Infarction Undergoing Percutaneous Coronary Intervention*. *Clinical cardiology*, 2007. **30**(S2).
197. Bassand, J.-P., R. Afzal, J. Eikelboom, L. Wallentin, R. Peters, A. Budaj, K.A. Fox, C.D. Joyner, S. Chrolavicius, and C.B. Granger, *Relationship between baseline haemoglobin and major bleeding complications in acute coronary syndromes*. *European heart journal*, 2009: p. ehp401.
198. Rousseau, M., R.T. Yan, M. Tan, C.J. Lefkowitz, A. Casanova, D. Fitchett, S.S. Jolly, A. Langer, S.G. Goodman, and A.T. Yan, *Relation between hemoglobin level and recurrent myocardial ischemia in acute coronary syndromes detected by continuous electrocardiographic monitoring*. *The American journal of cardiology*, 2010. **106**(10): p. 1417-1422.
199. Westenbrink, B., M. Alings, S. Connolly, J. Eikelboom, M. Ezekowitz, J. Oldgren, S. Yang, J. Pongue, S. Yusuf, and L. Wallentin, *Anemia predicts thromboembolic events, bleeding complications and mortality in patients with atrial fibrillation: insights from the RE-LY trial*. *Journal of Thrombosis and Haemostasis*, 2015. **13**(5): p. 699-707.
200. Marketou, M., A. Patrianakos, F. Parthenakis, E. Zacharis, D. Arfanakis, G. Kochiadakis, G. Chlouverakis, and P. Vardas, *Systemic blood pressure profile in hypertensive patients with low hemoglobin concentrations*. *International journal of cardiology*, 2010. **142**(1): p. 95-96.
201. Stenvinkel, P. and P. Bárány, *Anaemia, rHuEPO resistance, and cardiovascular disease in end-stage renal failure; links to inflammation and oxidative stress*. *Nephrology Dialysis Transplantation*, 2002. **17**(suppl 5): p. 32-37.
202. Herold, G., *Innere Medizin: eine vorlesungsorientierte Darstellung; unter Berücksichtigung des Gegenstandskataloges für die Ärztliche Prüfung; mit ICD 10-Schlüssel im Text und Stichwortverzeichnis*. 2011: Eigenverl.

203. WHO/Europe. *Definition of cardiovascular diseases*. Available from: <http://www.euro.who.int/en/health-topics/noncommunicable-diseases/cardiovascular-diseases/cardiovascular-diseases2/definition-of-cardiovascular-diseases> 03.03.2017.
204. Di Pietro, N., A. Giardinelli, V. Sirolli, C. Riganti, P. Di Tomo, E. Gazzano, S. Di Silvestre, C. Panknin, M.M. Cortese-Krott, and C. Csonka, *Nitric oxide synthetic pathway and cGMP levels are altered in red blood cells from end-stage renal disease patients*. *Molecular and cellular biochemistry*, 2016: p. 1-13.
205. Academic medical Center. University of Amsterdam, *LORRCA user's manual*. 2004.
206. Bauersachs, R., R. Wenby, and H. Meiselman, *Determination of specific red blood-cell aggregation indexes via an automated-system*. *Clinical Hemorheology*, 1989. **9**(1): p. 1-25.
207. Donner, M., M. Siadat, and J. Stoltz, *Erythrocyte aggregation: approach by light scattering determination*. *Biorheology*, 1987. **25**(1-2): p. 367-375.
208. Mechatronics,. *Lorrca*. Available from: <https://rrmechatronics.com/product/rbc-2/lorrca/> 04.01.2017.
209. Bowles, E.A., G.N. Moody, Y. Yeragunta, A.H. Stephenson, M.L. Ellsworth, and R.S. Sprague, *Phosphodiesterase 5 inhibitors augment UT-15C-stimulated ATP release from erythrocytes of humans with pulmonary arterial hypertension*. *Experimental Biology and Medicine* (Maywood, N.J.), 2015. **240**(1): p. 121-7.
210. Hanson, M.S., A.H. Stephenson, E.A. Bowles, M. Sridharan, S. Adderley, and R.S. Sprague, *Phosphodiesterase 3 is present in rabbit and human erythrocytes and its inhibition potentiates iloprost-induced increases in cAMP*. *Am J Physiol Heart Circ Physiol*, 2008. **295**(2): p. H786-93.
211. Olearczyk, J.J., M.L. Ellsworth, A.H. Stephenson, A.J. Lonigro, and R.S. Sprague, *Nitric oxide inhibits ATP release from erythrocytes*. *J Pharmacol Exp Ther*, 2004. **309**(3): p. 1079-84.
212. Sprague, R.S., E.A. Bowles, D. Achilleus, A.H. Stephenson, C.G. Ellis, and M.L. Ellsworth, *A selective phosphodiesterase 3 inhibitor rescues low PO₂-induced ATP release from erythrocytes of humans with type 2 diabetes: implication for vascular control*. *Am J Physiol Heart Circ Physiol*, 2011. **301**(6): p. H2466-72.
213. Sridharan, M., E.A. Bowles, J.P. Richards, M. Krantic, K.L. Davis, K.A. Dietrich, A.H. Stephenson, M.L. Ellsworth, and R.S. Sprague, *Prostacyclin receptor-mediated ATP release from erythrocytes requires the voltage-dependent anion channel*. *Am J Physiol Heart Circ Physiol*, 2012. **302**(3): p. H553-9.

214. Hanson, M.S., A.H. Stephenson, E.A. Bowles, and R.S. Sprague, *Insulin inhibits human erythrocyte cAMP accumulation and ATP release: role of phosphodiesterase 3 and phosphoinositide 3-kinase*. *Experimental Biology and Medicine* (Maywood, N.J.), 2010. **235**(2): p. 256-62.
215. Knebel, S.M., M.M. Elrick, E.A. Bowles, A.K. Zdanovec, A.H. Stephenson, M.L. Ellsworth, and R.S. Sprague, *Synergistic effects of prostacyclin analogs and phosphodiesterase inhibitors on cyclic adenosine 3', 5' monophosphate accumulation and adenosine 3' 5' triphosphate release from human erythrocytes*. *Experimental Biology and Medicine*, 2013. **238**(9): p. 1069-1074.
216. Traut, T.W., *Physiological concentrations of purines and pyrimidines*. *Molecular and cellular biochemistry*, 1994. **140**(1): p. 1-22.
217. Decherf, G., G. Bouyer, S. Egee, and S.L. Thomas, *Chloride channels in normal and cystic fibrosis human erythrocyte membrane*. *Blood Cells, Molecules and Diseases*, 2007. **39**(1): p. 24-34.
218. Boas, F.E., L. Forman, and E. Beutler, *Phosphatidylserine exposure and red cell viability in red cell aging and in hemolytic anemia*. *Proc Natl Acad Sci U S A*, 1998. **95**(6): p. 3077-81.
219. Nicolay, J.P., G. Liebig, O.M. Niemoeller, S. Koka, M. Ghashghaeinia, T. Wieder, J. Haendeler, R. Busse, and F. Lang, *Inhibition of suicidal erythrocyte death by nitric oxide*. *Pflügers Archiv-European Journal of Physiology*, 2008. **456**(2): p. 293-305.
220. Closse, C., J. Dachary-Prigent, and M.R. Boisseau, *Phosphatidylserine-related adhesion of human erythrocytes to vascular endothelium*. *British Journal of Haematology*, 1999. **107**(2): p. 300-2.
221. Abed, M., F. Artunc, K. Alzoubi, S. Honisch, D. Baumann, M. Föller, and F. Lang, *Suicidal erythrocyte death in end-stage renal disease*. *Journal of Molecular Medicine*, 2014. **92**(8): p. 871-879.
222. Sikora, J., S.N. Orlov, K. Furuya, and R. Grygorczyk, *Hemolysis is a primary ATP-release mechanism in human erythrocytes*. *Blood*, 2014. **124**(13): p. 2150-7.
223. Ellsworth, M.L., *Red blood cell-derived ATP as a regulator of skeletal muscle perfusion*. *Med Sci Sports Exerc*, 2004. **36**(1): p. 35-41.
224. Coade, S.B. and J.D. Pearson, *Metabolism of adenine nucleotides in human blood*. *Circulation Research*, 1989. **65**(3): p. 531-7.
225. Bischoff, E., *Potency, selectivity, and consequences of nonselectivity of PDE inhibition*. *International journal of impotence research*, 2004. **16**: p. S11-S14.

226. Sprague, R.S., A.H. Stephenson, E.A. Bowles, M.S. Stumpf, and A.J. Lonigro, *Reduced expression of G(i) in erythrocytes of humans with type 2 diabetes is associated with impairment of both cAMP generation and ATP release*. *Diabetes*, 2006. **55**(12): p. 3588-93.
227. Richards, J.P., E.A. Bowles, W.R. Gordon, M.L. Ellsworth, A.H. Stephenson, and R.S. Sprague, *Mechanisms of C-peptide-mediated rescue of low O₂-induced ATP release from erythrocytes of humans with Type 2 diabetes*. *American Journal of Physiology-Regulatory, Integrative and Comparative Physiology*, 2015. **308**(5): p. R411-R418.
228. Forst, T., D.D. De La Tour, T. Kunt, A. Pfützner, K. Goitom, T. Pohlmann, S. Schneider, B. Johansson, J. Wahren, and M. Löbig, *Effects of proinsulin C-peptide on nitric oxide, microvascular blood flow and erythrocyte Na⁺, K⁺-ATPase activity in diabetes mellitus type I*. *Clinical Science*, 2000. **98**(3): p. 283-290.
229. Wallerath, T., T. Kunt, T. Forst, E.I. Closs, R. Lehmann, T. Flohr, M. Gabriel, D. Schäfer, A. Göpfert, and A. Pfützner, *Stimulation of endothelial nitric oxide synthase by proinsulin C-peptide*. *Nitric Oxide*, 2003. **9**(2): p. 95-102.
230. Manganiello, V.C., M. Taira, E. Degerman, and P. Belfrage, *Type III cGMP-inhibited cyclic nucleotide phosphodiesterases (PDE 3 gene family)*. *Cellular signalling*, 1995. **7**(5): p. 445-455.
231. Sterling, K.M., S. Shah, R.J. Kim, N.I. Johnston, A.Y. Salikhova, and E.H. Abraham, *Cystic fibrosis transmembrane conductance regulator in human and mouse red blood cell membranes and its interaction with ecto-apyrase*. *Journal of cellular biochemistry*, 2004. **91**(6): p. 1174-1182.
232. Thiele, I., M. Hug, M. Hübner, and R. Greger, *Expression of cystic fibrosis transmembrane conductance regulator alters the responses to hypotonic cell swelling and ATP of Chinese hamster ovary cells*. *Cellular Physiology and Biochemistry*, 1998. **8**(1-2): p. 61-74.
233. Lang, F., G.L. Busch, and H. Völkl, *The diversity of volume regulatory mechanisms*. *Cellular Physiology and Biochemistry*, 1998. **8**(1-2): p. 1-45.
234. Braunstein, G.M., R.M. Roman, J.P. Clancy, B.A. Kudlow, A.L. Taylor, V.G. Shylonsky, B. Jovov, K. Peter, T. Jilling, and I.I. Ismailov, *Cystic fibrosis transmembrane conductance regulator facilitates ATP release by stimulating a separate ATP release channel for autocrine control of cell volume regulation*. *Journal of Biological Chemistry*, 2001. **276**(9): p. 6621-6630.
235. Al-Awqati, Q., *Regulation of ion channels by ABC transporters that secrete ATP*. *Science*, 1995. **269**(5225): p. 805.

236. Di Virgilio, F., P. Chiozzi, D. Ferrari, S. Falzoni, J.M. Sanz, A. Morelli, M. Torboli, G. Bolognesi, and O.R. Baricordi, *Nucleotide receptors: an emerging family of regulatory molecules in blood cells*. *Blood*, 2001. **97**(3): p. 587-600.
237. Guggino, W.B., *Cystic fibrosis and the salt controversy*. *Cell*, 1999. **96**(5): p. 607-610.
238. Schwiebert, E.M., D.J. Benos, M.E. Egan, M.J. Stutts, and W.B. Guggino, *CFTR is a conductance regulator as well as a chloride channel*. *Physiological reviews*, 1999. **79**(1): p. S145-S166.
239. Bradbury, N.A., *Intracellular CFTR: localization and function*. *Physiological reviews*, 1999. **79**(1): p. S175-S191.
240. Bertrand, C.A. and R.A. Frizzell, *The role of regulated CFTR trafficking in epithelial secretion*. *American Journal of Physiology-Cell Physiology*, 2003. **285**(1): p. C1-C18.
241. Abraham, E.H., K.M. Sterling, R.J. Kim, A.Y. Salikhova, H.B. Huffman, M.A. Crockett, N. Johnston, H.W. Parker, W.E. Boyle, Jr., A. Hartov, E. Demidenko, J. Eford, J. Kahn, S.A. Grubman, D.M. Jefferson, S.C. Robson, J.H. Thakar, A. Lorico, G. Rappa, A.C. Sartorelli, and P. Okunieff, *Erythrocyte membrane ATP binding cassette (ABC) proteins: MRP1 and CFTR as well as CD39 (ecto-apyrase) involved in RBC ATP transport and elevated blood plasma ATP of cystic fibrosis*. *Blood Cells, Molecules, and Diseases*, 2001. **27**(1): p. 165-80.
242. Stumpf, A., K. Wenners-Epping, M. Wälte, T. Lange, H. Koch, J. Häberle, A. Dübbers, S. Falk, L. Kiesel, and D. Nikova, *Physiological concept for a blood based CFTR test*. *Cellular Physiology And Biochemistry*, 2006. **17**(1-2): p. 29-36.
243. Conran, N., C. Oresco-Santos, H.C. Acosta, A. Fattori, S.T. Saad, and F.F. Costa, *Increased soluble guanylate cyclase activity in the red blood cells of sickle cell patients*. *British Journal of Haematology*, 2004. **124**(4): p. 547-54.
244. Bonomini, M., V. Sirolli, F. Gizzi, S. Di Stante, A. Grilli, and M. Felaco, *Enhanced adherence of human uremic erythrocytes to vascular endothelium: role of phosphatidylserine exposure*. *Kidney international*, 2002. **62**(4): p. 1358-1363.
245. Bonomini, M., A. Pandolfi, N. Di Pietro, V. Sirolli, A. Giardinelli, A. Consoli, L. Amoroso, F. Gizzi, M.A. De Lutiis, and M. Felaco, *Adherence of uremic erythrocytes to vascular endothelium decreases endothelial nitric oxide synthase expression*. *Kidney international*, 2005. **67**(5): p. 1899-1906.

246. Pandolfi, A., N. Di Pietro, V. Sirolli, A. Giardinelli, S. Di Silvestre, L. Amoroso, P. Di Tomo, F. Capani, A. Consoli, and M. Bonomini, *Mechanisms of uremic erythrocyte-induced adhesion of human monocytes to cultured endothelial cells*. Journal of cellular physiology, 2007. **213**(3): p. 699-709.
247. Brimble, K.S., A. McFarlane, N. Winegard, M. Crowther, and D.N. Churchill, *Effect of chronic kidney disease on red blood cell rheology*. Clinical hemorheology and microcirculation, 2006. **34**(3): p. 411-420.
248. Martinez, M., A. Vaya, J. Alvarino, J. Barbera, D. Ramos, A. Lopez, and J. Aznar, *Hemorheological alterations in patients with chronic renal failure. Effect of hemodialysis*. Clinical hemorheology and microcirculation, 1999. **21**(1): p. 1-6.
249. Tonelli, M., C. Bohm, S. Pandeya, J. Gill, A. Levin, and B.A. Kiberd, *Cardiac risk factors and the use of cardioprotective medications in patients with chronic renal insufficiency*. American Journal of Kidney Diseases, 2001. **37**(3): p. 484-489.
250. Leskinen, Y., J.P. Salenius, T. Lehtimäki, H. Huhtala, and H. Saha, *The prevalence of peripheral arterial disease and medial arterial calcification in patients with chronic renal failure: requirements for diagnostics*. American journal of kidney diseases, 2002. **40**(3): p. 472-479.
251. Seliger, S.L., D.L. Gillen, W. Longstreth, B. Kestenbaum, and C.O. Stehman-Breen, *Elevated risk of stroke among patients with end-stage renal disease*. Kidney international, 2003. **64**(2): p. 603-609.
252. Cortese-Krott, M.M., A. Rodriguez-Mateos, R. Sansone, G.G. Kuhnle, S. Thasian-Sivarajah, T. Krenz, P. Horn, C. Krisp, D. Wolters, C. Heiss, K.D. Kroncke, N. Hogg, M. Feelisch, and M. Kelm, *Human red blood cells at work: identification and visualization of erythrocytic eNOS activity in health and disease*. Blood, 2012. **120**(20): p. 4229-37.
253. Cortese-Krott, M.M., A. Rodriguez-Mateos, G.G.C. Kuhnle, G. Brown, M. Feelisch, and M. Kelm, *A multilevel analytical approach for detection and visualization of intracellular NO production and nitrosation events using diaminofluoresceins*. Free Radical Biology and Medicine, 2012. **53**(11): p. 2146-58.
254. Pytel, E., M. Olszewska-Banaszczyk, M. Koter-Michalak, and M. Broncel, *Increased oxidative stress and decreased membrane fluidity in erythrocytes of CAD patients*. Biochemistry and Cell Biology, 2013. **91**(5): p. 315-8.
255. Blankenberg, S., H.J. Rupprecht, C. Bickel, M. Torzewski, G. Hafner, L. Tiret, M. Smieja, F. Cambien, J. Meyer, K.J. Lackner, and I. AtheroGene, *Glutathione peroxidase 1 activity and cardiovascular events in patients with coronary artery disease*. N Engl J Med, 2003. **349**(17): p. 1605-13.

256. Attanasio, P., R. Bissinger, W. Haverkamp, B. Pieske, A. Wutzler, and F. Lang, *Enhanced suicidal erythrocyte death in acute cardiac failure*. European Journal of Clinical Investigation, 2015. **45**(12): p. 1316-24.
257. Sabatine, M.S., D.A. Morrow, R.P. Giugliano, P.B. Burton, S.A. Murphy, C.H. McCabe, C.M. Gibson, and E. Braunwald, *Association of hemoglobin levels with clinical outcomes in acute coronary syndromes*. Circulation, 2005. **111**(16): p. 2042-2049.
258. Yedgar, S., A. Koshkaryev, and G. Barshtein, *The red blood cell in vascular occlusion*. Pathophysiology of haemostasis and thrombosis, 2003. **32**(5-6): p. 263-268.
259. Arbel, Y., S. Banai, J. Benhorin, A. Finkelstein, I. Herz, A. Halkin, G. Keren, S. Yedgar, G. Barashtein, and S. Berliner, *Erythrocyte aggregation as a cause of slow flow in patients of acute coronary syndromes*. International Journal of Cardiology, 2012. **154**(3): p. 322-7.
260. Bindra, K., C. Berry, J. Rogers, N. Stewart, M. Watts, J. Christie, S. Cobbe, and H. Eteiba, *Abnormal haemoglobin levels in acute coronary syndromes*. QJM, 2006. **99**(12): p. 851-862.
261. González-Ferrer, J.J., J.C. García-Rubira, D.V. Balcones, I.N. Gil, R.C. Barrio, M. Fuentes-Ferrer, A. Fernández-Ortiz, and C. Macaya, *Influence of hemoglobin level on in-hospital prognosis in patients with acute coronary syndrome*. Revista Española de Cardiología (English Edition), 2008. **61**(9): p. 945-952.
262. Danesh, J., R. Collins, R. Peto, and G. Lowe, *Haematocrit, viscosity, erythrocyte sedimentation rate: meta-analyses of prospective studies of coronary heart disease*. European Heart Journal, 2000. **21**(7): p. 515-520.
263. Locatelli, F., A.R. Nissenson, B.J. Barrett, R.G. Walker, D.C. Wheeler, K.U. Eckardt, N.H. Lameire, and G. Eknoyan, *Clinical practice guidelines for anemia in chronic kidney disease: problems and solutions. A position statement from Kidney Disease: Improving Global Outcomes (KDIGO)*. Kidney international, 2008. **74**(10): p. 1237-1240.
264. Babitt, J.L. and H.Y. Lin, *Mechanisms of anemia in CKD*. Journal of the American Society of Nephrology, 2012: p. ASN. 2011111078.

Acknowledgment

This work was supported by the SFB1116 (B06) graduate program funded by the Deutsche Forschungsgemeinschaft.

This dissertation is the result of 3 years of hard work, frustration, but also much enthusiasm and passion. I would have never reached this point of my life without the help and support of special persons, who I would like to thank here.

Special thanks to:

Prof. Dr. rer. nat. Dr. Miriam M. Cortese-Krott, my mentor and supervisor, who gave me the chance to start my PhD thesis in the lab of cardiology and to gain a lot of new great experiences here. I would like to thank her for the support in discussions and inspiring ideas, which helped me hugely to successfully finish my thesis.

Prof. Dr. Peter Proksch, for being my supervisor in the faculty of Life Science (Mathematisch-Naturwissenschaftliche Fakultät).

Prof. Dr. med- Malte Kelm the head of the cardiology department, for his inspiring and constructive ideas.

A special thanks to Dr. rer. nat Tatsiana Surovara, the post doc of our group, who always had an open ear for my problems and helped me to solve challenges, which seemed even unbridgeable to me. I would also like to thank all the staff in the lab of cardiology, who not only were great colleges by supporting me in the lab, but also became great friends, who gave me the personal support I needed to successfully finish my thesis. These people made my thesis a unique time on what I will always look back with a smile.

The last lines of my acknowledgement are dedicated to the people, who always supported me and without who I would not be the person, who I am today.

I would like to thank my family, especially my parents, who always encouraged me to be myself and to follow my dreams. They gave me the strength to reach my goals even if they sometimes seemed unreachable. I would also like to

warmly thank my partner Julius Dann and my best friend Johanna Dierken for always motivating me in times of desperate and frustration. They intensively helped me to fulfill my dreams and never doubted my success. I will never forget your understanding and belief in me. I am also grateful for all other friends and people for their understanding and support in the past 3 years. They know that I will always be thankful that they are always there for me.

Curriculum vitae

Personal characteristics

First Name	Christina Monika
Family Name	Panknin
Date of Birth	03.01.1988
Place of Birth	Radevormwald
Nationality	German

Education

02/2014-	PhD candidate at Heinrich-Heine-University, Düsseldorf Division of Cardiology, Pulmonology and Angiology AG Cortese-Krott Title of PhD thesis: Characterization of RBC functions in health and coronary artery disease
02/2014-01/2017	Membership of iGRAD - Interdisciplinary Graduate and Research Academy Düsseldorf
02/2015-01/2017	Membership of graduate school SFB1116, Master switches in cardiac ischemia
10/2011 – 11/2013	RWTH Aachen, M. Sc. <ul style="list-style-type: none">• Applied and Molecular Biotechnology• Masterthesis at Grüenthal GmbH (Grade: 1,7)
09/2007 – 03/2011	FHOOW Emden, B. Sc. <ul style="list-style-type: none">• Biotechnology/Bioinformatics

Internships and further education

- 05/2013- 11/2013 **Masterthesis at Grünenthal GmbH**
- Research and Development Department: Pain
- Supervision: Dr. T. Christoph
- Functional characterization of TRPV1 in rat dorsal root ganglions
 - Fluorescence microscopy and preparation
 - Analytics of pain-signaling in rats for therapeutics development
- 10/2012 – 12/2012 **Research-internship at University hospital Aachen,**
- Institute of Pharmacology and Toxicology
 - Supervisor: Prof. Dr. G. Schmalzing
- 09/2010 – 11/2010 **Internship-semester at Miavit GmbH, Essen (Oldb)**
- Department: Microbiology

Workshops

Presenting (in) Science - How to own the stage on (international) conferences

Good Scientific Practice for (Post)Doctoral Researchers

Upward Leadership (medRSD)

Success in companies

Emotional Intelligence

SPSS (basic course)

Other specifications

Languages	English:	fluent (spoken and written)
	French:	good
	Spanish:	basic
EDV		MS Excel, MS PowerPoint, MS Word, GraphPad Prism and SPSS

Publications

“Red Blood Cell Function and Dysfunction: Redox Regulation, Nitric Oxide Metabolism, Anemia.”

Kuhn V, Diederich L, Keller Iv TC, Kramer CM, Lückstädt W, **Panknin C**, Suvorava T, Isakson B, Kelm M, Cortese-Krott MM. ARS. 2016.

„Nitric oxide synthetic pathway and cGMP levels are altered in red blood cells from end-stage renal disease patients.“

Di Pietro N, Giardinelli A, Sirolli V, Riganti C, Di Tomo P, Gazzano E, Di Silvestre S, **Panknin C**, Cortese-Krott MM, Csonka C, Kelm M, Ferdinandy P, Bonomini M, Pandolfi A. Mol. Cell Biochem. 2016.

„Left ventricular diastolic dysfunction in Nrf2 knock out mice is associated with cardiac hypertrophy, decreased expression of SERCA2a, and preserved endothelial function.“ E

Erkens R, Kramer CM, Lückstädt W, **Panknin C**, Krause L, Weidenbach M, Dirzka J, Krenz T, Mergia E, Suvorava T, Kelm M, Cortese-Krott MM. Free Radic. Biol Med. 2015.